lek. Aleksandra Pilśniak

“Obrazy kliniczno-dermoskopowe zmian skórnych w przebiegu ostrego i przewlekłego zapalenia skóry wywołanego radioterapią u chorych z rozpoznanym złośliwym nowotworem głowy i szyi.”

“Clinical and dermoscopic images of skin lesions in the course of acute and chronic radiation-induced dermatitis in patients diagnosed with head and neck malignancy.”

Rozprawa doktorska na stopień doktora

w dziedzinie nauk medycznych i nauk o zdrowiu

w dyscyplinie nauk medycznych

przedkładana Radzie Naukowej Narodowego Instytutu Onkologii,

im. Marii Skłodowskiej-Curie Państwowego Instytutu Badawczego,

Oddział w Warszawie

Promotor: Prof. dr hab. n. med. Grażyna Kamińska-Winciorek

Gliwice, 2024

Praca wykonana w I Klinice Radioterapii i Chemioterapii, Narodowego Instytutu Onkologii,

im. Marii Skłodowskiej-Curie, Państwowego Instytutu Badawczego,

w Oddziale w Gliwicach

Pragnę serdecznie podziękować

Mojemu Promotorowi, Pani Prof. dr hab. n. med. Grażynie Kamińskiej-Winciorek, za inspirację, opiekę naukową, wsparcie merytoryczne oraz motywację do dalszego rozwoju.

Panu Dr hab. n. med. Tomaszowi Rutkowskiemu, za wsparcie merytoryczne i logistyczne.

Kierownikowi I Kliniki Radioterapii i Chemioterapii, Prof. dr hab. n. med. Krzysztofowi Składowskiemu, za życzliwość i umożliwienie realizacji pracy doktorskiej.

Panu Prof. dr hab. n. med. Andrzejowi Tukiendorfowi, za cierpliwość i konsultacje statystyczne.

Pani Dr n. med. Anastazji Szlauer - Stefańskiej, za pomoc w ocenie obrazów dermoskopowych oraz udzieleniu cennych wskazówek dotyczących pracy naukowej.

Chciałbym również podziękować Panu Prof. dr hab. n. med. Michałowi Holeckiemu oraz wszystkim Współpracownikom Katedry i Kliniki Chorób Wewnętrznych, Autoimmunologicznych i Metabolicznych, bez których moja naukowa droga byłaby o wiele trudniejsza i zdecydowanie mniej przyjemna.

Pracę tę dedykuję Mojemu Mężowi Pawłowi i Moim Rodzicom,

Jesteście moim największym wsparciem i motywacją.

Spis treści

1.Wykaz stosowanych skrótów:

AJCC - *(ang. American Joint Committee on Cancer),* Amerykański Wspólny Komitet ds. Raka;

ARD - *(ang. acute radiodermatitis)*, ostre popromienne zapalenie skóry;

CB - *(ang. contominant boost*), jednoczasowy boost;

CHT - *(ang. chemotherapy)*, chemioterapia;

CI - *(ang. confidence interval),* przedział ufności;

CRD - *(ang. chronic radiodermatitis)*, przewlekłe popromienne zapalenie skóry;

CTCAE - *(ang. Common Terminology Criteria for Adverse Events)*, Wspólne Kryteria Terminologiczne dotyczące Zdarzeń Niepożądanych;

CTV1 - *(ang. clinical target volume 1)*, pierwsza kliniczna objętość tarczowa;

CTV2 - *(ang. clinical target volume 2)*, druga kliniczna objętość tarczowa;

D - *(ang. day*), dzień;

G - *(ang. grade)*, stopień nasilenia toksyczności zgodnie z kryteriami toksyczności Grupy Radioterapii Onkologicznej i Europejskiej Organizacji Badań i Leczenia Raka;

GLOBOCAN - *(ang. Global Cancer Statistics)*, Globalne Statystyki dotyczące Raka;

HNC - *(ang. head and neck cancer)*, nowotwory głowy i szyi;

HNSCC - *(ang. head and neck squamous cell carcinoma)*, rak płaskonabłonkowy głowy i szyi;

IDS - *(ang. International Dermoscopy Society),* Międzynarodowe Towarzystwo Dermoskopowe;

IMRT - *(ang. intensity modulated radiation therapy)*, modulacja intensywności wiązki napromieniania;

LENT SOMA - *(ang. Late Effects Normal Tissue Task Force-Subjective scale, and the Objective, Management, Analytic scale)*, Efekty Późne – Subiektywna Skala Grupy Zadaniowej ds. Tkanek oraz Skala Analityczna, Celu i Postępowania;

OR - *(ang. odds ratio)*, iloraz szans;

RT - *(ang. radioteraphy)*, radioterapia;

RTOG/EORTC - *(ang. Radiation Therapy Oncology Group and the European Organization for Research and Treatment of Cancer),* Grupa Radioterapii Onkologicznej i Europejskiej Organizacji Badań i Leczenia Raka.

2. Wykaz publikacji stanowiących rozprawę doktorską:

Rozprawa doktorska powstała w oparciu o cykl dwóch prospektywnych prac oryginalnych i dwóch prac poglądowych, opublikowanych w recenzowanych czasopismach naukowych o sumarycznym wskaźniku **IF 7,8** oraz sumie punktów **MEiN 410**. Ponadto wyniki badań zostały zaprezentowane na IX Zjeździe Polskiego Towarzystwa Radioterapii Onkologicznej (*Polska, Łódź, 18-19.10.2019*), XVIII Kongresie European Association of Dermato-Oncology (*Hiszpania, Sewilla, 21-23.04.2022*) oraz XXXII Zjeździe Polskiego Towarzystwa Dermatologicznego (*Polska, Lublin, 31.05-01.06.2023*).

Prace oryginalne:

PUBLIKACJA A:

Pilśniak A, Szlauer-Stefańska A, Tukiendorf A, Rutkowski T, Składowski K, Kamińska-Winciorek G. Dermoscopy of acute radiation-induced dermatitis in patients with head and neck cancers treated with radiotherapy. Sci Rep. 2023;13(1):15711.

DOI: 10.1038/s41598-023-42507-1

IF: 4,6

MEiN: 140 pkt

PUBLIKACJA B:

Pilśniak A, Szlauer-Stefańska A, Tukiendorf A, Rutkowski T, Składowski K, Kamińska-Winciorek G. Dermoscopy of Chronic Radiation-Induced Dermatitis in Patients with Head and Neck Cancers Treated with Radiotherapy. Life. 2024; 14 (3): 399.

DOI: 10.3390/life14030399

IF: 3,2

MEiN: 70 pkt

Prace poglądowe:

PUBLIKACJA C:

Dudek A, Rutkowski T, Kamińska-Winciorek G, Składowski K. What is new when it comes to acute and chronic radiation-induced dermatitis in head and neck cancer patients? NOWOTWORY J Oncol 2020; 70, 1: 9–15.

DOI: 10.5603/NJO.2020.0002

MEiN: 100 pkt

PUBLIKACJA D

Kamińska-Winciorek G, Pilśniak A. The role of dermoscopy in dermato-oncological diagnostics – new trends and perspectives. NOWOTWORY J Oncol 2021; 71: 103–110.

DOI: 10.5603/NJO.a2021.0013

MEiN: 100 pkt

3. Wykaz rycin:

Rycina 1. Obrazy makroskopowe (A,C,E,G) ARD w stopniach (G) od G1 do G4, oceniane klinicznie zgodnie z kryteriami RTOG [12] i obrazy dermoskopowe (B,D,F,H) opisane zgodnie z konsensusem IDS [19] u wybranego chorego w trakcie leczenia RT. (A) Słaby rumień (G1); (B) obraz dermoskopowy (G1) ARD przestawia naczynia linijne z rozgałęzieniami i linijne, zakrzywione naczynia o skupionym rozmieszczeniu i białe obszary bezstrukturalne; (C) obraz makroskopowy przedstawia jasny rumień, utratę włosów, wilgotne złuszczanie i umiarkowany obrzęk (G2); (D) obraz dermoskopowy ARD (G2) przedstawia naczynia linijne z rozgałęzieniami i linijne, zakrzywione naczynia o siateczkowym rozmieszczeniu oraz czopy mieszkowe o układzie rozet; (E) obraz makroskopowy przedstawia jasny rumień, utratę włosów, zlewające się wilgotne złuszczanie i obrzęk wżerowy (G3); (F) obraz dermoskopowy przedstawia (G3) naczynia linijne z rozgałęzieniami o rozmieszczeniu siateczkowym, pigmentacją okołomieszkową i czopy mieszkowe o układzie rozet; (G) owrzodzenie w ARD (G4); (H) obraz dermoskopowy (G4) uwidacznia naczynia linijne z rozgałęzieniami o rozmieszczeniu siateczkowym oraz białą i żółtą łuskę o niejednolitym rozmieszczeniu.

Rycina 2. Obrazy dermoskopowe ARD opisane zgodnie z konsensusem IDS [19] (A) Obraz dermoskopowy ARD przedstawia naczynia linijne z rozgałęzieniami, linijne, zakrzywione naczynia o rozmieszczeniu siateczkowym oraz białe okołomieszkowe koloru; (B) obraz dermoskopowy ARD ujawnia biało-żółtą łuskę o niejednolitym rozmieszczeniu (C) obraz dermoskopowy ukazuje naczynia linijne z rozgałęzieniami i linijne, zakrzywione o rozmieszczeniu skupionym, oraz brązową łuskę o niejednolitym rozmieszczeniu; (D) obraz dermoskopowy ukazuje naczynia linijne z rozgałęzieniami i linijne, zakrzywione o nieswoistym rozmieszczeniu oraz pigmentację okołomieszkową; (E) naczynia linijne z rozgałęzieniami i linijne, zakrzywione o rozmieszczeniem siateczkowym oraz czopy mieszkowe o układzie rozet.

Rycina 3. Obrazy makroskopowe (A, C) CRD w stopniach (G) od G1 do G2, oceniane klinicznie według kryteriów RTOG [12] oraz obrazy dermoskopowe (B, D) opisane według IDS [19] u wybranego chorego. (A) – niewielki zanik, zmiana pigmentacji (G1); (B) — obraz dermoskopowy (G1) CRD ujawnia naczynia linijne (pomarańczowe strzałki) o niespecyficznym rozmieszczeniu, brązowe kropki i ciałka (czerwone strzałki) i białe linie (białe strzałki); (C) – plamisty zanik, całkowita utrata włosów (G2); (D) — obraz dermoskopowy CRD (G2) przedstawia naczynia kropkowane (czarne strzałki) o nieswoistym rozmieszczeniu, brązowe kropki i ciałka (czerwone strzałki) i białe linie (białe strzałki).

Rycina 4. Obrazy dermoskopowe CRD opisane zgodnie z konsensusem IDS [20]. (A) — w obrazie dermoskopowym CRD widoczne są naczynia kropkowane (czarne strzałki) i linijne (pomarańczowe strzałki) o nieswoistym rozmieszczeniu oraz pigmentacja okołomieszkowa (fioletowe strzałki); (B) — obraz dermoskopowy CRD ujawnia naczynia kropkowane (czarne strzałki) i linijne z rozgałęzieniami (niebieskie strzałki) o rozmieszczeniu skupionym; (C) — obraz dermoskopowy CRD ujawnia białą łuskę o niejednolitym rozmieszczeniu (żółte strzałki) oraz brązowe kropki i ciałka (czerwone strzałki); (D) — obraz dermoskopowy CRD ujawnia naczynia linijne z rozgałęzieniami, (niebieskie strzałki) o rozmieszczeniu siateczkowym, okołomieszkowe białe zabarwienie (zielone strzałki), białą łuskę o niejednolitym rozmieszczeniu (żółte strzałki), białe linie (białe strzałki); (E) — obraz dermoskopowy CRD ujawnia naczynia z rozgałęzieniami (niebieskie strzałki) i kropkowane naczynia (czarne strzałki) o rozmieszczeniu skupionym oraz białe obszary bezstrukturalne (różowe strzałki); (F) — obraz dermoskopowy CRD ujawnia naczynia linijne (pomarańczowe strzałki) o nieswoistym rozmieszczeniu, brązowe kropki i ciałka (czerwone strzałki) oraz białe linie (białe strzałki); (G) — obraz dermoskopowy CRD ujawnia białą łuskę o niejednolitym rozmieszczeniu (żółte strzałki) i białe linie (białe strzałki); (H) — obraz

dermoskopowy CRD ujawnia kropkowane naczynia (czarne strzałki) o rozmieszczeniu skupionym i białe obszary bezstrukturalne (różowe strzałki).

4. Wstęp:

Nowotwory głowy i szyi (*ang. head and neck - HNC*) to grupa, do której zgodnie z definicją Amerykańskiego Wspólnego Komitetu ds. Raka z 2017 r. (*ang. American Joint Committee on Cancer - AJCC*) zalicza się nowotwory złośliwe wywodzące się z błony śluzowej jamy ustnej, gardła, krtani, zatok przynosowych oraz dużych i małych gruczołów ślinowych [1]. Najczęstszym typem histologicznym nowotworu w tym obszarze jest rak płaskonabłonkowy [2]. Według najnowszych szacunków globalnych statystyk dotyczących raka (*ang. Global Cancer Statistics - GLOBOCAN*), rak płaskonabłonkowy głowy i szyi (*ang. head and neck squamous cell carcinoma - HNSCC*) jest siódmym pod względem częstości występowania nowotworem na świecie i odpowiada za około 890 000 nowych przypadków i 450 000 zgonów rocznie [3]. Na podstawie Krajowego Rejestru Nowotworów w Polsce odnotowujemy ok. 5500 do 6000 nowych zachorowań na HNC rocznie, a ich odsetkowy udział wśród wszystkich nowotworów złośliwych waha się od 5,5 do 6,2% [4].

Diagnoza zwykle jest stawiana na etapie choroby o zaawansowaniu miejscowym i wymaga wielokierunkowego leczenia. Obecne metody terapii łączą chirurgię, chemioterapię (*ang. chemotherapy, CHT*), radioterapię (*ang. radiotherapy, RT*), immunoterapię i terapie celowane [5]. Na dzień dzisiejszy stosuje się liczne zaawansowane techniki RT, takie jak modulacja intensywności wiązki napromieniania (*ang.intensity modulated radiation therapy, IMRT*), w której wykorzystuje się sterowane komputerowo akceleratory liniowe w celu dostarczania precyzyjnych dawek promieniowania do nowotworu złośliwego, minimalizując dawkę podawaną zdrowym sąsiadującym tkankom. Technika ta poprawia w ten sposób wskaźnik terapeutyczny i równocześnie zmniejsza ryzyko ostrej i przewlekłej toksyczności [6].

Pomimo tego RT może powodować uszkodzenie zdrowych tkanek znajdujących się w obszarze napromieniania. Zmiany pojawiające się po RT możemy podzielić na toksyczność ostrą, gdy pojawia się w ciągu 90 dni od rozpoczęcia leczenia lub toksyczność późną, gdy

pojawia się po 90 dniach napromieniania [7]. Do ostrych zmian mogących wystąpić u chorych po radioterapii nowotworu głowy i szyi zaliczamy: zapalenie błony śluzowej jamy ustnej i gardła, odynofagię, dysfagię, chrypkę, kserostomię, ból w obrębie jamy ustnej i twarzy, popromienną martwicę krtani, zapalenie skóry, wypadanie włosów, nudności, wymioty, niewłaściwe odżywianie i nawodnienie oraz utratę masy ciała [8]. Z kolei toksyczność późna obejmuje: trwałą utratę śliny, martwicę popromienną kości, zapalenie mięśni wywołane promieniowaniem, zwężenie gardła i przełyku, próchnicę zębów, martwicę jamy ustnej, zwłóknienie, zaburzenia gojenia się ran, zapalenie skóry i nowotwory skóry, obrzęk limfatyczny, niedoczynność tarczycy, nadczynność przytarczyc, zawroty i bóle głowy, wtórne nowotwory oraz uszkodzenia gałki ocznej, uszu, struktur neurologicznych i szyi [9].

Ostre popromienne zapalenie skóry (*ang. acute radiation-induced dermatitis, ARD*) może wystąpić w ciągu pierwszych 24 godzin od rozpoczęcia RT, ale zwykle pojawia się w ciągu kilku dni lub nawet tygodni od rozpoczęcia RT [10]. Z kolei przewlekłe popromienne zapalenie skóry (*ang. chronic radiation-induced dermatitis, CRD*) pojawia się zwykle kilka miesięcy po RT [11].

Ocena kliniczna popromiennego zapalenia skóry nie jest wystandaryzowana i opisano wiele skal klinicznych. Do najczęściej stosowanych zaliczamy: Kryteria Toksyczności Grupy Radioterapii Onkologicznej i Europejskiej Organizacji Badań i Leczenia Raka *(ang. Radiation Therapy Oncology Group and the European Organization for Research and Treatment of Cancer, RTOG/EORTC*) [12], Wspólne Kryteria Terminologiczne dotyczące zdarzeń niepożądanych (*ang. Common Terminology Criteria for Adverse Events, CTCAE v. 5.0*) [13], Efekty późne – subiektywna skala Grupy Zadaniowej ds. Tkanek oraz skala Analityczna, Celu i Postępowania (*ang. the Late Effects Normal Tissue Task Force-Subjective scale, and the Objective, Management, Analytic scale, LENT SOMA*) [14,15]. Według klasyfikacji RTOG/EORTC [12], w ARD możemy obserwować rumień, utratę włosów, suche lub wilgotne złuszczanie, obrzęk, zmniejszoną potliwość oraz owrzodzenia i martwicę krwotoczną [12]. Typowymi objawami

skórnymi CRD są teleangiektazje, przebarwienia, zanik skóry, zgrubienie, a także zwłóknienie skóry [16].

Dermoskopia jest uznaną metodą diagnostyczną stanowiącą pomost między badaniem klinicznym i histopatologicznym [17]. W aktualnym piśmiennictwie znaleziono tylko jedno opublikowane badanie dotyczące dermoskopowego obrazowania rumienia w przebiegu ARD [18]. Do czasu opublikowania wyników moich prac nie opisywano w literaturze danych dotyczących analizy cech dermoskopowych w ARD i CRD. Innowacyjne zastosowanie dermoskopii w ARD i CRD może pozwolić na standaryzację oceny klinicznej popromiennego zapalenia skóry. Charakterystyka dermoskopowa z archiwizacją uzyskanych obrazów (fotografii) poszerzyła dotychczasową wiedzę na temat biologii ostrego i przewlekłego popromiennego zapalenia skóry. Do tej pory nie było innego obiektywnego narzędzia do analizy ARD i CRD. Wykazane w moich badaniach cechy dermoskopowe odzwierciedlają biologiczną reakcję skóry na promieniowanie i mogą w przyszłości zostać wykorzystane do parametryzacji ARD i CRD pod kątem intensywności i innych konsekwencji klinicznych.

5. Cele pracy:

1) Analiza aktualnego stanu wiedzy na temat ostrego i popromiennego zapalenia skóry wywołanego leczeniem metodą radioterapii.
2) Analiza przydatności dermoskopii jako metody badawczej w onkologii.
3) Określenie czy istnieją charakterystyczne cechy dermoskopowe w ostrym i przewlekłym popromiennym zapaleniu skóry u chorych poddawanych radioterapii?
4) Ocena, czy istnieje zależność między cechami dermoskopowymi w ostrym i przewlekłym popromiennym zapaleniu skóry a cechami makroskopowymi charakterystycznymi dla tych toksyczności.
5) Ustalenie przydatności badania dermoskopowego w diagnostyce ostrego i przewlekłego popromiennego zapalenia skóry.
6) Ustalenie związku pomiędzy cechami makroskopowymi i dermoskopowymi w ostrym i przewlekłym popromiennym zapaleniu skóry, a demograficznymi i klinicznymi czynnikami ryzyka.

6. Materiał i metody:

A) Materiał i metody w pracach oryginalnych (A, B)

6.1 Grupa badana

W badaniu o charakterze prospektywnym, nierandomizowanym przeprowadzono ocenę dermoskopową wraz z oceną kliniczną, u 26 chorych obserwowanych w kierunku ARD, którzy zostali poddani RT z powodu HNC w I Klinice Radioterapii i Chemioterapii w Narodowym Instytucie Onkologii im. Marii Skłodowskiej-Curie, Państwowego Instytutu Badawczego w Oddziale w Gliwicach w okresie od września 2020 r. do marca 2021 r.

W drugim badaniu prospektywnym, nierandomizowanym, przeprowadzono ocenę kliniczną i dermoskopową u 32 chorych obserwowanych w kierunku CRD, którzy zostali poddani RT z powodu HNC w I Klinice Radioterapii i Chemioterapii w Narodowym Instytucie Onkologii im. Marii Skłodowskiej-Curie, Państwowego Instytutu Badawczego w Oddziale w Gliwicach, a następnie pozostawali pod opieką Przyklinicznej Poradni Onkologicznej w okresie od września 2020 r. do marca 2021 r.

Zarówno w pierwszym jak i drugim badaniu kryteriami włączenia były wiek > 18 lat, intencja radykalnego leczenie i podpisana świadoma zgoda na udział w badaniu. Z badania wyłączono chorych leczonych lekami biologicznymi (*bio radiodermitis*) oraz z aktywnymi dermatozami mogącymi wpływać na obraz kliniczny i dermoskopowy badanego obszaru skóry.

6.2 Leczenie

Mediana całkowitej dawki RT wynosiła 70 Gy (50–72 Gy) i była podawana w 25–40 frakcjach. Radioterapię prowadzono przez 7 tygodni, włączając pięć frakcji na tydzień w połączeniu z CHT (cisplatyna, 100 mg/m^2 dni (d) 1, 22, 43) lub jako jednoczasowy boost (*ang. contominant boost, CB*) z siedmioma frakcjami na tydzień bez CHT. Pierwsza kliniczna objętość

tarczowa (*ang. clinical target volume, CTV1*) obejmowała guz pierwotny i zajęte grupy węzłów chłonnych z marginesem. Druga kliniczna objętość tarczowa (*ang. clinical target volume, CTV2*) obejmowała CTV1 i obszary narażone na ryzyko mikroskopowego rozprzestrzeniania się guza pierwotnego i grup wybranych węzłów chłonnych. Wszyscy chorzy byli leczeni dawkami 70 Gy w 35 frakcjach (2,0 Gy/frakcję) przez 7 tygodni lub 70,2 Gy w 39 frakcjach (1,8 Gy/frakcję) przez pięć i pół tygodnia, aż do osiągnięcia pierwotnego celu. Obszary napromieniano elektywnie, objęto dawkę 50 Gy w 25 frakcjach (2,0 Gy/frakcję) lub 54 Gy w 30 frakcjach (1,8 Gy/frakcję). Chemioterapia indukcyjna składała się z dwóch do trzech cykli TPF (docetaksel 75 mg/m^2, cisplatyna 75 mg/m^2, d1 i 5-fluorouracyl 750 mg/m^2 d1–5) lub PF (cisplatyna 100 mg/m^2, d1 i 5-fluorouracyl 1000 mg/m^2 d1–5) podawanych co 21 dni.

6.3 Ocena kliniczna i dermoskopowa:

W badaniu dotyczącym ARD chorzy byli oceniani klinicznie i dermoskopowo średnio w 15 punktach czasowych – na początku badania (przed RT), następnie co drugi dzień aż do końca hospitalizacji: w 1, 2, 4, 6, 8, 10 itd. W całym okresie u wszystkich chorych wykonano 374 obserwacje. Podczas każdej obserwacji wykonano cztery zdjęcia dermoskopowe obszaru napromienianego oraz dwa zdjęcia obszaru kontrolnego. W sumie zarchiwizowano 2244 obrazów (fotografii) dermoskopowych i 374 obrazów (fotografii) klinicznych. Spośród nich 1496 obrazów (fotografii) przedstawiało badane obszary narażone na napromienianie.

Chorzy włączeni do badania CRD byli oceniani w trakcie kontrolnych wizyt w Przyszpitalnej Poradni Onkologicznej w 3, 6 lub 12 miesiącu po RT. Zarchiwizowano łącznie 216 obrazów (fotografii) dermoskopowych i 36 obrazów (fotografii) klinicznych. Spośród nich 144 obrazy (fotografie) przedstawiały obszary poddane działaniu RT. Przewlekłe zapalenie skóry wywołane promieniowaniem oceniano w jednym punkcie czasowym i w dwóch punktach czasowych odpowiednio u 28 i 4 chorych. Łącznie wykonano 36 obserwacji u 32 chorych. W 3

miesiącu po RT obserwowano 16 chorych (96 obrazów dermoskopowych), 10 chorych (60 obrazów dermoskopowych) obserwowano w 6 miesiącu po RT i 10 chorych (60 obrazów dermoskopowych) obserwowano w 12 miesiącu po RT.

W każdym badaniu chorzy byli obserwowani i oceniani w tych samych symetrycznych czterech obszarach (prawa i lewa okolica szyjna, prawa i lewa okolica podżuchwowa) narażonych na promieniowanie jonizujące oraz w dwóch obszarach kontrolnych (prawa i lewa dolna część okolicy zausznej).

Wyniki badania dermoskopowego opisano zgodnie z konsensusem Międzynarodowego Towarzystwa Dermoskopowego (*ang. International Dermoscopy Society, IDS*) [19].

Dermoskopową ocenę oraz archiwizację obrazów przeprowadzałam osobiście przy użyciu dermoskopu DermLiteFoto (3Gen, LLC, San Juan Capistrano, Kalifornia, Stany Zjednoczone) w świetle spolaryzowanym, w dziesięciokrotnym powiększeniu. Zarchiwizowane obrazy (fotografie) dermoskopowe i kliniczne zostały następnie niezależnie przeanalizowane i opisane przez dwóch dermoskopistów (A.P. i A.S.-S.), nie znających żadnych danych chorych. W przypadku rozbieżności pomiędzy nimi ostateczną decyzję co do opisu podejmował trzeci dermoskopista (G.K.-W.).

Ocenę kliniczną przeprowadzono według skali RTOG/EORTC [12]. W ocenie klinicznej określano obecność rumienia, utraty włosów, suchego i wilgotnego złuszczania, obrzęku, owrzodzeń, krwotoków, martwicy, teleangiektazji, zmiany pigmentacji, zaniku skóry oraz zgrubienia i zwłóknienie skóry.

W ocenie dermoskopowej sprawdzano obecność i opisywano morfologię i rozmieszczenie naczyń, kolor i rozmieszczenie łuski, zmiany mieszkowe (czopy mieszkowe, czerwone kropki mieszkowe, białe zabarwienie okołomieszkowe, pigmentacja okołomieszkowa), kolor i morfologię innych struktur oraz sprawdzano czy istnieją określone wskazówki sugerujące konkretne rozpoznanie.

6.4 Analiza statystyczna:

W końcowej ocenie statystycznej przeanalizowano bazę danych sporządzoną na podstawie zarchiwizowanych oraz opisanych 2244 obrazów dermoskopowych i 374 obrazów klinicznych dotyczących ARD i 216 obrazów dermoskopowych i 36 obrazów klinicznych dotyczących CRD.

Stopień zgodności pomiędzy dwoma niezależnymi badaczami oraz stopień zgodności pomiędzy cechami klinicznymi a cechami dermoskopowymi oceniano za pomocą współczynnika rzetelności Kappa Cohena (κ).

Ponadto do oceny wpływu frakcji RT na binarne wyniki diagnostyki skóry zastosowano jednoczynnikową i wieloczynnikową regresję logistyczną binarną.

Do oszacowania wpływu zebranych czynników ryzyka na obserwowane cechy dermoskopowe wykorzystano wieloczynnikową regresję logistyczną porządkową. Wyniki statystyczne wyrażono za pomocą klasycznego ilorazu szans (*ang. odds ratio, OR*) z 95% przedziałem ufności (*ang. confidence interval, CI*); Wartość testową $p < 0,05$ uznano za przesłankę zależności istotnej statystycznie. Ze względu na powtarzane pomiary z kolejnymi frakcjami RT dla każdego chorego, w zastosowanych regresjach uwzględniono tzw. efekty losowe.

6.5 Zgoda Komisji Bioetycznej

Badania zostały zaaprobowane przez Komisję Bioetyczną Narodowego Instytutu Onkologii im. Marii Skłodowskiej-Curie Państwowego Instytutu Badawczego w Gliwicach w dniu 02.04.2019 (sygn. KB/430-44/19). Badania przeprowadzono zgodnie z Deklaracją Helsińską z 1964 r. i jej późniejszymi zmianami. Wszyscy chorzy wyrazili świadomą pisemną zgodę na udział w badaniu i publikację.

B) Metodyka w pracach poglądowych (C,D)

Publikacje poglądowe oparto na informacjach opublikowanych w artykułach polskojęzycznych i anglojęzycznych uzyskanych z elektronicznej bazy PubMed i Google Scholar opublikowanych w latach 1982 - 2020.

7. Wyniki:

PUBLIKACJA A

U wszystkich chorych (26) obserwowanych w trakcie RT rozwinęło się ARD. U 14 chorych pod koniec leczenia RT stwierdzono ARD w 2 stopniu toksyczności, u 10 chorych w 3 stopniu, a u dwóch chorych rozwinęła się ARD w stopniu 4 wg RTOG/EORTC [12]. Stopień 1 obserwowano w pierwszym tygodniu (4,69 dniu) (Ryc.1A), stopień 2 w trzecim tygodniu obserwacji (20,69 dzień) (Ryc.1C), stopień 3 w 6. tygodniu obserwacji (37,81 dzień) (Ryc.1E) i stopień 4 w 5. tygodniu obserwacji (34,66 dzień) (Ryc.1G).

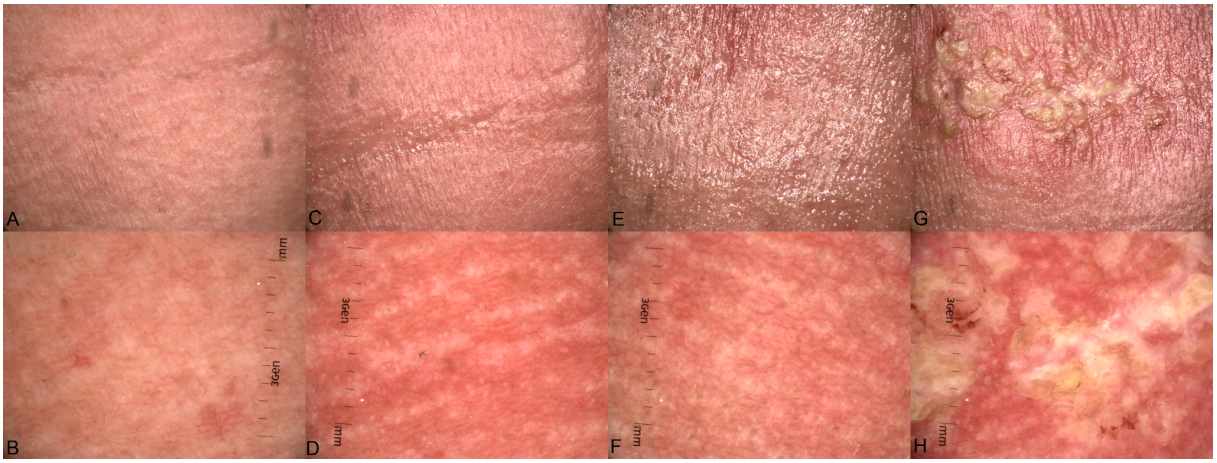

Rycina 1. Obrazy makroskopowe (A,C,E,G) ARD w stopniach (G) od G1 do G4, oceniane klinicznie zgodnie z kryteriami RTOG [12] i obrazy dermoskopowe (B,D,F,H) opisane zgodnie z konsensusem IDS [19] u wybranego chorego w trakcie leczenia RT. (A) Słaby rumień (G1); (B) obraz dermoskopowy (G1) ARD przestawia naczynia linijne z rozgałęzieniami i linijne, zakrzywione naczynia o skupionym rozmieszczeniu i białe obszary bezstrukturalne; (C) obraz makroskopowy przedstawia jasny rumień, utratę włosów, wilgotne złuszczanie i umiarkowany obrzęk (G2); (D) obraz dermoskopowy ARD (G2) przedstawia naczynia linijne z rozgałęzieniami i linijne, zakrzywione naczynia o siateczkowym rozmieszczeniu oraz czopy mieszkowe o układzie rozet; (E) obraz makroskopowy przedstawia jasny rumień, utratę włosów, zlewające się wilgotne złuszczanie i obrzęk wżerowy (G3); (F) obraz dermoskopowy przedstawia (G3) naczynia linijne z rozgałęzieniami o rozmieszczeniu siateczkowym, pigmentacją okołomieszkową i czopy mieszkowe o układzie rozet; (G) owrzodzenie w ARD (G4); (H) obraz dermoskopowy (G4) uwidacznia naczynia linijne z rozgałęzieniami o rozmieszczeniu siateczkowym oraz białą i żółtą łuskę o niejednolitym rozmieszczeniu.

W każdym stopniu ARD obserwowano polimorficzne naczynia. Rozmieszczenie naczyń było niejednorodne i nie było typowego układu dla konkretnego stopnia ARD. W zdrowej skórze nie stwierdziłam naczyń o rozmieszczeniu siateczkowym, ale ich obecność wykryto w każdym stopniu ARD. Nieswoiste rozmieszczenie występowało częściej w zdrowej skórze niż

w ARD. W każdym stopniu ARD zaobserwowano niejednolicie rozmieszczoną łuskę, a częstotliwość jej występowania wzrastała wraz ze stopniem rozwoju według RTOG [12]. Ponadto cechą występującą we wszystkich stopniach, ale nie obserwowaną w zdrowej skórze, były czopy mieszkowe o układzie rozet.

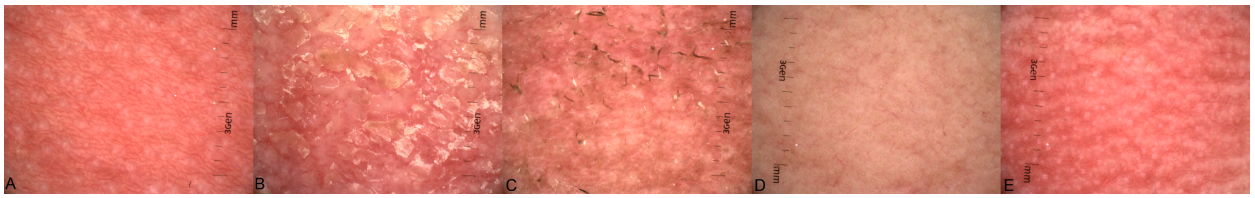

Rycina 2. Obrazy dermoskopowe ARD opisane zgodnie z konsensusem IDS [19] (A) Obraz dermoskopowy ARD przedstawia naczynia linijne z rozgałęzieniami, linijne, zakrzywione naczynia o rozmieszczeniu siateczkowym oraz białe okołomieszkowe koloru; (B) obraz dermoskopowy ARD ujawnia biało-żółtą łuskę o niejednolitym rozmieszczeniu (C) obraz dermoskopowy ukazuje naczynia linijne z rozgałęzieniami i linijne, zakrzywione o rozmieszczeniu skupionym, oraz brązową łuskę o niejednolitym rozmieszczeniu; (D) obraz dermoskopowy ukazuje naczynia linijne z rozgałęzieniami i linijne, zakrzywione o nieswoistym rozmieszczeniu oraz pigmentację okołomieszkową; (E) naczynia linijne z rozgałęzieniami i linijne, zakrzywione o rozmieszczeniem siateczkowym oraz czopy mieszkowe o układzie rozet.

Zgodność cech dermoskopowych z klinicznymi wynosiła zgodnie z współczynnikiem Kappa Cohena (κ) 0,03–0,54.

W kolejnym etapie pracy analizowano związek cech dermoskopowych i makroskopowych oraz wpływu czasu, wieku, płci, chemioterapii indukcyjnej, chemioterapii towarzyszącej, całkowitej dawki promieniowania, dawki frakcyjnej, lokalizacji guza, a także rozpoznania histopatologicznego nowotworu złośliwego.

Każdy dzień obserwacji podczas leczenia RT generuje statystycznie większe prawdopodobieństwo wystąpienia naczyń o rozmieszczeniu siateczkowym ($p<0,0001$) (Ryc.1D,F,H;2A,E), białej ($p<0,0001$) (Ryc.1H;2B), żółtej ($p<0,0001$) (Ryc.1H;2B) i brązowej łuski ($p<0,0001$) (Ryc.2C) o niejednolitym rozmieszczeniu ($p<0,0001$) (Ryc.1H;2B,C), pigmentacji okołomieszkowej ($p<0,0001$) (Ryc.1F;2D), czopów mieszkowych o układzie rozet ($p<0,0001$) (Ryc.1D,F;2E), przy jednoczesnym zmniejszeniu prawdopodobieństwa na nieswoiste rozmieszczenie naczyń ($p<0,0001$) (Ryc.2E). W kontekście odpowiedzi makroskopowej, każdy dzień obserwacji podczas RT determinuje statystycznie większe ryzyko wystąpienia jasnego

rumienia (p<0,0001) (Ryc.1C,E), utraty włosów (p<0,0001) (Ryc.1C,E), suchego (p=0,0001) i wilgotnego złuszczania (p<0,0001) (Ryc.1C,E), umiarkowanego (p<0,0001) (Ryc.1C) i obrzęku wżerowego (p<0,0001) (Ryc.1E) oraz owrzodzenia (p=0,0012) (Ryc.1G), przy jednoczesnym zmniejszeniu ryzyka wystąpienia rumienia mieszkowego (p=0,0158) i słabo nasilonego rumienia (p<0,0001) (Ryc.1A). Wyniki dotyczące wpływu zebranych czynników ryzyka na reakcję skórną u w modelu wieloczynnikowym były porównywalne.

W analizie jednoczynnikowej wiek był istotnym czynnikiem ryzyka występowania naczyń o rozmieszczeniu siateczkowym (p=0,0031), naczyń o rozmieszczeniu nieswoistym (p=0,0157), czopów mieszkowych o układzie rozet (p=0,0053), pigmentacji okołomieszkowej (p=0,0194), a w grupie cech makroskopowych rumienia mieszkowego (p=0,0104). Analiza wieloczynnikowa nie wykazała jednak tej zależności w przypadku nieswoistego rozmieszczenia naczyń, czopów mieszkowych o układzie rozet. czy pigmentacji okołomieszkowej.

Płeć ma znaczenie dla występowania naczyń o rozmieszczeniu siateczkowym (p=0,0001), naczyń o nieswoistym rozmieszczeniu (p=0,0110), białej (p<0,0001) i żółtej łuski (p=0,0001) o niejednolitym rozmieszczeniu (p<0,0001), czopów mieszkowych o układzie rozet (p=0,0293), a w przypadku cech makroskopowych w przypadku nieznacznego (p=0,0212) i jasnego rumienia (p=0,0012) oraz suchego złuszczania (p=0,0084). Analiza wieloczynnikowa wykazała, że w każdym przypadku efekt płci był silniejszy.

Chemioterapia indukcyjna zwiększa ryzyko wystąpienia żółtej łuski (p=0,0095) i zmniejsza ryzyko występowania naczyń o rozmieszczeniu siateczkowym (p<0,0001). W modelu wieloczynnikowym zależności te rosną.

Jednoczasowa chemioterapia jest istotna dla występowania naczyń o rozmieszczeniu siateczkowym (p=0,0149), czopów mieszkowych o układzie rozet (p=0,0207), pigmentacji okołomieszkowej (p=0,0029) i cech makroskopowych, takich jak rumień mieszkowy (p=0,0290), delikatny rumień (p=0,0295) i wilgotne złuszczanie (p=0,0497). Z kolei analiza

wieloczynnikowa nie wykazała tej zależności w przypadku czopów mieszkowych o układzie rozet, rumienia mieszkowego i wilgotnego złuszczania. Brak jednoczesnej chemioterapii zmniejsza ryzyko naczyń w rozmieszczeniu siateczkowym (p=0,0149) i pigmentacji okołomieszkowej (p=0,0029).

PUBLIKACJA B

U wszystkich chorych (32) obserwowanych po zakończeniu radioterapii rozwinął się CRD. U 21 chorych stwierdzono 2 stopień toksyczności, u pozostałych chorych rozwinęła się CRD w stopniu 1 wg RTOG/EORTC. W trzecim miesiącu obserwacji u dziesięciu chorych rozwinął się CRD w stopniu 2, a u pozostałych sześciu CRD w stopniu 1. W 6. miesiącu obserwacji u pięciu chorych wystąpił CRD w stopniu 2, a u pozostałych dwóch – w stopniu 1. W 12. miesiącu obserwacji u sześciu chorych pojawił się CRD w stopniu 2., a u pozostałych trzech – w stopniu 1. U dwóch chorych wystąpiła zmiana stopnia reakcji, u jednego chorego z 1 do 2, a u drugiego z 2 do 1, odpowiednio po 3 i 6 miesiącach obserwacji. Typowe cechy kliniczne i dermoskopowe CRD przedstawiono na rycinie 3 ABCD.

Naczynia w każdym stopniu CRD były polimorficzne, podobnie jak w zdrowej skórze. Na uwagę zasługuje znacznie zwiększony udział naczyń kropkowanych (Ryc.3D;4A,B,E,H), które – w skórze zdrowej – stwierdzono w 18,75% obserwacji, natomiast w obszarach poddanych RT częstość występowania wzrosła do 82,6–84,6 %. Rozmieszczenie naczyń było niejednorodne. W skórze zdrowej nie zaobserwowałam łuski w kolorze żółtym i brązowym, jednak jej obecność stwierdziłam w każdym stopniu CRD. Ponadto odsetek białej łuski (Ryc.4C,D,G) w porównaniu ze skórą zdrową (15,63%) wzrósł do 53,9% w stopniu 1 CRD i do 52,2% w stopniu 2. Wraz ze wzrostem stopnia CRD wzrasta częstość występowania białych obszarów bezstrukturalnych (Ryc.4E,H), brązowych kropek i globuli (Ryc.3B,D;4C,F) oraz białych linii (Ryc.3B,D;4D,F,G).

Zgodność cech dermoskopowych z klinicznymi zgodnie z współczynnikiem Kappa Cohena (κ) wynosiła 0,226–0,423.

W kolejnym etapie pracy analizowałam związek cech dermoskopowych i makroskopowych oraz wpływu czasu, wieku, płci, chemioterapii w tym indukcyjnej, całkowitej dawki promieniowania, dawki frakcyjnej, lokalizacji, a także rozpoznania histopatologicznego guza.

W analizie jednoczynnikowej wiek był istotnym czynnikiem wpływającym na obecność łuski o niejednolitym rozmieszczeniu (p=0,0264) (Ryc.4C,D,G), pigmentacji okołomieszkowej (P=0,0243) (Ryc.4A) i białych obszarów bezstrukturalnych (P=0,0105) (Ryc.4E,H).

Płeć ma znaczenie dla występowania naczyń linijnych (p=0,0400) (Ryc.3B;4A,F) i zmiany pigmentacji (p=0,0098) (Ryc.3A).

Operacja w wywiadzie zwiększa ryzyko wystąpienia łuski białej (p=0,0402) (Ryc. 4C,D,G).

Zwiększanie liczby frakcji i dawki całkowitej zwiększa ryzyko wystąpienia białych obszarów bezstrukturalnych (Ryc.4E,H), brązowych kropek i globuli (Ryc.3B,D;4C,F), zmiany pigmentacji (Ryc.3A), a także częściowej i całkowitej utraty włosów (Ryc.3C). Liczba frakcji i dawka całkowita są również powiązane ze stopniem rozwoju według RTOG/EORTC.

W związku z tym, że chorych obserwowano w trzech różnych punktach czasowych, sprawdzono wpływ czasu na występowanie cech klinicznych i dermoskopowych.

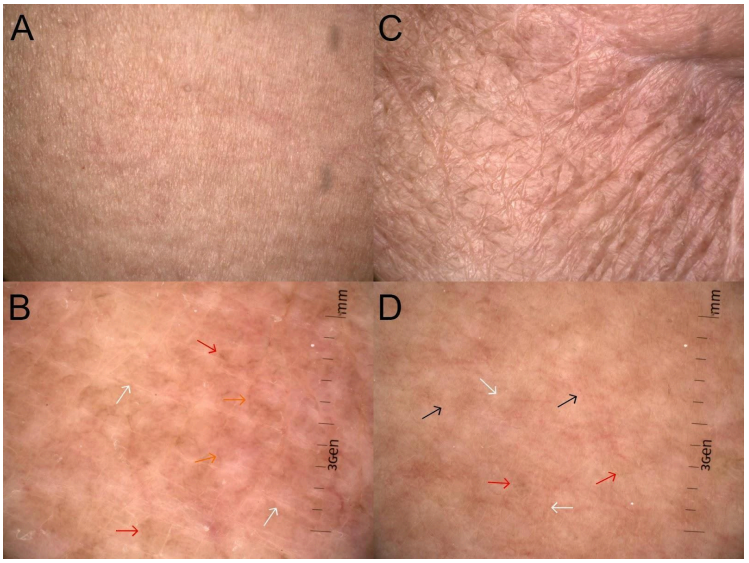

Rycina 3 Obrazy makroskopowe (A, C) CRD w stopniach (G) od G1 do G2, oceniane klinicznie według kryteriów RTOG [12] oraz obrazy dermoskopowe (B, D) opisane według IDS [19] u wybranego chorego. (A) – niewielki zanik, zmiana pigmentacji (G1); (B) — obraz dermoskopowy (G1) CRD ujawnia naczynia linijne (pomarańczowe strzałki) o niespecyficznym rozmieszczeniu, brązowe kropki i ciałka (czerwone strzałki) i białe linie (białe strzałki); (C) – plamisty zanik, całkowita utrata włosów (G2); (D) — obraz dermoskopowy CRD (G2) przedstawia naczynia kropkowane (czarne strzałki) o nieswoistym rozmieszczeniu, brązowe kropki i ciałka (czerwone strzałki) i białe linie (białe strzałki).

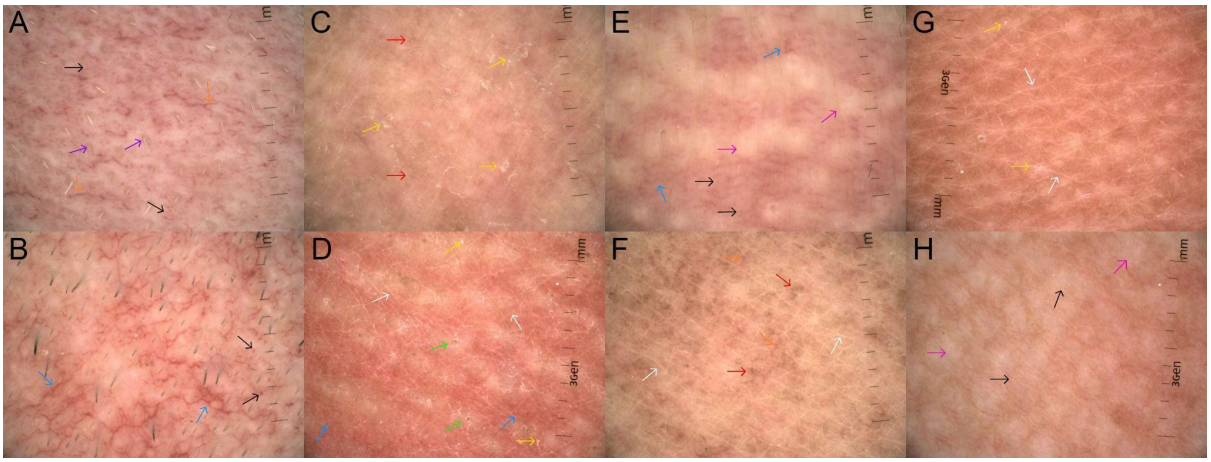

Rycina 4. Obrazy dermoskopowe CRD opisane zgodnie z konsensusem IDS [20]. (A) — w obrazie dermoskopowym CRD widoczne są naczynia kropkowane (czarne strzałki) i linijne (pomarańczowe strzałki) o nieswoistym rozmieszczeniu oraz pigmentacja okołomieszkowa (fioletowe strzałki); (B) — obraz dermoskopowy CRD ujawnia naczynia kropkowane (czarne strzałki) i linijne z rozgałęzieniami (niebieskie strzałki) o rozmieszczeniu skupionym; (C) — obraz dermoskopowy CRD ujawnia białą łuskę o niejednolitym rozmieszczeniu (żółte strzałki) oraz brązowe kropki i ciałka (czerwone strzałki); (D) — obraz dermoskopowy CRD ujawnia naczynia linijne z rozgałęzieniami, (niebieskie strzałki) o rozmieszczeniu siateczkowym, okołomieszkowe białe zabarwienie (zielone strzałki), białą łuskę o niejednolitym rozmieszczeniu (żółte strzałki), białe linie (białe strzałki); (E) — obraz dermoskopowy CRD ujawnia naczynia z rozgałęzieniami (niebieskie strzałki) i kropkowane naczynia (czarne strzałki) o rozmieszczeniu skupionym oraz białe obszary bezstrukturalne (różowe strzałki); (F) — obraz dermoskopowy CRD ujawnia naczynia linijne (pomarańczowe strzałki) o nieswoistym rozmieszczeniu, brązowe kropki i ciałka (czerwone strzałki) oraz białe linie (białe strzałki); (G) — obraz dermoskopowy CRD ujawnia białą łuskę o niejednolitym rozmieszczeniu (żółte strzałki) i białe linie (białe strzałki); (H) — obraz dermoskopowy CRD ujawnia kropkowane naczynia (czarne strzałki) o rozmieszczeniu skupionym i białe obszary bezstrukturalne (różowe strzałki).

Czas w miesiącach generuje statystycznie większe prawdopodobieństwo wystąpienia naczyń kropkowanych (p=0,0002) (Ryc.3A;4A,B,E,H), białej łuski (p=0,0068) (Ryc.4C,D,G), łuski o niejednolitym rozmieszczeniu (p=0,0011) (Ryc.4C,D,G), okołomieszkowego białego koloru (p=0,0047) (Ryc.4D), białych obszarów bezstrukturalnych (p<0,0001) (Ryc.4E,H), brązowych kropek i globuli (p <0,0001) (Ryc.3B,D;4C,F) i białych linii (p=0,0008) (Ryc.3B,D;4D,F,G).

PUBLIKACJA C

W pracy przeanalizowano aktualną wiedzę dotyczącą ARD i CRD. Mimo optymalnego leczenia w wyniku radioterapii nadal u prawie 90% chorych pojawiają się objawy skórne. Patogeneza nie jest do końca poznana i wciąż pozostaje wiele do wyjaśnienia. W chwili obecnej ARD i CRD rozpoznaje się zwykle na podstawie kryteriów klinicznych. Ocenę nasilenia toksyczności zarówno w przebiegu ARD i CRD umożliwia skala RTOG/EORTC.

PUBLIKACJA D

Dermoskopia jest nieinwazyjną metodą diagnostyczną stanowiącą pomost pomiędzy badaniem klinicznym a histopatologicznym. Znajduje zastosowanie w przedoperacyjnej i pooperacyjnej diagnostyce różnicowej zmian skórnych oraz w monitorowaniu chorych w trakcie i po zakończeniu leczenia onkologicznego, w związku z tym jest jest multidyscyplinarną metodą diagnostyczną z uwzględnieniem onkologii klinicznej.

8. Wnioski:

1) Na podstawie analizy aktualnego stanu wiedzy na temat ostrego i przewlekłego popromiennego zapalenia skóry wywołanego radioterapią stwierdzono, że mimo istnienia wielu doniesień na temat czynników, które mogą być zaangażowane w patogenezę ostrego i przewlekłego popromiennego zapalenia skóry nadal potrzebne są dalsze badania, aby potwierdzić i poznać rzeczywistą naturę tego procesu. Mimo, że ocena kliniczna przeprowadzana jest w oparciu o użyciu różne skale kliniczne, brak jednak jednolitego systemu oceny. Ponadto tylko w jednym badaniu stworzono system punktacji obejmujący czynniki dozymetryczne i kliniczne, aby ocenić ryzyko wystąpienia ciężkich, ostrych reakcji skórnych u pacjentów poddawanych radioterapii o modulowanej intensywności (IMRT) w leczeniu HNC.
2) Dermoskopia jest multidyscyplinarną metodą diagnostyczną z uwzględnieniem onkologii klinicznej. Znajdując zastosowanie w przedoperacyjnej i pooperacyjnej diagnostyce różnicowej zmian skórnych oraz w monitorowaniu chorych w trakcie i po zakończeniu leczenia onkologicznego.
3) Wyodrębniono charakterystyczne cechy dermoskopowe dla ostrego i przewlekłego popromiennego zapalenia skóry u chorych poddanych radioterapii.
    a) Do cech dermoskopowych w ostrym popromiennym zapaleniu skóry zaliczono naczynia o rozmieszczeniu siateczkowym, białą, żółtą i brązową łuskę o niejednolitym rozmieszczeniu, przebarwienia okołomieszkowe i czopy mieszkowe o układzie rozet.
    b) Do cech dermoskopowych w przewlekłym popromiennym zapaleniu skóry zaliczono: naczynia kropkowane, rozmieszczone w skupiskach, białą łuskę o niejednolitym rozmieszczeniu, białą barwę okołomieszkową, białe obszary bezstrukturalne, brązowe kropki i ciałka oraz białe linie.

4) Istnieją zależności między cechami dermoskopowymi w ostrym i przewlekłym popromiennym zapaleniu skóry z cechami makroskopowymi charakterystycznymi dla tych toksyczności.
5) Badanie dermoskopowe jest nowatorską metodą diagnostyczną w ocenie ostrego i przewlekłego popromiennego zapalenia skóry. Do tej pory nie wykorzystywano jej jako obiektywnego narzędzia do analizy ARD i CRD.
6) Ustalono związek pomiędzy cechami dermoskopowymi a demograficznymi i klinicznymi czynnikami ryzyka, do których należy:
    a) płeć oraz jednoczasowa chemioterapia w ostrym popromiennym zapaleniu skóry,
    b) wiek, płeć, operacja przed RT w przewlekłym popromiennym zapaleniu skóry.

9. Bibliografia:

1. Lydiatt WM, Patel SG, O'Sullivan B, Brandwein MS, Ridge JA, Migliacci JC, Loomis AM, Shah JP. Head and Neck cancers-major changes in the American Joint Committee on cancer eighth edition cancer staging manual. CA Cancer J Clin. 2017;67(2):122-137.
2. Curado MP, Hashibe M. Recent changes in the epidemiology of head and neck cancer. Curr Opin Oncol. 2009;21(3):194-200.
3. Bray F, Ferlay J, Soerjomataram I, Siegel RL, Torre LA, Jemal A. Global cancer statistics 2018: GLOBOCAN estimates of incidence and mortality worldwide for 36 cancers in 185 countries. CA Cancer J Clin. 2018;68(6):394-424.
4. https://onkologia.org.pl/pl/nowotwory-narzadow-glowy-i-szyi-czym-sa (16.09.2021).
5. Pandruvada S, Kessler R, Thai A. Head and neck cancer treatment in the era of molecular medicine. Adv Cancer Res. 2023;160:205-252.
6. Alfouzan AF. Radiation therapy in head and neck cancer. Saudi Med J. 2021;42(3):247-254.
7. Sroussi HY, Epstein JB, Bensadoun RJ, Saunders DP, Lalla RV, Migliorati CA, Heaivilin N, Zumsteg ZS. Common oral complications of head and neck cancer radiation therapy: mucositis, infections, saliva change, fibrosis, sensory dysfunctions, dental caries, periodontal disease, and osteoradionecrosis. Cancer Med. 2017;6(12):2918-2931.
8. Brook I. Early side effects of radiation treatment for head and neck cancer. Cancer Radiother. 2021;25(5):507-513.
9. Brook I. Late side effects of radiation treatment for head and neck cancer. Radiat Oncol J. 2020;38(2):84-92.
10. Hegedus F, Mathew LM, Schwartz RA. Radiation dermatitis: an overview. Int J Dermatol. 2017;56(9):909-914.

11. Robijns, J.; Laubach, H.J. Acute and chronic radiodermatitis. Journal of the Egyptian Women's Dermatologic Society. 2018,15(1):2–9.

12. Cox JD, Stetz J, Pajak TF. Toxicity criteria of the Radiation Therapy Oncology Group (RTOG) and the European Organization for Research and Treatment of Cancer (EORTC). Int J Radiat Oncol Biol Phys. 1995;31(5):1341-1346.

13. https://ctep.cancer.gov/protocolDevelopment/electronic_applications/ctc.htm#ctc_50

14. Routledge JA, Burns MP, Swindell R, Khoo VS, West CM, Davidson SE. Evaluation of the LENT-SOMA scales for the prospective assessment of treatment morbidity in cervical carcinoma. Int J Radiat Oncol Biol Phys. 2003;56(2):502-510.

15. Dudek A, Rutkowski T, Kamińska-Winciorek G, Krzysztof Składowski K. What is new when it comes to acute and chronic radiation-induced dermatitis in head and neck cancer patients? NOWOTWORY J Oncol 2020;70(1):9–15.

16. Wong RK, Bensadoun RJ, Boers-Doets CB, Bryce J, Chan A, Epstein JB, Eaby-Sandy B, Lacouture ME. Clinical practice guidelines for the prevention and treatment of acute and late radiation reactions from the MASCC Skin Toxicity Study Group. Support Care Cancer. 2013;21(10):2933-2948.

17. Kaminska-Winciorek G, Spiewak R. Tips and tricks in the dermoscopy of pigmented lesions. BMC Dermatol. 2012, 12, 14.

18. Kišonas J, Venius J, Grybauskas M, Dabkevičienė D, Burneckis A, Rotomskis R. Acute Radiation Dermatitis Evaluation with Reflectance Confocal Microscopy: A Prospective Study. Diagnostics. 2021;13;11(9):1670.

19. Errichetti E, Zalaudek I, Kittler H, Apalla Z, Argenziano G, Bakos R, Blum A, Braun RP, Ioannides D, Lacarrubba F, Lazaridou E, Longo C, Micali G, Moscarella E, Paoli J, Papageorgiou C, Russo T, Scope A, Stinco G, Thomas L, Toncic RJ, Tschandl P, Cabo H, Hallpern A, Hofmann-Wellenhof R, Malvehy J, Marghoob A, Menzies S, Pellacani G,

Puig S, Rabinovitz H, Rudnicka L, Vakirlis E, Soyer P, Stolz W, Tanaka M, Lallas A. Standardization of dermoscopic terminology and basic dermoscopic parameters to evaluate in general dermatology (non-neoplastic dermatoses): an expert consensus on behalf of the International Dermoscopy Society. Br J Dermatol. 2020;182(2):454-467.

10. Streszczenie w języku angielskim:

Introduction: We conducted two prospective studies, one on acute radiation dermatitis (ARD) and chronic radiation dermatitis (CRD), along with two review papers.

Aim of the study: The original studies examined whether there are characteristic dermoscopic features in ARD and CRD, and the relationship between dermoscopic and macroscopic features in ARD and CRD was evaluated. Additionally, the aim was to explore the association between macroscopic and dermoscopic features in ARD and CRD and demographic and clinical risk factors. The reviews analyzed the current knowledge about ARD and CRD and the usefulness of dermoscopy as a research method in oncology.

Materials and Methods: In the first prospective, non-randomized study, we conducted dermoscopic and clinical evaluations in 26 patients observed for ARD at an average of 15 time points, at the Inpatient Department of Radiation and Clinical Oncology, Maria Sklodowska Curie National Research Institute of Oncology (MSCNRIO), in Gliwice from September 2020 to March 2021. A total of 2244 dermoscopic images and 374 clinical images were archived. In the second prospective, non-randomized study, clinical and dermoscopic evaluations were performed on 32 patients observed for CRD at 3, 6, or 12 months following radiotherapy treatment at the MSCNRIO. A total of 216 dermoscopic images and 36 clinical images were archived. In both studies, the control area consisted of skin areas from the same patient not exposed to radiotherapy, and the dermoscopic images were assessed by two independent dermoscopists. Dermoscopic assessment of ARD and CRD was based on the diagnostic criteria in the current literature. Clinical assessment of ARD and CRD was graded according to RTOG/EORTC.

The review publications were based on information published in Polish and English-language articles from the PubMed electronic database and Google Scholar.

Results: Dermoscopic features of ARD included: vessels in reticular distribution, white, yellow, or brown scale in a patchy distribution, perifollicular pigmentation, and follicular plugs arranged

in rosettes. Two independent risk factors for acute toxicity were identified: gender and concurrent chemotherapy.

Dermoscopic features in CRD included: dotted vessels, clustered vessel distribution, white patchy scale, perifollicular white color, white structureless areas, brown dots and globules, and white lines. Three independent risk factors of chronic toxicity, such as age, gender, and surgery before radiotherapy were identified.

The current literature contains only one published study on dermoscopic imaging of erythema in ARD. Dermoscopy is a useful diagnostic method with a well-established position in oncology diagnosis.

Conclusions: These are the first studies showing the potential role of dermoscopy in the assessment of ARD and CRD. Until now there was no other objective tool for qualitative analyses of ARD and CRD. The dermoscopic features that had been shown in our study reflect the biological reaction of the skin toward radiation and may be used for the parametrization of ARD and CRD regarding its intensity and any other clinical consequences in the future.

11. Słowa kluczowe w języku angielskim: head and neck cancers, acute radiation-induced dermatitis, chronic radiation-induced dermatitis, dermoscopy, dermatoscopy, RTOG/EORTC, side effects.

scientific reports

Check for updates

OPEN

Dermoscopy of acute radiation-induced dermatitis in patients with head and neck cancers treated with radiotherapy

Aleksandra Pilśniak[1], Anastazja Szlauer-Stefańska[2], Andrzej Tukiendorf[3], Tomasz Rutkowski[4], Krzysztof Składowski[4] & Grażyna Kamińska-Winciorek[5]✉

Head and neck cancer (HNC) was the seventh most common cancer in the world in 2018. Treatment of a patient may include surgery, radiotherapy (RT), chemotherapy, targeted therapy, immunotherapy, or a combination of these methods. Ionizing radiation used during RT covers relatively large volumes of healthy tissue surrounding the tumor. The acute form of radiation-induced dermatitis (ARD) are skin lesions that appear usually within 90 days of the start of RT. This is a prospective study which compares 2244 dermoscopy images and 374 clinical photographs of irradiated skin and healthy skin of 26 patients at on average 15 time points. Dermoscopy pictures were evaluated independently by 2 blinded physicians. Vessels in reticular distribution, white, yellow or brown scale in a patchy distribution, perifollicular pigmentation and follicular plugs arranged in rosettes were most often observed. For these dermoscopic features, agreement with macroscopic features was observed. Two independent predictors of severe acute toxicity were identified: gender and concurrent chemotherapy. Knowledge of dermoscopic features could help in the early assessment of acute toxicity and the immediate implementation of appropriate therapeutic strategies. This may increase the tolerance of RT in these groups of patients.

Abbreviations

HNC	Head and neck cancer
RT	Radiotherapy
ARD	Acute radiation-induced dermatitis
AJCC	American Joint Committee on Cancer
CTV1	Clinical target volume 1
PTV1	Planned target volume 1
RTOG/EORTC	Radiation Therapy Oncology Group and the European Organization for Research and Treatment of Cancer
CTCAE	Common Terminology Criteria for Adverse Events
LENT SOMA	Late Effects Normal Tissue Task Force-Subjective scale, and the Objective, Management, Analytic scale
indCHT	Induction chemotherapy
CHRT	Radiochemotherapy
IDS	International Dermoscopy Society
OR	Odds ratio
CI	Confidence interval
PBMT	Photobiomodulation therapy

[1]Department of Internal Medicine, Autoimmune and Metabolic Diseases, Faculty of Medical Sciences in Katowice, Medical University of Silesia, Katowice, Poland. [2]Department of Bone Marrow Transplantation and Onco-Hematology, Maria Sklodowska-Curie National Research Institute of Oncology (MSCNRIO), Gliwice, Poland. [3]Institute of Health Sciences, Opole University, Opole, Poland. [4]Inpatient Department of Radiation and Clinical Oncology, Maria Sklodowska Curie National Research Institute of Oncology (MSCNRIO), Gliwice, Poland. [5]Department of Bone Marrow Transplantation and Onco-Hematology, Skin Cancer and Melanoma Team, Maria Sklodowska-Curie National Research Institute of Oncology (MSCNRIO), Wybrzeże Armii Krajowej 15, 44-101 Gliwice, Poland. ✉email: dermatolog.pl@gmail.com

Head and neck cancer (HNC) is one of the most common cancers and continues to be a significant challenge in clinical practice[1]. Each year, around 800 thousand patients worldwide develop HNC, and approximately half of them die from the disease[1]. Head and neck cancers are more than twice as common in men than in women[2]. According to the definition of the American Joint Committee on Cancer (AJCC), this group of neoplasms includes those originating from the mucosa of the oral cavity, pharynx, larynx, paranasal sinuses, or major and minor salivary glands[3]. The most common histological type of neoplasm in this area is squamous cell carcinoma[4]. Treatment is multimodal and depends on many tumor and patient-related factors and usually includes surgery, radiotherapy (RT), and chemotherapy which are often combined [5]. The prognosis depends mainly on the stage of the disease. Despite aggressive multimodal treatment strategies, poor results are still observed. The 5-year survival is only 40–50%[6]. Ionizing radiation used during RT covers relatively large volumes of healthy tissue surrounding the tumor because irradiated volume extends beyond gross tumor volume to clinical tumor volume 1 (CTV1) covering the potential microscopic spread of the tumor and to planned target volume 1 (PTV1) that cover margin dedicated to technical aspects of radiotherapy. A typical therapeutic dose is usually from the range of 66–74 Gy in fractions of 2.0 Gy or even higher doses (e.g. 81.6 Gy in fractions of 1.2 Gy)[7]. To improve local control and reduce the toxic effect, fractionation approaches can be divided into hyperfractionation and accelerated fractionation[8]. Early skin reactions to RT can occur within the first 24 h of starting RT but usually begin within a few days or even weeks from the beginning of RT. The acute form of radiation-induced dermatitis is skin lesions that appear within 90 days of RT begining[9]. Acute radiation-dermatitis (ARD) is responsible for discomfort, pain, aesthetic changes, and may reduce patient's quality of life. Intense ARD may even cause the need to reduce the RT dose or stop RT for some time to heal the mucosal or skin reaction. Both situations increase the risk of treatment failure[10–12]. Clinical evaluation of radiation-induced dermatitis is not standardized, and multiple clinical scales have been described. The most frequently used are the scale of the Radiation Therapy Oncology Group and the European Organization for Research and Treatment of Cancer (RTOG/EORTC)[13], Common Terminology Criteria for Adverse Events (CTCAE) v. 5.0[14], the Late Effects Normal Tissue Task Force-Subjective scale, and the Objective, Management, Analytic scale (LENT SOMA)[15,16]. According to the RTOG/EORTC classification[13], in grade I, we can observe follicular, faint, or dull erythema, epilation, dry desquamation, and decreased sweating. Grade II occurs when the following features are observed: tender or bright erythema, patchy moist desquamation, and moderate edema. In grade III of ARD, there is confluent, moist desquamation other than skin fold and pitting edema may occur. In grade IV, the presence of ulceration, and hemorrhage necrosis is stigmatized. Grade V is known as death[13]. Dermoscopy is a recognized diagnostic method combining clinical and pathological examination. There is no data concerning the evaluation of dermoscopic features of ARD in current literature. The innovative application of dermoscopy in the assessment of ARD may allow the standardization of its clinical evaluation. Consequently, a proper assessment of the severity of ARD skin damage will make it possible to decide how to manage the patients who undergo RT due to HNC.

Materials and methods

This study aimed to assess dermoscopic features of ARD among patients with HNC qualified for RT, with a subsequent analysis of clinical and dermoscopic patterns of the treated and control areas, based on obtained macroscopic and dermoscopic photographs of ARD for further comparison.

Patients

The study group consisted of 26 patients who underwent RT due to HNC (24 squamous cell carcinomas, one lymphoepithelial carcinoma, and one undifferentiated nasopharyngeal carcinoma) at the Maria Skłodowska-Curie National Research Institute of Oncology, Gliwice Branch, between September 2020 and March 2021.The inclusion criteria were age > 18 years, radical treatment signed consent. Patients treated with biological drugs (bio radiodermatitis), and with active dermatoses that could affect the clinical and dermoscopic picture of the examined skin area under observation were excluded from the study. Details of the patients' clinical and histopathological characteristics, the location of the tumor, are shown in Table 1. The control group consisted of skin regions not exposed to ionizing irradiation from the same patients (748 images).

Treatment

In seven cases, induction chemotherapy (indCHT) prior to radiochemotherapy (CHRT) was given; CHRT and RT alone was applied in 12 and four patients, respectively. The median total RT dose was 70 Gy (50–72 Gy) given in 25–40 daily fractions. Radiotherapy was delivered for over 7 weeks by incorporating five fractions per week combined with chemotherapy (CHT) (cisplatin, 100 mg/m^2 days (d) 1, 22, 43) or as a concomitant boost (CB) with seven fractions per week without CHT. Clinical target volume 1 (CTV1) included a primary tumor and involved lymph node groups with a margin. Clinical target volume 2 (CTV2) included CTV1 and areas at risk of harboring microscopic spread of primary tumor and elective lymph node groups. All patients were treated with

Median age (range)	Gender (M/F)	Location of tumor	Histopathological type (WHO) classification
61 (34–74)	21/5	Lower (3), middle (7), and upper (2) pharynx; epiglottis (1), glottis (1); larynx (8); palatine tonsil (2), an alveolar triangle of palatine tonsil (1); metastasis to the lymphatic system of the neck from an unknown primary site (1)	Carcinoma planoephiteliale (24) Lymphoepitelial carcinoma (1) Undifferentiated nasopharyngeal carcinoma (1)

Table 1. Clinical characteristics, location of the tumor, and histopathological type of the group of observed patients.

doses of 70 Gy in 35 fractions (2.0 Gy/fraction) for over 7 weeks or 70.2 Gy in 39 fractions (1.8 Gy/fraction) for over five and a half weeks to the primary target. Doses to the elective target were 50 Gy in 25 fractions (2.0 Gy/fraction) or 54 Gy in 30 fractions (1.8 Gy/ fraction). Induction chemotherapy consisted of two to three cycles of TPF (docetaxel 75 mg/m^2, cisplatin 75 mg/m^2, d1 and 5-fluorouracil 750 mg/m^2 d1–5) or PF (cisplatin 100 mg/m^2, d1 and 5-fluorouracil 1000 mg/m^2 d1–5).

Clinical and dermoscopic evaluation

Patients were evaluated clinically and dermoscopically on average at 15-time points—at the beginning of the study (prior to RT), then every other day until the end of the hospitalization: in 1, 2, 4, 6, 8, 10, etc. Each patient was assessed in the same symmetric four areas (right and left cervical areas, right and left submandibular areas) exposed to ionizing irradiation and in two control areas (right and left retroauricular regions). During the entire period, 374 observations were made in all patients; during each, four dermoscopic photos of the irradiated area and two photos of the non-treated area were taken. A total of 2244 dermoscopic photographs and 374 clinical photographs were recorded. Out of them, 1496 photographs represented the investigated areas exposed to irradiation. Clinical evaluation was performed in line with the RTOG/EORTC radiation-induced dermatitis scale (I–V). The presence of erythema, epilation, dry desquamation, moist desquamation, moderate edema, pitting edema, ulceration, hemorrhages, and necrosis was assessed. Dermoscopic findings were described in line with the consensus of experts in non-neoplastic dermatoses on behalf of the International Dermoscopy Society (IDS) by Errichetti et al.[17]. The presence or absence of 31 clinical features was described, including vessels (morphology and distribution); scale (color and distribution); follicular findings (follicular plugs, follicular red dots, perifollicular white color, follicular pigmentation); other structures (color and morphology); and specific clues. Dermoscopic assessment of skin lesions was performed using the DermLiteFoto dermoscope (*3Gen, LLC*, *San Juan Capistrano*, CA, USA) at tenfold magnification. Dermoscopy was performed by a medical doctor experienced in dermoscopy (A. P.). Dermoscopic images were then independently analyzed by two dermoscopists (A. P. and A. S.-S.), blinded to any patient/protocol data. When there was a discrepancy between them, the third dermoscopist (G. K.-W.) made the final decision regarding the description.

Statistical analysis

A photographic database of 2244 dermoscopic photographs and 374 clinical photographs was analyzed in the final statistical assessment. Concordance based on Cohen's κ coefficient in the assessment of dermoscopic and macroscopic photographs between two independent observers in 89% of the results was greater than or equal to 0.9. In particular, the value of κ ranges between − 1 and + 1 (κ equal to + 1 implies a perfect agreement between the two ratings, while that of − 1 implies perfect disagreement; if κ assumes the value 0, then this implies that there is no relationship between the two ratings, and any agreement or disagreement is random). Univariate and multivariate binary logistic regression was applied to evaluate the impact of the RT fractions on binary skin diagnostic outcomes. In turn, to estimate the influence of the collected risk factors on the observed dermoscopic features, a multivariate ordinal logistic model was used. The statistical outcomes were expressed by a classical odds ratio (OR) with a 95% confidence interval (CI); a p value of < 0.05 was considered statistically significant. Due to repeated measures with consecutive RT fractions for each patient, the regressions were extended for random effects. The statistical outcomes were expressed by a classical odds ratio (OR) together with a 95% confidence interval (CI 95%) and a p value.

Ethical approval

The authors have received approval from the local ethics committee of the National Research Institute of Oncology (reference number KB/430-44/19). The study was conducted in accordance with the Helsinki Declaration of 1964, and its later amendments. All subjects provided informed consent to participate in the study as well as for publication.

Results

There were oral cavity carcinoma, oropharyngeal carcinoma, hypopharyngeal carcinoma, laryngeal carcinoma nasopharyngeal carcinoma and neck lymph nodes tumor as a metastatic cancer from unknown primary in 1, 8, 3, 10, 3 and 1 patients, respectively. There were five women and 21 men with the mean age of 60.5 years (range 34–74) in this group.

All patients (26) observed during the course of RT developed ARD. The highest noted grade according to RTOG/EORTC, at the end of the RT treatment, was grade II in 14 patients, grade III in 10 patients, and the remaining two developed grade IV ARD. Grade I was observed in the first week (on average on Day 4.69) (Fig. 1A), grade II in the third week of the follow-up (Day 20.69) (Fig. 1C), grade III in the 6th week of the follow-up (Day 37.81) (Fig. 1E), and grade IV in the 5th week of the follow-up (Day 34.66) (Fig. 1G). The percentage occurrence of dermoscopic features depending on the grade of radiation-induced dermatitis per RTOG/EORTC [13] is presented in Table 2 and Fig. 1B,D,F,H (Table 2).

Summary of dermoscopic findings: vessels in each grade of ARD were polymorphic. The arrangement of the vessels was also heterogeneous, and there was no typical arrangement for a particular grade of ARD. In healthy skin, we did not observe vessels in reticular distribution, but their presence was detected in every degree of ARD. Unspecific distribution was more common in healthy skin than in ARD. In each grade of ARD, a patchy scale was observed and the frequency of scale occurrence increased with the grade of development according to RTOG without characteristic color was observed. However, the incidence of scale increases with the degree of development in RTOG (Fig. 1H). Moreover, a feature present in all grades but not observed in healthy skin was follicular plugs arranged in rosettes.

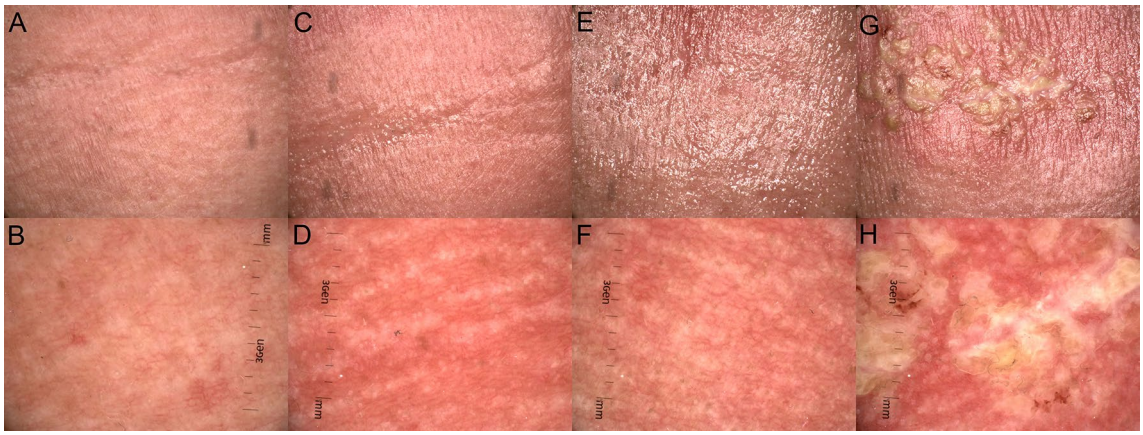

Figure 1. Macroscopic images (**A**,**C**,**E**,**G**) of ARD in grades (G) from G1 to G4, clinically assessed in line with RTOG criteria[13] and dermoscopic findings (**B**,**D**,**F**,**H**) described in line with the consensus of experts in non-neoplastic dermatoses on behalf of the International Dermoscopy Society in one of the patients observed during the course of the RT treatment. (**A**) Faint erythema (G1); (**B**) dermoscopic image (G1) of ARD reveals linear branched and linear curved vessels in clustered distribution and white structureless areas; (**C**) bright erythema, epilation, moist desquamation and moderate edema (G2); (**D**) dermoscopic image of ARD (G2) shows linear branched and linear curved vessels in reticular distribution of vessels, and follicular plugs arranged in rosettes; (**E**) bright erythema, epilation, confluent moist desquamation and pitting edema (G3); (**F**) dermoscopic image (G3) with linear branched vessels in reticular distribution, perifollicular pigmentation and follicular plugs arranged in rosettes; (**G**) ulceration in ARD (G4); (**H**) dermoscopic image (G4) reveals linear branched vessels in reticular distribution, white, yellow, patchy scale.

Statistically significant results are underlined in bold in Table 3. A relationship between the observed dermoscopic and clinical features was checked using κ coefficient (Table 3).

The agreement between dermoscopic and clinical features was 0.03–0.54 and bright erythema, epilation, dry and moist desquamation, moderate edema, and dermoscopic features such as vessels in reticular distribution, white, yellow, brown scale and patchy scale distribution, follicular plugs arranged in rosettes and perifollicular pigmentation. Negative results mean incompatibility: when a given macroscopic feature is present, the dermoscopic feature is not present. In the next step, dermoscopic and clinical features were analyzed in terms of the influence of time, age, gender, induction chemotherapy, concurrent chemotherapy, total radiation dose, fractional dose, tumor location, as well as the histopathological diagnosis during the whole RT treatment on the skin diagnostic outcomes using logistic regression. The statistically significant relationships between clinical features and possible ARD risk factors—time, age, gender, indCHT, concurrent CHT, and fractional dose—are expressed by odds ratios reported in Table 4 whereas OR is a measure of association between radiation exposure and a clinical outcome; OR > 1 indicates the increased occurrence of any event, while OR < 1 a protective exposure) (Table 3).

Based on the results in Table 4, we observed the relationship between the presence of vessels in reticular distribution and time, age, gender, induction chemotherapy, and concurrent CHT (Table 4). The statistical interpretation of the OR (univariate regression) may be as follows: 1 day of observation generates an increased risk of vessels in reticular distribution by 8%, and 5 days of observation ($1.08^5 = 1.47$), so by almost one and a half. A 10-year difference in the age of patients generates a $(1–0.97^{10}) \times 100\% = 26\%$ reduction in the occurrence of vessels in reticular distribution. The risk of vessels in reticular distribution is 64% lower in men than in women. Induction chemotherapy reduces the risk of vessels in reticular distribution almost three times (OR = 2.94). Concurrent CHT reduces the risk of vessels in reticular distribution by 1.83 (OR = 1.83). The results regarding the effect of collected risk factors on skin reaction in a multivariate model showed that the effect of gender and induction chemotherapy increased. Moreover, in the multivariate model, the lack of concurrent CHT reduces the risk of vessels in reticular distribution by 53% (see the right panel of Table 4). Other results in the table should be interpreted analogously. Considering individual factors affecting clinical response, each day of observation during RT treatment statistically generates a higher chance of occurrence of vessels in reticular distribution (Figs. 1D,F,H, 2A,E), white scale and yellow scale (Fig. 2B), and brown scale (Fig. 2C) with patchy distribution (Figs. 1B,H, 2C), perifollicular pigmentation (Fig. 2D), follicular plugs arranged in rosettes (Fig. 2E), while the chance of unspecific distribution of vessels decreases (Fig. 2D). In the context of a macroscopic response, each day of observation during RT treatment statistically generates a higher chance of occurrence of bright erythema (Fig. 1C,E), epilation (Fig. 1C,E), dry and moist desquamation (Fig. 1C,E), moderate (Fig. 1C) and pitting edema (Fig. 1E), and ulceration (Fig. 1G) while the chance of follicular and faint erythema decreases (Fig. 1A). The results regarding the effect of collected risk factors on skin reaction in a multivariate model were comparable. In a univariate analysis, age was a significant factor for vessels in reticular distribution, vessels in unspecific distribution, follicular plugs arranged in rosettes, and perifollicular pigmentation as well as in the group of macroscopic features for follicular erythema. However, multivariate analysis did not show this relationship for the unspecific distribution of vessels, follicular plugs arranged in rosettes, or perifollicular pigmentation (the association is on the border of statistical significance, i.e., $p < 0.1$). Gender is important for the occurrence of vessels in reticular distribution, vessels in unspecific distribution, white, yellow, patchy scale, follicular plugs arranged in rosettes,

Dermoscopic features	Prior RT (%)	RTOG I (%)	RTOG II (%)	RTOG III (%)	RTOG IV (%)
Vessels morphology					
Dotted	61.5	62.0	71.7	59.3	100
Linear (without bends or branches)	2.6	0.7	0.6	0	0
Linear with branches	87.2	95.6	97.0	100.0	100
Linear curved	92.3	97.8	98.8	100.0	100
Vessels distribution					
Uniform	0	0	0	0	0
Clustered	35.9	79.6	59.6	70.4	33.33
Peripheral	0	0	0	0	0
Reticular	0	30.7	62.7	70.4	66.67
Unspecific	97.4	52.6	35.5	18.5	33.33
Scale color					
White	0	21.9	48.2	70.4	100
Yellow	0	8.8	33.7	63.0	100.0
Brown	0	4.4	34.9	63.0	66.7
Scale distribution					
Diffuse	0	0	0	0	0
Central	0	0	0	0	0
Peripheral	0	0	0	0	0
Patchy	0	24.8	74.1	92.6	100.0
Follicular findings					
Follicular plugs arranged in rosettes	0	8.0	54.2	44.4	100.0
Follicular red dots	0	0	0	0	0
Perifollicular white color	38.5	21.9	41.0	18.5	33.3
Perifollicular pigmentation	12.8	27.0	61.5	44.4	66.7
Other structures					
White structureless	46.2	59.1	47.0	63.0	66.7
Brown structureless	0	0	0	0	0
Yellow structureless	0	0	0	0	0
White dots or globules	0	0	0	0	0
Brown dots or globules	20.5	26.3	19.3	3.7	0
Yellow dots or globules	0	0	0	0	0
White lines	35.9	54.0	44.0	14.8	0
Brown lines	25.6	37.2	25.3	14.8	0
Yellow lines	7.7	1.5	1.8	0	0

Table 2. Percentage share (%) of dermoscopic non-neoplastic features[17] depending on the grade of radiodermatitis in line with RTOG/EORTC[13].

and for macroscopic features for faint and bright erythema and dry desquamation. Multivariate analysis showed that the gender effect was stronger in each case. The risk of vessels in reticular distribution, white scale, yellow scale, patchy scale, and follicular plugs arranged in rosettes is 85%, 89%, 80%, 95%, and 69% lower in men than in women, respectively. The risk of faint erythema is 118% higher for men than women, while the chance of bright erythema and dry desquamation is 88% and 74% lower in men than in women, respectively. Induction chemotherapy increases the risk of yellow scale and reduces the risk of vessels in reticular distribution. In the multivariate model, these dependencies increase, and we observe that induction chemotherapy increases the risk of yellow scale occurrence by two-thirds (OR = 0.34) and reduces the risk of vessels in reticular distribution almost six times (OR = 5.90). Concurrent chemotherapy is important for the occurrence of vessels in reticular distribution, follicular plugs arranged in rosettes, perifollicular pigmentation and macroscopic features such as follicular erythema, tender erythema, and moist desquamation. In turn, multivariate analysis did not show this relationship for follicular plugs arranged in rosettes, follicular erythema and moist desquamation (the association is on the border of the statistical significance, i.e., $p < 0.1$). Non-concurrent chemotherapy reduces the risk of vessels in reticular distribution, perifollicular pigmentation and tender erythema by 53%, 51% and 94%, respectively.

Discussion

Graham et al. emphasized the importance of archiving photographs, which are a useful source of documents for auditing and monitoring radiotherapy-induced skin toxicity[18]. In turn, the study by Ni et al. used deep learning-based method for the automatic assessment of radiation-induced dermatitis in patients with nasopharyngeal carcinoma[19]. In our study, 2244 dermoscopic photographs and 374 clinical photographs were archived, creating

Dermoscopic features	Clinical features							
	Faint erythema	Bright erythema	Epilation	Dry desquamation	Moist desquamation	Moderate edema	Pitting edema	Ulceration
Dotted vessels	− 0.04	0.07	− 0.02	0.03	0.00	0.02	0.00	− 0.02
Linear vessels	0.00	− 0.01	− 0.01	− 0.02	0.01	0.00	− 0.01	− 0.01
Linear witch branches vessels	0.00	0.03	0.04	0.01	0.00	0.00	0.01	0.00
Linear curved vessels	0.00	0.02	0.02	0.00	0.01	0.01	0.00	0.00
Clustered vessels	**0.18**	− 0.09	**− 0.16**	0.05	**− 0.15**	**− 0.15**	0.00	0.01
Reticular vessels	**− 0.21**	**0.42**	**0.35**	0.02	**0.30**	**0.22**	**0.09**	− 0.02
Unspecific vessels	0.06	**− 0.29**	**− 0.21**	0.05	**− 0.21**	**− 0.18**	**− 0.09**	**− 0.03**
White scale	**− 0.19**	**0.34**	**0.29**	**0.23**	**0.19**	**0.17**	**0.15**	**0.08**
Yellow scale	**− 0.23**	**0.32**	**0.32**	**0.42**	**0.23**	**0.23**	**0.24**	**0.13**
Brown scale	**− 0.26**	**0.34**	**0.34**	**0.14**	**0.42**	**0.45**	**0.23**	**0.07**
Patchy scale	**− 0.31**	**0.54**	**0.53**	**0.23**	**0.35**	**0.41**	**0.14**	**0.04**
Follicular plugs arranged in rosettes	**− 0.35**	**0.47**	**0.46**	**0.15**	**0.44**	**0.52**	**0.09**	0.01
Perifollicular white color	**− 0.16**	**0.11**	0.06	**0.11**	− 0.08	0.07	− 0.05	− 0.03
Perifollicular pigmentation	**− 0.20**	**0.32**	**0.45**	**0.16**	**0.12**	**0.20**	0.02	− 0.02
White structureless	**0.10**	− 0.07	0.00	− 0.04	0.03	− 0.02	0.03	**0.03**
Brown dots or globules	**0.12**	**− 0.09**	**− 0.09**	− 0.07	**− 0.14**	− 0.02	**− 0.11**	− 0.04
White lines	**0.15**	**− 0.13**	**− 0.13**	**0.10**	**− 0.24**	**− 0.13**	**− 0.11**	**− 0.04**
Brown lines	**0.12**	**− 0.13**	− 0.06	− 0.03	**− 0.11**	**− 0.14**	− 0.07	− 0.04
Yellow lines	− 0.01	**− 0.03**	0.01	− 0.04	− 0.04	0.02	− 0.03	− 0.02

Table 3. Level of agreement between the presence of selected dermoscopic features[17] and clinical features[13] in ARD assessed with values of κ statistics.

a database that in the future could be used as a database to automate clinical assessment. In the current literature, only one study used dermoscopy, but only for the presence of erythema in ARD[20]. So far, only clinical features have been described, and there are no data on the analysis of dermoscopic features in ARD. One of the previous studies reported dermoscopic changes in the surrounding tissue of basal cell carcinoma in patients who underwent brachytherapy[21]. Radiation-induced dermatitis occurs in about 90–95% of patients exposed to ionizing radiation[22–24]. Published reports on the share of individual grades per RTOG are ambiguous. This is probably due to many variables affecting the development of this type of skin toxicity. Elliot et al. showed in their observation that 1% of patients did not develop any grade of ARD, 20% developed grade I, 57% grade II, and 23% grade III or IV[25]. Kang et al. observed radiation-induced dermatitis of the maximum grade I-IV in 46.6%, 18.0%, 5.5%, and 0.9% of the patients, respectively[26]. In turn, in the report from Franco et al., the toxicity profile at the end of RT was Grade 0 in 3.5% of patients, Grade I in 32%, Grade II in 61%, Grade III in 3.5%[27]. Mild erythema may appear as early as a few hours after exposure to ionizing radiation[28], but usually develops about 7–10 days after starting therapy[29]. Dry desquamation (RTOG/EORTC grade I) usually occurs after 3–4 weeks from the start of treatment. More intense erythema, hair loss, and hyperpigmentation are usually observed between 2 and 4 weeks of therapy[30]. Moist desquamation (RTOG/EORTC grade II) usually occurs after 4 weeks when the total RT dose to the skin is 40 Gy or higher[31,32]. In the study of Franco et al., grade II appeared between treatment weeks 4–5; for those having grade III acute skin toxicity, this event mainly began during weeks 5 and 6[27]. Data variability is also likely to be influenced by treatment and clinical risk factors. ARD can lead to pain, discomfort, reduced quality of life, and premature discontinuation of treatment. Therefore, it is important to make a rapid diagnosis when the first symptoms appear and to implement appropriate prevention and treatment. Dermoscopy can be a complementary tool to support macroscopic ARD evaluation. Our study is the first in the published papers to attempt to identify the correlations between the clinical and dermoscopic features of ARD with its dermoscopic follow-up. The importance of the total dose during RT is well known[33,34]. Moreover, in our study, we selected patients scheduled for RT at comparable total doses to minimize the risk of a dose effect. A statistical dependence of the influence of days of observation during RT was observed for the features correlating in the test of compatibility of clinical and dermoscopic features. Predicting the risk of radiation-induced dermatitis is essential for proper prevention and treatment. Kawamura et al. in their study created a scoring system taking into account V60Gy, concurrent chemotherapy status, age, and body mass index[35]. Age ≥ 67 years was significant in their study for the development of ARD.

Meyer et al. showed that gender is important in the context of the development of radiation-induced dermatitis[33]. Kawamura et al. showed that concurrent chemotherapy with platinum and cetuximab (cetuximab > platinum) had significant importance in the development of radiation-induced dermatitis. Gold standards of management have not yet been established, and treatment, as well as prevention, are common and empirical, based on personal experience supported by weak scientific evidence[9,36]. Based on the study by Robijn et al., there could be a strong recommendation to use photobiomodulation therapy (PBMT) in the prevention and management of ARD in cancer patients[37]. The identified dermoscopic features may facilitate the selection of topical

	Univariate analysis		Multivariate analysis	
Dermoscopic features				
Reticular vessels				
Time	1.08 (1.06–1.10)	**<0.0001**	1.10 (1.08–1.12)	**<0.0001**
Age	0.97 (0.94–0.99)	**0.0031**	0.95 (0.92–0.98)	**0.0009**
Gender	0.34 (0.18–0.60)	**0.0001**	0.15 (0.07–0.33)	**<0.0001**
Induction chemotherapy	2.94 (1.85–4.74)	**<0.0001**	5.90 (3.10–11.7)	**<0.0001**
Radiochemotherapy	1.83 (1.12–3.03)	**0.0149**	0.47 (0.23–0.96)	**0.0379**
Unspecific vessels				
Time	0.95 (0.93–0.96)	**<0.0001**	0.94 (0.93–0.96)	**<0.0001**
Age	1.03 (1.01–1.06)	**0.0157**	1.03 (1.00–1.05)	0.0505
Gender	1.97 (1.17–3.38)	**0.0110**	2.15 (1.21–3.86)	**0.0085**
White scale				
Time	1.06 (1.04–1.08)	**<0.0001**	1.07 (1.05–1.09)	**<0.0001**
Gender	0.14 (0.06–0.31)	**<0.0001**	0.11 (0.04–0.25)	**<0.0001**
Yellow scale				
Time	1.07 (1.05–1.09)	**<0.0001**	1.08 (1.05–1.10)	**<0.0001**
Gender	0.23 (0.08–0.51)	**0.0001**	0.20 (0.07–0.48)	**0.0001**
Induction chemotherapy	0.47 (0.25–0.84)	**0.0095**	0.34 (0.17–0.66)	**0.0011**
Brown scale				
Time	1.09 (1.07–1.12)	**<0.0001**		
Patchy scale				
Time	1.11 (1.09–1.14)	**<0.0001**	1.13 (1.10–1.16)	**<0.0001**
Gender	0.27 (0.15–0.47)	**<0.0001**	0.12 (0.05–0.25)	**<0.0001**
Follicular plugs arranged in rosettes				
Time	1.12 (1.09–1.15)	**<0.0001**	1.13 (1.10–1.16)	**<0.0001**
Age	0.97 (0.94–0.99)	**0.0053**	0.97 (0.94–1.01)	0.1226
Gender	0.51 (0.27–0.94)	**0.0293**	0.31 (0.14–0.66)	**0.0020**
Radiochemotherapy	1.89 (1.10–3.37)	**0.0207**	1.12 (0.54–2.34)	0.7650
Perifollicular pigmentation				
Time	1.06 (1.04–1.08)	**<0.0001**	1.07 (1.05–1.09)	**<0.0001**
Age	1.03 (1.00–1.06)	**0.0194**	1.02 (0.99–1.05)	0.1250
Radiochemotherapy	0.48 (0.30–0.78)	**0.0029**	0.49 (0.26–0.95)	**0.0334**
Fraction dose	0.02 (0.00–0.18)	**0.0005**	0.04 (0.00–0.54)	**0.0143**
Clinical features				
Follicular erythema				
Time	0.89 (0.74–0.98)	**0.0158**	0.89 (0.73–0.99)	**0.0276**
Age	1.30 (1.05–1.69)	**0.0104**	1.31 (1.01–1.82)	**0.0417**
Radiochemotherapy	0.13 (0.01–0.81)	**0.0290**	0.42 (0.04–2.71)	0.3654
Faint erythema				
Time	0.94 (0.92–0.95)	**<0.0001**	0.93 (0.92–0.95)	**<0.0001**
Gender	1.85 (1.10–3.14)	**0.0212**	2.18 (1.23–3.92)	**0.0081**
Tender erythema				
Radiochemotherapy	0.06 (0.00–0.77)	**0.0295**		
Bright erythema				
Time	1.19 (1.15–1.23)	**<0.0001**	1.21 (1.17–1.26)	**<0.0001**
Gender	0.41 (0.23–0.71)	**0.0012**	0.12 (005–0.27)	**<0.0001**
Epilation				
Time	1.30 (1.24–1.38)	**<0.0001**		
Dry desquamation				
Time	1.04 (1.02–1.07)	**0.0001**	1.04 (1.02–1.07)	**0.0001**
Gender	0.28 (0.07–0.74)	**0.0084**	0.26 (007–0.71)	**0.0064**
Moist desquamation				
Time	1.31 (1.24–1.41)	**<0.0001**	1.32 (1.24–1.42)	**<0.0001**
Radiochemotherapy	1.82 (1.00–3.50)	**0.0497**	0.51 (0.19–1.33)	0.1701
Moderate edema				
Time	1.13 (1.10–1.17)	**<0.0001**		

Continued

	Univariate analysis		Multivariate analysis	
Pitting edema				
Time	1.19 (1.13–1.27)	**<0.0001**		
Ulceration				
Time	1.09 (1.03–1.18)	**0.0012**		

Table 4. Statistically significant ORs ($p < 0.05$) of the influence of clinical data on the occurrence of dermoscopic and macroscopic features in ARD (univariate and multivariate logistic regression). Significant values are in [bold].

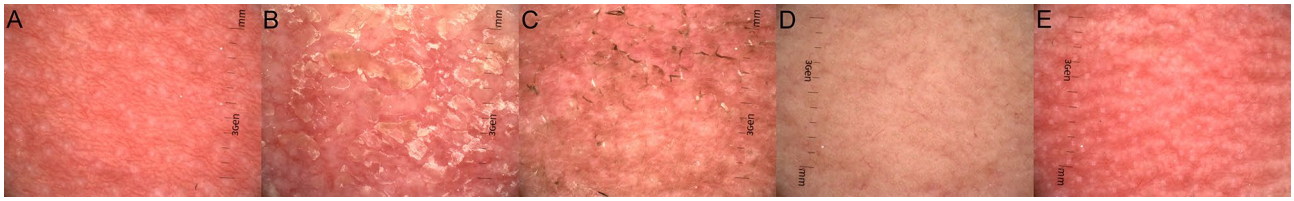

Figure 2. Dermoscopic images of ARD described in line with the consensus of experts in non-neoplastic dermatoses on behalf of the International Dermoscopy Society by Errichetti et al.[17]. (**A**) Dermoscopic image of ARD reveals linear branched, linear curved vessels with reticular distribution and perifollicular white color; (**B**) dermoscopic image of acute radiodermatitis reveals white and yellow, patchy scale; (**C**) dermoscopic image reveals linear branched and linear curved vessels with clustered distribution, brown, patchy scale; (**D**) dermoscopic image reveals linear branched and linear curved vessels with unspecific distribution, and perifollicular pigmentation; (**E**) linear branched and linear curved vessels with reticular distribution and follicular plugs arranged in rosettes.

preparations in further studies, which will consider dermoscopic image in the skin and facilitate non-invasive adjustment of prophylaxis and treatment of ARD. Because very frequent observations of patients showed the appearance of the first features on average on 4.69 days from the first dose of ARD, appropriate prevention should be implemented rapidly, especially in males, who in a recent study were found to develop a higher degree of ARD.

Conclusions (PURE)

Knowledge of dermoscopic features and predictors could help in rapid early assessment and new therapeutic strategies, that can help reduce toxicities among patients treated with RT for HNC.

Data availability

The datasets used and/or analysed during the current study available from the corresponding author on reasonable request.

Received: 16 April 2023; Accepted: 11 September 2023
Published online: 21 September 2023

References

1. Bray, F. *et al.* Global cancer statistics 2018: GLOBOCAN estimates of incidence and mortality worldwide for 36 cancers in 185 countries. *CA Cancer J. Clin.* **68**, 394–424 (2018).
2. Siegel, R. L., Miller, K. D., Fuchs, H. E. & Jemal, A. Cancer statistics, 2021. *CA A Cancer J. Clin.* **1**, 7–33 (2021).
3. Lydiatt, W. M. *et al.* Head and Neck cancers-major changes in the American Joint Committee on cancer eighth edition cancer staging manual. *CA Cancer J. Clin.* **67**(2), 122–137 (2017).
4. Curado, M. & Hashibe, M. Recent changes in the epidemiology of head and neck cancer. *Curr. Opin. Oncol.* **21**, 194–200 (2009).
5. Gamerith, G. & Fuereder, T. Treating head and neck cancer—a multidisciplinary effort. *Memo* **13**, 359–360 (2020).
6. Leemans, C. R., Braakhuis, B. J. & Brakenhoff, R. H. The molecular biology of head and neck cancer. *Nat. Rev. Cancer* **11**(27), 9–22 (2011).
7. Pfister, D. G. *et al.* Head and neck cancers. *J. Natl. Compr. Cancer Netw.* **9**, 596–650 (2011).
8. Alfouzan, A. F. Radiation therapy in head and neck cancer. *Saudi Med. J.* **42**(3), 247–254 (2021).
9. Hegedus, F., Mathew, L. M. & Schwartz, R. A. Radiation dermatitis: an overview. *Int. J. Dermatol.* **56**(9), 909–914 (2017).
10. Singh, M., Alavi, A., Wong, R. & Akita, S. Radiodermatitis : a review of our current understanding. *Am. J. Clin. Dermatol.* **17**(3), 277–292 (2016).
11. Yee, C. *et al.* Radiation-induced skin toxicity in breast cancer patients: a systematic review of randomized trials. *Clin. Breast Cancer* **18**(5), e825–e840 (2018).
12. Sekiguchi, K. *et al.* Efficacy of heparinoid moisturizer as a prophylactic agent for radiation dermatitis following radiotherapy after breast-conserving surgery: a randomized controlled trial. *Jpn. J. Clin. Oncol.* **48**(5), 450–457 (2018).
13. Cox, J. D., Stetz, J. & Pajak, T. F. Toxicity criteria of the Radiation Therapy Oncology Group (RTOG) and the European Organization for Research and Treatment of Cancer (EORTC). *Int. J. Radiat. Oncol. Biol. Phys.* **31**(5), 1341–1346 (1995).
14. https://ctep.cancer.gov/protocolDevelopment/electronic_applications/ctc.htm#ctc_50.

15. Routledge, J. A. *et al.* Evaluation of the LENT-SOMA scales for the prospective assessment of treatment morbidity in cervical carcinoma. *Int. J. Radiat. Oncol. Biol. Phys.* **56**(2), 502–510 (2003).
16. Dudek, A., Rutkowski, T., Kaminska-Winciorek, G. & Składowski, K. What is new when it comes to acute and chronic radiation induced dermatitis in head and neck cancer patients? Acute and chronic radiation—induced dermatitis. *Nowotwory* **5**(42), 11–17 (2020).
17. Errichetti, E. *et al.* Standardization of dermoscopic terminology and basic dermoscopic parameters to evaluate in general dermatology (non-neoplastic dermatoses): an expert consensus on behalf of the International Dermoscopy Society. *Br. J. Dermatol.* **182**(2), 454–467 (2020).
18. Graham, P. H. *et al.* Digital photography as source documentation of skin toxicity: An analysis from the Trans Tasman Radiation Oncology Group (TROG) 04.01 Post-Mastectomy Radiation Skin Care Trial. *J. Med. Imaging Radiat. Oncol.* **56**, 458–463 (2012).
19. Ni, R. *et al.* Deep learning-based automatic assessment of radiation dermatitis in patients with nasopharyngeal carcinoma. *Int. J. Radiat. Oncol. Biol. Phys.* **113**(3), 685–694 (2022).
20. Kišonas, J. *et al.* Acute radiation dermatitis evaluation with reflectance confocal microscopy: a prospective study. *Diagnostics* **11**(9), 1670 (2021).
21. Krzysztofiak, T., Kamińska-Winciorek, G., Tukiendorf, A., Suchorzepka, M. & Wojcieszek, P. Basal cell carcinoma treated with high dose rate (HDR) brachytherapy-early evaluation of clinical and dermoscopic patterns during irradiation. *Cancers* **13**(20), 5188 (2021).
22. Brown, K. R. & Rzucidlo, E. Acute and chronic radiation injury. *J. Vasc. Surg.* **53**, 15S (2011).
23. Hymes, S. R., Strom, E. A. & Fife, C. Radiation dermatitis: clinical presentation, pathophysiology, and treatment 2006. *J. Am. Acad. Dermatol.* **54**(1), 28–46 (2006).
24. Denhama, J. W. & Hauer-Jensenb, M. The radiotherapeutic injury—a complex 'wound'. *Radiother. Oncol.* **63**(2), 129–145 (2002).
25. Elliott, E. A. *et al.* Radiation Therapy Oncology Group Trial 99-13. Phase III Trial of an emulsion containing trolamine for the prevention of radiation dermatitis in patients with advanced squamous cell carcinoma of the head and neck: results of Radiation Therapy Oncology Group Trial 99-13. *J. Clin. Oncol.* **24**(13), 2092–2097 (2006).
26. Kang, H. C. *et al.* The safety and efficacy of EGF-based cream for the prevention of radiotherapy-induced skin injury: results from a multicenter observational study. *Radiat. Oncol. J.* **32**(3), 156–162 (2014).
27. Franco, P. *et al.* Hypericum perforatum and neem oil for the management of acute skin toxicity in head and neck cancer patients undergoing radiation or chemo-radiation: a single-arm prospective observational study. *Radiat. Oncol.* **9**, 297 (2014).
28. Koenig, T. R., Wolff, D., Mettler, F. A. & Wagner, L. K. Skin injuries from fluoroscopically guided procedures: part 1, characteristics of radiation injury. *Am. J. Roentgenol.* **177**(1), 3–11 (2001).
29. Kole, A. J., Kole, L. & Moran, M. S. Acute radiation dermatitis in breast cancer patients: challenges and solutions. *Breast Cancer (Dove Med. Press)* **9**, 313–323 (2017).
30. McQuestion, M. Evidence-based skin care management in radiation therapy: clinical update. *Semin. Oncol. Nurs.* **27**, e1-17 (2011).
31. Hymes, S. R., Strom, E. A. & Fife, C. Radiation dermatitis: clinical presentation, pathophysiology and treatment. *J. Am. Acad. Dermatol.* **54**(1), 28–46 (2006).
32. Bray, F. N., Simmons, B. J., Wolfson, A. H. & Nouri, K. Acute and chronic cutaneous reactions to ionizing radiation therapy. *Dermatol. Ther.* **6**(2), 185–206 (2016).
33. Meyer, F., Fortin, A., Wang, C. S., Liu, G. & Bairati, I. Predictors of severe acute and late toxicities in patients with localized head-and-neck cancer treated with radiation therapy. *Int. J. Radiat. Oncol. Biol. Phys.* **15**(824), 1454–1462 (2012).
34. Mendelsohn, F. A., Divino, C. M., Reis, E. D. & Kerstein, M. D. Wound care after radiation therapy. *Adv. Skin Wound Care* **15**, 216–224 (2002).
35. Kawamura, M. *et al.* A scoring system predicting acute radiation dermatitis in patients with head and neck cancer treated with intensity-modulated radiotherapy. *Radiat. Oncol.* **14**(1), 14 (2019).
36. Wong, R. K. *et al.* Clinical practice guidelines for the prevention and treatment of acute and late radiation reactions from the MASCC Skin Toxicity Study Group. *Support Care Cancer* **21**(10), 2933–2948 (2013).
37. Robijns, J., Lodewijckx, J. & Mebis, J. Photobiomodulation therapy for acuteradiodermatitis. *Curr. Opin. Oncol.* **31**(4), 291–298 (2019).

Acknowledgements

The authors thank the patients for their participation in the study.

Author contributions

Conceptualization: A.P., G.K.W., T.R. Data curation: A.P. Formal analysis: A.P., A.S.Z.S., A.T., G.K.W. Funding acquisition: G.K.W. Investigation: A.P. Methodology: A.P., G.K.W., T.R. Project administration: A.P., G.K.W., T.R. Resources: A.P., A.S.Z.S. Software: A.T. Supervision: G.K.W. Validation: A.P., A.T. Visualization: A.P. Writing—original draft preparation: A.P. Writing—review and editing: A.P., G.K.W., A.T., T.R., K.S.

Competing interests

The authors declare no competing interests.

Additional information

Correspondence and requests for materials should be addressed to G.K.-W.

life

Article

Dermoscopy of Chronic Radiation-Induced Dermatitis in Patients with Head and Neck Cancers Treated with Radiotherapy

Aleksandra Pilśniak [1], Anastazja Szlauer-Stefańska [2], Andrzej Tukiendorf [3], Tomasz Rutkowski [4], Krzysztof Składowski [4] and Grażyna Kamińska-Winciorek [5,*]

[1] Department of Internal Medicine, Autoimmune and Metabolic Diseases, Faculty of Medical Sciences, Medical University of Silesia, 40-055 Katowice, Poland; aleksandra.pilsniak@gmail.com
[2] Department of Bone Marrow Transplantation and Onco-Hematology, Maria Sklodowska-Curie National Research Institute of Oncology (MSCNRIO), 44-102 Gliwice, Poland; anastazja.szlauer@gmail.com
[3] Institute of Health Sciences, Opole University, 45-040 Opole, Poland; andrzej.tukiendorf@gmail.com
[4] Inpatient Department of Radiation and Clinical Oncology, Maria Sklodowska-Curie National Research Institute of Oncology (MSCNRIO), Gliwice Branch, 44-102 Gliwice, Poland; tomasz.rutkowski@gliwice.nio.gov.pl (T.R.); krzysztof.skladowski@io.gliwice.pl (K.S.)
[5] Department of Bone Marrow Transplantation and Onco-Hematology, Skin Cancer and Melanoma Team, Maria Sklodowska-Curie National Research Institute of Oncology (MSCNRIO), 44-102 Gliwice, Poland
* Correspondence: dermatolog.pl@gmail.com; Tel.: +48-32-278-8523

Abstract: Radiotherapy (RT) is an integral part of many cancer treatment protocols. Chronic radiation-induced dermatitis (CRD) is a cutaneous toxicity that occurs in one-third of all patients treated with this method. CRD is usually observed several months after completion of treatment. Typical symptoms of CRD are telangiectasia, skin discoloration, atrophy, thickening, and cutaneous fibrosis. There are currently no data in the literature on the evaluation of the dermoscopic features of CRD. The aim of this prospective study was the identification of clinical and dermoscopic features in a group of 32 patients with head and neck cancer (HNC) in whom CRD developed after RT. CRD was assessed at 3, 6, and 12 months after RT in 16, 10, and 10 patients, respectively. CRD was assessed at one time point and two time points in 28 and 4 patients, respectively. The control included skin areas of the same patient not exposed to RT. The dataset consisted of 36 clinical and 216 dermoscopic photos. Clinical evaluation was performed according to the RTOG/EORTC radiation-induced dermatitis scale. The highest score was grade 2 observed in 21 patients. Clinical observations revealed the presence of slight and patchy atrophy, pigmentation change, moderate telangiectasias, and some and total hair loss. Dotted vessels, clustered vessel distribution, white patchy scale, perifollicular white color, white structureless areas, brown dots and globules, and white lines were the most frequently noted features in dermoscopy. Three independent risk factors for chronic toxicity, such as age, gender, and surgery before RT, were identified. The dermoscopic features that had been shown in our study reflect the biological reaction of the skin towards radiation and may be used for the parametrization of CRD regarding its intensity and any other clinical consequences in the future.

Keywords: chronic radiation-induced dermatitis; radiotherapy; head and neck cancers; dermoscopy; side effects

Citation: Pilśniak, A.; Szlauer-Stefańska, A.; Tukiendorf, A.; Rutkowski, T.; Składowski, K.; Kamińska-Winciorek, G. Dermoscopy of Chronic Radiation-Induced Dermatitis in Patients with Head and Neck Cancers Treated with Radiotherapy. *Life* **2024**, *14*, 399. https://doi.org/10.3390/life14030399

Academic Editor: Alin Laurentiu Tatu

Received: 30 January 2024
Revised: 5 March 2024
Accepted: 12 March 2024
Published: 18 March 2024

1. Introduction

According to estimates by the American Cancer Society, more than 2 million new cases of cancer will be diagnosed in the USA in 2024. This estimated number of new cases of cancers excludes squamous and basal cell carcinoma of the skin, and cancer in situ (non-invasive cancer) [1].

Surgery, radiotherapy (RT), chemotherapy (CHT), and combinations of these methods in patients with head and neck cancer (HNC) depend on both patient- and tumor-related factors [2,3].

While RT is a crucial part of many cancer treatment protocols [4], preventing side effects, long-term disability, and discomfort from this therapy is important. The side effects mentioned above can affect the patient's quality of life to such an extent that treatment is interrupted, which impairs the effect of RT. This problem particularly concerns patients in whom the skin is involved in irradiated areas as in HNC [5,6]. Chronic radiation-induced dermatitis (CRD) is an important and increasingly common problem because it occurs in one-third of patients after RT [7]. CRD is a cutaneous toxicity that appears several months after RT [8,9].

Typical cutaneous symptoms of CRD include telangiectasia, discoloration, skin atrophy, thickening, and cutaneous fibrosis [10–12]. In the course of CRD, there is histologic evidence of reduced microvascular network density and changes in blood vessel morphology [13]. Ionizing radiation activates cytokine cascades and fibrous inflammatory pathways at the molecular level, which can progress over many years and lead to significant fibrosis [14].

Dermoscopic examination combines clinical and pathological examination [15]. There are currently no data in the literature on the evaluation of the dermoscopic features of CRD. The use of dermoscopy in the assessment of CRD is an innovative approach. In the future, it may facilitate clinical assessment and thus make appropriate decisions about the further management of a patient with developed chronic skin toxicity. The evaluation of clinical and dermoscopic features in the course of CRD was the main assumption of this study.

2. Materials and Methods

The clinical and dermoscopic evaluation in the CRD study is a continuation of our earlier published cutaneous toxicity study in patients with HNC who are eligible for RT [16]. The first study focused on acute radiation dermatitis (ARD). However, this study looks at CRD, and although the study group is different, it is a continuum of the assessment of skin toxicity following RT. The location of the study, the methodology, the treatment protocols for the included patients, the inclusion and exclusion criteria, the clinical and dermoscopic assessment, and the statistical methods used are consistent with the first study on ARD [16].

2.1. Patients

The study was conducted at the Maria Skłodowska-Curie National Institute of Oncology, Gliwice Branch (MSCNRIO), from September 2020 to March 2021. The study group consisted of 32 patients who underwent RT treatment at the MSCNRIO and were under the care of the hospital oncology clinic. The observational group consisted of patients with oral cavity cancer, oropharyngeal cancer, hypopharyngeal cancer, laryngeal cancer, and nasopharyngeal cancer in 11, 7, 3, 7, and 2 cases, respectively. There was also 1 patient with sphenoid sinus cancer and 1 patient with a primary unknown tumor involved in this group. The study included 32 patients (inclusion criteria: signed informed consent, age > 18 years, radical RT) with a mean age of 60 years (range: 30–75 years). There were 10 women and 22 men in this group. Patients with active dermatoses or patients being treated with biological drugs were excluded from the study.

2.2. Treatment

The treatment protocol for the patients included in this study was consistent with a previously published ARD study [16]. Induction chemotherapy (indCHT) was carried out in 7 cases. Radiochemotherapy (CHRT) was performed simultaneously in 18 patients, and only RT was performed in 14 patients. Clinical target volume 1 (CTV1) included a primary tumor and involved lymph node groups. Clinical target volume 2 (CTV2) included areas at risk of harboring microscopic disease and elective lymph node groups. All patients were

treated with a dose of 70 Gy, divided into 35 fractions (2.0 Gy/fraction), over 7 weeks or 70.2 Gy, divided into 39 fractions (1.8 Gy/fraction), over 5.5 weeks towards the primary target. The dose for the elective target was 50 Gy in 25 fractions (2.0 Gy/fraction) or 54 Gy in 30 fractions (1.8 Gy/ fraction). IndCHT was given as 2 to 3 cycles of TPF (docetaxel 75 mg/m^2, cisplatin 75 mg/m^2, d1, and 5-fluorouracil 750 mg/m^2 d1–5) or PF (cisplatin 100 mg/m^2, d1 and 5-fluorouracil 1000 mg/m^2 d1–5). CHRT included RT with 2–3 cycles of concomitant cisplatin given at a dose of 100 mg/m^2 each 21 days.

2.3. Clinical and Dermoscopic Evaluation

During each observation of the study, 4 dermoscopic images of the irradiated area (right cervical area, left cervical area, right submandibular area, left submandibular area) and 2 images of the control non-irradiated area (right and left lower part of retroauricular area) were obtained. The control areas (not exposed to RT) were within the same patients. The areas selected as controls were the most similar in thickness and texture to the skin on the neck and mandible. The lower part of the retroauricular area (specifically, the area behind the earlobe) is the area of the skin closest to the neck but not exposed to RT, with very similar UV exposure.

The collection consisted of 36 clinical and 216 dermoscopic photos. Of this set, 144 photos showed areas treated with RT. CRD was assessed at one time point and two time points in 28 and 4 patients, respectively. In total, 36 observations in 32 patients were collected.

Criteria for regular follow-ups in a structured form were checked at 3, 6, and 12 months after the end of RT. In total, 16 patients (96 dermoscopic images) were evaluated 3 months after RT, 10 patients (60 dermoscopic images) were evaluated 6 months after RT, and 10 patients (60 dermoscopic images) 12 months after RT. Radiation-induced dermatitis was clinically evaluated from grades 1 to 5 according to the RTOG/EORTC scale [17].

The first author performed a dermoscopic assessment each time using a DermLite-Foto dermatoscope (3Gen, LLC, San Juan Capistrano, CA, USA) at tenfold magnification. In the next step, the archived dermoscopic images were described by 2 independent dermoscopists (A.P. and A.S.-S.) blinded to patient/protocol data. Analysis of 31 dermoscopic features, according to the International Dermoscopic Society (IDS) consensus of non-neoplastic diseases, was performed [18]. Our description includes morphology and distribution of vessels, color and distribution of scale, follicular findings such as follicular plugs, follicular red dots, perifollicular white color, follicular pigmentation, as well as color and morphology of other structures, and specific clues [16,18]. In the event of disagreement between the dermoscopists, the final decision on the description was made by a third dermoscopist (G.K.-W.).

2.4. Statistical Analysis

In the final statistical evaluation, a database based on archived and described 216 dermoscopic images and 36 clinical images was analyzed. The degree of agreement between 2 independent researchers and the degree of agreement between the clinical and dermoscopic features was assessed using Cohen's kappa coefficient. Univariate binary logistic regression was applied to assess the influence of RT fractions on the binary outcomes of skin diagnosis. A multivariate ordinal logistic model was used to estimate the influence of the collected risk factors on the dermoscopic images and clinical features, consistent with the methodology of the study. Due to repeated measures with consecutive RT fractions for each patient, the regressions were extended for random effects (we fitted our data using Generalized Linear Mixed Models via Penalized Quasi-Likelihood for binomial families). The statistical results were expressed by a classical odds ratio (OR) together with a 95% confidence interval (CI 95%) and a *p*-value. The computation was performed using the R statistical platform [19] with the MASS package [20].

3. Results

In 82% of the dermoscopic and macroscopic image evaluations, the agreement between two independent observers based on Cohen's κ coefficient was equal to 1.0. All 32 patients observed during the follow-up after RT developed CRD. The highest score per RTOG/EORTC [17] was grade 2 observed in 21 patients. The remaining patients developed grade 1 CRD. In the 3rd month of observation, 10 patients developed grade 2 CRD, and the remaining 6 developed grade 1 CRD. In the 6th month of observation, five patients developed grade 2 CRD, and the remaining two developed grade 1. In the 12th month of observation, six patients developed grade 2 CRD, and the remaining three developed grade 1. Two patients had a change in reaction grade, i.e., from 1 to 2 for one patient and from 2 to 1 for the other patient, at 3 and 6 months of follow-up, respectively.

Table 1 shows the percentage of dermoscopic features in the respective clinical grade of CRD.

Table 1. The proportion of dermoscopic features, based on the consensus of the experts for non-neoplastic dermatoses on behalf of the IDS [18], to the grade of CRD according to the RTOG/EORTC scale [17]. The proportion was based on the analysis of 216 dermoscopy images in 6 areas (4 irradiated areas and 2 control areas) in 32 patients (in 28 patients with one time point and 4 patients with two time point observations).

		CRD	
RTOG/EORTC	**0**	**Grade 1**	**Grade 2**
Vessel morphology			
Dotted	18.75%	84.6%	82.6%
Linear (without bends or branches)	3.13%	7.7%	4.4%
Linear with branches	65.63%	61.5%	69.6%
Linear curved	46.88%	76.9%	47.8%
Vessel distribution			
Uniform	0.0%	0.0%	0.0%
Clustered	18.75%	53.9%	43.5%
Peripheral	0.0%	0.0%	0.0%
Reticular	0.0%	0.0%	4.4%
Unspecific	75.0%	84.6%	91.3%
Scale color			
White	15.63%	53.9%	52.2%
Yellow	0.0%	7.7%	13.0%
Brown	0.0%	15.4%	17.4%
Scale distribution			
Diffuse	0.0%	0.0%	0.0%
Central	0.0%	0.0%	0.0%
Peripheral	0.0%	7.7%	0.0%
Patchy	15.63%	46.2%	56.5%
Follicular findings			
Follicular plugs	0.0%	0.0%	0.0%
Follicular red dots	0.0%	0.0%	0.0%
Perifollicular white color	3.13%	15.4%	43.5%
Perifollicular pigmentation	9.38%	23.1%	0.0%

Table 1. *Cont.*

	CRD		
RTOG/EORTC	**0**	**Grade 1**	**Grade 2**
Other structures			
White structureless	3.13%	92.3%	100.0%
Brown structureless	0.0%	0.0%	0.0%
Yellow structureless	0.0%	0.0%	0.0%
White dots or globules	0.0%	0.0%	0.0%
Brown dots or globules	31.25%	69.2%	95.7%
Yellow dots or globules	0.0%	0.0%	0.0%
White lines	21.88%	84.6%	78.3%
Brown lines	0.0%	0.0%	0.0%
Yellow lines	0.0%	0.0%	0.0%

The typical clinical and dermoscopic features are presented in Figure 1A–D.

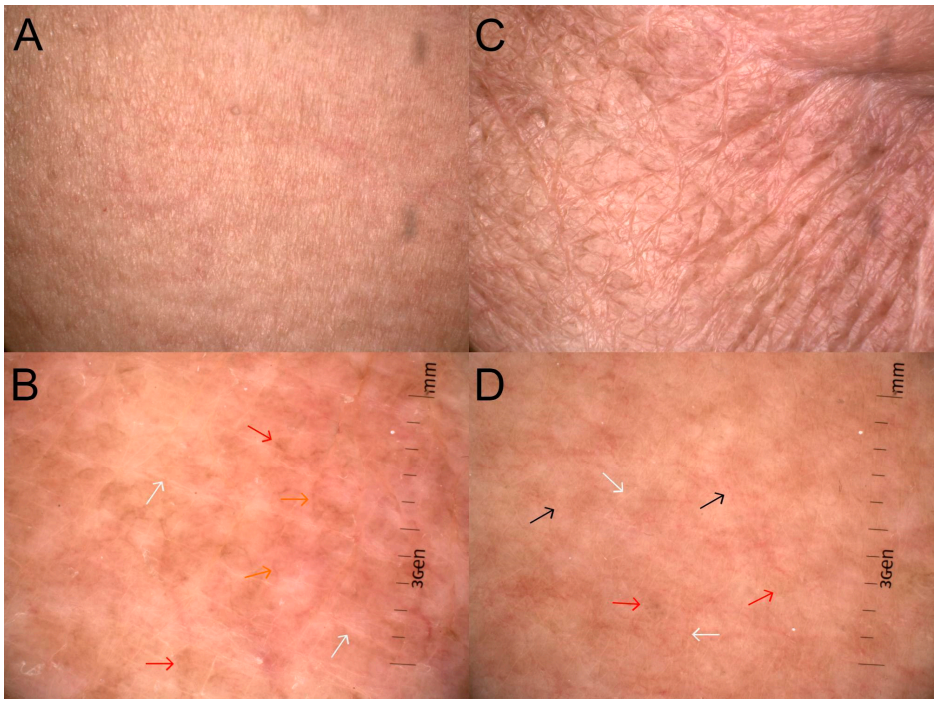

Figure 1. CRD on macroscopic images (**A**,**C**) across grades (G) G1 to G2, assessed according to RTOG criteria [17]. Dermoscopic images (**B**,**D**) are described according to the International Dermoscopy Society (IDS) by Errichetti et al. [18]. (**A**)—slight atrophy, pigmentation change (G1); (**B**)—linear vessels (orange arrows) in unspecific distribution, brown dots or globules (red arrows), and white lines (white arrows); (**C**)—patchy atrophy, total hair loss (G2); (**D**)—dotted vessels (black arrows) with unspecific distribution, brown dots or globules (red arrows), and white lines (white arrows).

The vascular polymorphisms observed in healthy skin were also found in all degrees of CRD. Of note is the significantly increased proportion of dotted vessels (Figure 2A,B,E,H), which—in healthy skin—was revealed in 18.75% of observations, while in areas subjected to RT, the incidence increased to 82.6–84.6%. The arrangement of vessels was also heterogeneous. In healthy skin, clustered distribution (Figure 2B,E,H) was evident in 18.75% of observations, in 53.9% of observations in grade 1 CRD, and 43.5% of grade 2 observations. In all degrees of CRD, yellow and brown scales were present, which was not observed in healthy skin. Moreover, the proportion of white scales (Figure 2C,D,G) compared to healthy skin (15.63%) increased to 53.9% in grade 1 CRD and to 52.2% in grade 2. Regarding follicular findings, an increase in the incidence of perifollicular white color (Figure 2D) was

observed. In healthy skin, this feature was found only in 3.13% of observations, whereas in grades 1 and 2, it was noted in 15.4%, and 42.5%, respectively. With the increase in the grade of CRD, an increase in the incidence of white structureless areas (Figure 2E,H), brown dots and globules (Figure 1B,D and Figure 2C,F), and white lines (Figure 1B,D and Figure 2D,F,G) was observed. Such features were found in grade 1 in 92.3%, 69.2%, and 84.6% of patients, respectively, and in grade 2 in 100%, 95.7%, and 78.3% of patients, respectively. In healthy skin, white structureless areas (Figure 2E,H), brown dots and globules (Figure 1B,D and Figure 2C,F), and white lines (Figure 1B,D and Figure 2D,F,G) appeared in 3.13%, 31.25%, and 21.88% of patients, respectively.

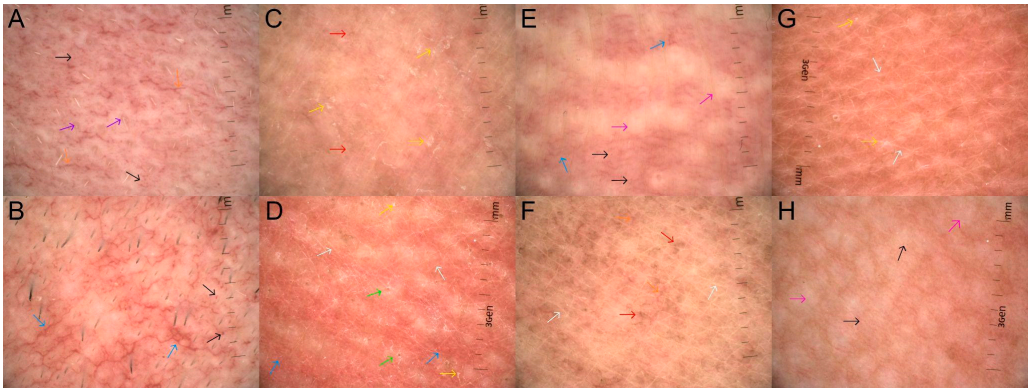

Figure 2. The description of the dermoscopic images of CRD based on the consensus of the experts for non-neoplastic dermatoses on behalf of the IDS [18]. (**A**)—dotted vessels (black arrows) and linear vessels (orange arrows) with unspecific distribution, and perifollicular pigmentation (purple arrows); (**B**)—dotted (black arrows) and linear with branch vessels (blue arrows) with clustered distribution; (**C**)—white patchy scale (yellow arrows), and brown dots and globules (red arrows); (**D**)—linear with branch vessels (blue arrows) with reticular distribution, perifollicular white color (green arrows), white patchy scale (yellow arrows), white lines (white arrows); (**E**)—linear with branches (blue arrows) and dotted vessels (black arrows) with clustered distribution and white structureless areas (pink arrows); (**F**)—linear vessels (orange arrows) with unspecific distribution, brown dots and globules (red arrows) and white lines (white arrows); (**G**)—white patchy scale (yellow arrows) and white lines (white arrows); (**H**)—dotted vessels (black arrows) in clustered distribution and white structureless areas (pink arrows).

Table 2 shows the relationship between dermoscopic and clinical features using the K coefficient. Statistically significant results are highlighted in bold (Table 2).

Table 2. The degree of agreement between the presence of selected clinical [17] and dermoscopic features [18] in CRD was assessed with values of κ statistics.

Dermoscopic Features	Clinical Features						
	Slight Atrophy	**Patchy Atrophy**	**Pigmentation Change**	**Some Hair Loss**	**Total Hair Loss**	**Thin Telangiectasias**	**Moderate Telangiectasias**
Dotted vessels	−0.05	0.0625	0.0357	0.111	−0.111	0.16	−0.0125
Linear vessels	0.0217	−0.0161	0.0188	0.111	−0.111	−0.0112	−0.0862
Linear vessels with branches	−0.105	0.118	0.0488	0	0	**0.423**	0.149
Linear curved vessels	0.135	−0.143	−0.0105	0.278	−0.278	0.264	**0.207**
Clustered vessels	0.103	−0.101	−0.0682	0.167	−0.167	0.0613	0.19
Reticular vessels	−0.0549	0.04	0.00917	0.0556	−0.0556	−0.0559	**0.301**
Unspecific vessels	−0.0328	0.0426	**0.366**	0	0	0.027	0.0395

Table 2. *Cont.*

Dermoscopic Features	Clinical Features						
	Slight Atrophy	**Patchy Atrophy**	**Pigmentation Change**	**Some Hair Loss**	**Total Hair Loss**	**Thin Telangiectasias**	**Moderate Telangiectasias**
White scale	−0.101	0.103	0.074	0.0556	−0.0556	0.161	0.145
Yellow scale	−0.0851	0.0656	0.0395	0	0	0.0795	−0.141
Brown scale	−0.0625	0.05	−0.0125	0.111	−0.111	0.069	0.0357
Peripheral scale	0.0769	−0.056	0.00917	0.0556	−0.0556	0.0447	−0.0485
Patchy scale	−0.211	0.215	0.074	0.0556	−0.0556	0.0497	0.145
Perifollicular white color	**−0.353**	**0.316**	0.149	0	0	−0.0714	−0.0976
Perifollicular pigmentation	**0.226**	**−0.171**	**−0.11**	0.167	−0.167	0.136	−0.116
White structureless areas	−0.06	0.08	**0.30**	−0.06	0.06	0.07	0.01
Brown dots or globules	−0.19	0.24	0.30	−0.17	0.17	−0.15	−0.02
White lines	0.09	−0.11	0.01	0.06	−0.06	−0.25	0.00

Described compatibility was 0.226–0.423 for slight atrophy, pigmentation change, thin telangiectasias, moderate telangiectasias, and dermoscopic features such as linear vessels with branches, linear curved vessels, reticular vessels, and perifollicular pigmentation.

In the next phase of the analysis, the influence of age, gender, indCHT, concomitant CHT, total radiation dose, fractional dose, tumor location, and histopathological diagnosis on the tumor size and the presence of dermoscopic and clinical features were investigated. This analysis was performed using logistic regression.

Table 3 shows statistically significant dermoscopic and clinical features and possible risk factors for CRD using odds ratios, whereas OR is a measure of association between radiation exposure and the clinical outcome; OR > 1 indicates the increased occurrence of any event, while OR < 1 indicates protective exposure.

We observed a relationship between the presence of white structureless areas (Figure 2E,H) and age, fraction dose, number of fractions, and total dose. The statistical interpretation of the OR (univariate regression) may be as follows: a 5-year difference in the age of patients generates a (1.20^5) × 100% = 249% higher risk in the occurrence of white structureless areas (Figure 2E,H). An increase of 5 fractions generates a (1.15^5) × 100% = 201% higher risk in the occurrence of white structureless areas (Figure 2E,H). A 10 Gy difference in the total dose generates a (1–1.20^10) × 100% = 137% higher risk in the occurrence of white structureless areas (Figure 2E,H). The other results in the table are to be interpreted in a similar way.

Age was a significant factor for patchy scale (Figure 2C,D,G), perifollicular pigmentation (Figure 2A), and white structureless areas (Figure 2E,H) in a univariate analysis.

Gender is an important individual factor for the presence of linear vessels (Figures 1B and 2A,F) and pigmentation change (Figure 1A). The risk of linear vessels (Figures 1B and 2A,F) is 94% lower for women than men, while pigmentation change (Figure 1A) is almost 1077% (almost 11 times) higher for women than men.

The presence of surgery increases the risk of the occurrence of white scale (Figure 2C,D,G) more than 4 times.

As the number of fractions and the total dose increases, the risk of white structureless areas (Figure 2E,H), brown dots and globules (Figure 1B,D and Figure 2C,F), pigmentation change (Figure 1A), as well as some and total hair loss (Figure 1C) increases. Not surprisingly, the number of fractions and total dose are also related to development grades per RTOG/EORTC [17].

Table 3. The influence of clinical data on the occurrence of macroscopic and dermoscopic features in CRD. The table shows statistically significant OR ($p < 0.05$) (in univariate binary logistic regression).

Dermoscopic Features		**Univariate Analysis (OR (95%CI) *p*-Value)**	
Linear vessels (without bends or branches)	Gender	0.06 (0.00–0.89)	0.0400
White scale	Operation	4.06 (1.06–17.68)	0.0402
Patchy scale	Age	1.10 (1.01–1.23)	0.0264
Perifollicular pigmentation	Age	1.31 (1.03–1.98)	0.0243
White structureless areas	Age	1.20 (1.04–1.71)	0.0105
	Fraction dose	0.17 (0.00–0.65)	0.0092
	Number of fractions	1.15 (1.02–3.48)	0.0235
	Total dose	1.09 (1.02–1.77)	0.0168
Brown dots or globules	Number of fractions	1.10 (1.02–1.20)	0.0171
	Total dose	1.05 (1.00–1.10)	0.0339
Clinical Features			
Pigmentation change	Gender	11.77 (1.79–133.87)	0.0098
	Number of fractions	1.11 (1.03–1.21)	0.0088
	Total dose	1.06 (1.02–1.12)	0.0086
Some hair loss	Number of fractions	0.87 (0.59–0.97)	0.0070
	Total dose	0.84 (0.67–0.98)	0.0038
	Radiochemotherapy	0.18 (0.04–0.69)	0.0123
Total hair loss	Number of fractions	1.12 (1.02–1.45)	0.0141
	Total dose	1.16 (1.02–1.45)	0.0067
	Radiochemotherapy	6.20 (1.59–28.18)	0.0080
RTOG	Number of fractions	1.07 (1.00–1.18)	0.0479
	Total dose	1.04 (1.00–1.11)	0.0494

Concurrent CHT increases the risk of complete hair loss by more than 6 times (OR = 6.20 (1.59–28.18)).

In the next step, as shown in Table 4, the influence of time on the occurrence of clinical and dermatoscopic characteristics was included in the analysis due to the different observation periods (Table 4).

Table 4. The influence of time on the occurrence of macroscopic and dermoscopic features in CRD. The table presents only dermoscopic structures that appeared statistically significant over time, extracted from all assessed dermoscopic structures presented in CRD. The table shows statistically significant ORs ($p < 0.05$) (in univariate binary logistic regression).

Dermoscopic Features	**Univariate Analysis (OR (95%CI) *p*-Value)**	
Dotted vessels	1.31 (1.12–1.59)	0.0002
White scale	1.18 (1.04–1.34)	0.0068
Patchy scale	1.22 (1.08–1.40)	0.0011
Perifollicular white color	1.21 (1.06–1.39)	0.0047
White structureless areas	2.67 (1.78–4.46)	<0.0001
Brown dots or globules	1.82 (1.35–2.69)	<0.0001
White lines	1.25 (1.09–1.50)	0.0008

Time in a month statistically generates a higher probability of the appearance of dotted vessels (Figure 2A,B,E,H), white scale (Figure 2C,D,G), patchy scale (Figure 2C,D,G), perifollicular white color (Figure 2D), white structureless areas (Figure 2E,H), brown dots and globules (Figure 1B,D and Figure 2C,F), and white lines (Figure 1B,D and Figure 2D,F,G).

4. Discussion

CRD is a subset of side effects of RT that can develop after treatment [8]. According to the literature, CRD occurs in one-third of all patients up to at least 10 years after RT [7]. Other authors believe that we cannot be precise on the time of its occurrence [21]. In our study, all observed patients developed CRD after RT. CRD is often a permanent, progressive, and potentially irreversible complication. In contrast to ARD, CRD does not heal on its own and can persist indefinitely [22].

Looking at the results of our study, in each month of observation (3rd, 6th, and 12th), grade 2 prevailed and it was the highest achieved grade among the observed patients.

In the current literature, dermoscopy has not been used to describe CRD and only clinical features have been described [23]. In the published data, we could not find a description involving the severity of CRD with dermoscopic observation. Dermoscopy assessment allows for the correlation of the macroscopic and dermoscopic features and therefore expands our knowledge about the presence and evolution of CRD. It is a much more accurate examination method than the unaided eye to confirm our diagnosis and can also result in a list of different diagnoses. Understanding the biology of dermoscopic changes observed during long-term follow-up may indicate prognostic factors for reaction severity and predictive factors for effective future treatments.

The basic mechanism for the development of chronic skin reactions is a persistent inflammatory response that begins after the first RT session and then continues for months or years [21,24].

Dotted vessels can be seen on inflamed or damaged skin [25], as confirmed by our study, which revealed an over fourfold increase in the incidence of this type of vessels in skin with diagnosed CRD compared to healthy skin. Moreover, clustered vessels can also be seen in dermatitis, and this is due to vasodilation in focally elongated dermal papillae [18,25]. The incidence of this type of distribution increased twofold in the skin with developed CRD compared to healthy skin in our results. The white scale, which is a feature of dermatoses characterized by hyperkeratosis (especially parakeratosis) without serous exudate, was also observed twice as often in CRD [18]. A greater incidence of perifollicular white color with a higher degree of CRD was noted. Histologically, perifollicular white color may correspond to perifollicular fibrosis [18].

According to our first study on ARD [16], we also attempted to investigate the correlation between clinical and dermoscopic features of CRD. The macroscopic features corresponded with dermoscopic features such as linear vessels with branches, linear curved vessels, vessels with reticular distribution, vessels with unspecific distribution, perifollicular white color, white structureless areas, and perifollicular pigmentation.

Radiation dermatitis can occur as a result of occupational or accidental exposure to ionizing radiation [26]. The risk factors for this disorder can be classified as intrinsic, extrinsic, or both.

Intrinsic factors include age, gender, smoking, nutritional status, genetic factors, connective tissue and skin diseases, concurrent CHT, and targeted therapy [27]. Extrinsic factors, on the other hand, are mainly related to the type and dose of radiation received [28].

Meyer et al. [29] showed that the risk of late severe toxicity increases with age. In our data, age was a significant factor for patchy scale and white structureless areas, the frequency of which increases in CRD compared to healthy skin. Moreover, gender also had a significant impact on the development of CRD [29]. In our study, women were more than 11 times more likely to have a pigmentation change. An increase in the number of fractions and the total dose raises the risk of white structureless areas, brown dots and globules, pigmentation change as well as some and total hair loss.

Not surprisingly, the number of fractions and total irradiation dose are also related to the development of higher grades per RTOG/EORTC. According to the previous study by Kawamura et al. [30], concomitant CHT is important for the development of ARD.

Toledano et al. in their study found that after breast-conserving surgery in patients, the simultaneous use of adjuvant CHT and RT increases late toxicity [31]. In our study, concurrent CHT increased the risk of complete hair loss by more than 6 times.

Limitations of the Study

The study group in our prospective observational study included a cohort of patients undergoing RT due to HNC. Despite the significant prevalence of this malignancy and the prevalent ARD in the course of this RT procedure, it should be emphasized that the small group of patients is due to the rarer occurrence of CRD and the longer follow-up time is required for its diagnosis and the unfavorable prognosis of treated patients, resulting in the possibility of losing patients from follow-up.

Criteria for regular follow-ups in a structured form were checked at 3, 6, and 12 months after the end of RT. However, the lack of regular follow-ups was mainly due to the loss of patients in this group with an unfavorable prognosis. In our study, only four patients were followed at two time points.

Another limitation of this study is the absence of cohorts of patients who do not develop CRD. Such a control group should be included in further research, or the group size should be increased by including subsequent patients after RT, regardless of clinically expressed reaction.

5. Conclusions

This is the first study showing the potential role of dermoscopy in CRD evaluation. Until now, there was no other objective tool for qualitative analyses of CRD. The dermoscopic features that had been shown in our study reflect the biological reaction of the skin towards radiation and may be used for the parametrization of CRD regarding its intensity and any other clinical consequences in the future. However, further research is needed to confirm the role of dermoscopy and to gather more clinical data on its utilization in CRD assessment.

Author Contributions: Conceptualization: A.P., G.K.-W. and T.R. Data curation: A.P. Formal analysis: A.P., A.S.-S., A.T. and G.K.-W. Funding acquisition: G.K.-W. Investigation: A.P. Methodology: A.P., G.K.-W. and T.R. Project administration: A.P., G.K.-W. and T.R. Resources: A.P. and A.S.-S. Software: A.T. Supervision: G.K.-W. Validation: A.P. and A.T. Visualization: A.P. Writing—original draft preparation: A.P. Writing—review and editing: A.P., A.S.-S., G.K.-W., A.T., T.R. and K.S. All authors have read and agreed to the published version of the manuscript.

Funding: This research received funding from Maria Sklodowska-Curie National Research Institute of Oncology (MSCNRIO), financing from the Institute's own funds not related to the grant.

Institutional Review Board Statement: The authors received approval (02.04.2019) from the local ethics committee of the National Research Institute of Oncology (reference number KB/430-44/19). The study was conducted in accordance with the Declaration of Helsinki in 1964, as amended.

Informed Consent Statement: Informed consent was obtained from all subjects involved in the study. Written informed consent has been obtained from the patients to publish this paper.

Data Availability Statement: The data presented in this study are available upon request from the corresponding author.

Acknowledgments: The authors thank the patients for their participation in the study.

Conflicts of Interest: The authors declare no conflicts of interest.

References

1. American Cancer Society. Cancer Facts & Figures 2024. Available online: https://www.cancer.org (accessed on 17 January 2024).
2. Gamerith, G.; Fuereder, T. Treating head and neck cancer—A multidisciplinary effort. *Memo* **2020**, *13*, 359–360. [CrossRef]
3. Ziółkowska, E.; Biedka, M.; Windorbska, W. Odczyn popromienny u chorych na raka regionu głowy i szyi: Mechanizmy i konsekwencje. *Otorynolaryngologia* **2011**, *10*, 147–153.
4. Borrelli, M.R.; Shen, A.H.; Lee, G.K.; Momeni, A.; Longaker, M.T.; Wan, D.C. Radiation-Induced Skin Fibrosis: Pathogenesis, Current Treatment Options, and Emerging Therapeutics. *Ann. Plast Surg.* **2019**, *83*, S59–S64. [CrossRef] [PubMed]
5. DeSantis, C.E.; Lin, C.C.; Mariotto, A.B.; Siegel, R.L.; Stein, K.D.; Kramer, J.L.; Alteri, R.; Robbins, A.S.; Jemal, A. Cancer treatment and survivorship statistics. *CA Cancer J. Clin.* **2014**, *64*, 252–271. [CrossRef] [PubMed]
6. Dudek, A.; Rutkowski, T.; Kamińska-Winciorek, G.; Krzysztof Składowski, K. What is new when it comes to acute and chronic radiation-induced dermatitis in head and neck cancer patients? *Nowotw. J. Oncol.* **2020**, *70*, 9–15. [CrossRef]
7. Whelan, T.J.; Pignol, J.P.; Levine, M.N.; Julian, J.A.; MacKenzie, R.; Parpia, S.; Shelley, W.; Grimard, L.; Bowen, J.; Lukka, H.; et al. Long-term results of hypofractionated radiation therapy for breast cancer. *N. Engl. J. Med.* **2010**, *362*, 513–520. [CrossRef] [PubMed]
8. Hegedus, F.; Mathew, L.M.; Schwartz, R.A. Radiation dermatitis: An overview. *Int. J. Dermatol.* **2017**, *56*, 909–914. [CrossRef]
9. Robijns, J.; Laubach, H.J. Acute and chronic radiodermatitis. *J. Egypt. Women's Dermatol. Soc.* **2018**, *15*, 2–9. [CrossRef]
10. Wong, R.K.; Bensadoun, R.J.; Boers-Doets, C.B.; Bryce, J.; Chan, A.; Epstein, J.B.; Eaby-Sandy, B.; Lacouture, M.E. Clinical practice guidelines for the prevention and treatment of acute and late radiation reactions from the MASCC Skin Toxicity Study Group. *Support. Care Cancer* **2013**, *21*, 2933–2948. [CrossRef]
11. Lanigan, S.W.; Joannides, T. Pulsed dye laser treatment of telangiectasia after radiotherapy for carcinoma of the breast. *Br. J. Dermatol.* **2003**, *148*, 77–79. [CrossRef]
12. Yarnold, J.; Brotons, M.C. Pathogenetic mechanisms in radiation fibrosis. *Radiother. Oncol.* **2010**, *97*, 149–161. [CrossRef] [PubMed]
13. Phulpin, B.; Gangloff, P.; Tran, N.; Bravetti, P.; Merlin, J.L.; Dolivet, G. Rehabilitation of irradiated head and neck tissues by autologous fat transplantation. *Plast. Reconstr. Surg.* **2009**, *123*, 1187–1197. [CrossRef] [PubMed]
14. Martin, M.; Lefaix, J.L.; Delanian, S. TGF-β1 and radiation fibrosis: A master switch and a specific therapeutic target? *Int. J. Radiat. Oncol. Biol. Phys.* **2000**, *47*, 277–290. [CrossRef] [PubMed]
15. Kamińska-Winciorek, G.; Pilśniak, A. The role of dermoscopy in dermato-oncological diagnostics—New trends and perspectives. *Nowotw. J. Oncol.* **2021**, *71*, 103–110. [CrossRef]
16. Pilśniak, A.; Szlauer-Stefańska, A.; Tukiendorf, A.; Rutkowski, T.; Składowski, K.; Kamińska-Winciorek, G. Dermoscopy of acute radiation-induced dermatitis in patients with head and neck cancers treated with radiotherapy. *Sci. Rep.* **2023**, *13*, 15711. [CrossRef] [PubMed]
17. Cox, J.D.; Stetz, J.; Pajak, T.F. Toxicity criteria of the Radiation Therapy Oncology Group (RTOG) and the European Organization for Research and Treatment of Cancer (EORTC). *Int. J. Radiat. Oncol. Biol. Phys.* **1995**, *31*, 1341–1346. [CrossRef] [PubMed]
18. Errichetti, E.; Zalaudek, I.; Kittler, H.; Apalla, Z.; Argenziano, G.; Bakos, R.; Blum, A.; Braun, R.P.; Ioannides, D.; Lacarrubba, F.; et al. Standardization of dermoscopic terminology and basic dermoscopic parameters to evaluate in general dermatology (non-neoplastic dermatoses): An expert consensus on behalf of the International Dermoscopy Society. *Br. J. Dermatol.* **2020**, *182*, 454–467. [CrossRef]
19. R Core Team. *R: A Language and Environment for Statistical Computing*; R Foundation for Statistical Computing: Vienna, Austria, 2022. Available online: https://www.R-project.org (accessed on 31 October 2023).
20. Venables, W.N.; Ripley, B.D. *Modern Applied Statistics with S*, 4th ed.; Springer: New York, NY, USA, 2022.
21. Spałek, M. Chronic radiation-induced dermatitis: Challenges and solutions. *Clin. Cosmet. Investig. Dermatol.* **2016**, *9*, 473–482. [CrossRef]
22. Hymes, S.R.; Strom, E.A.; Fife, C. Radiation dermatitis: Clinical presentation, pathophysiology, and treatment. *J. Am. Acad. Dermatol.* **2006**, *54*, 28–46. [CrossRef]
23. Bray, F.N.; Simmons, B.J.; Wolfson, A.H.; Nouri, K. Acute and Chronic Cutaneous Reactions to Ionizing Radiation Therapy. *Dermatol. Ther.* **2016**, *6*, 185–206. [CrossRef]
24. Vozenin-Brotons, M.C.; Milliat, F.; Sabourin, J.C.; de Gouville, A.C.; François, A.; Lasser, P.; Morice, P.; Haie-Meder, C.; Lusinchi, A.; Antoun, S. Fibrogenic signals in patients with radiation enteritis are associated with increased connective tissue growth factor expression. *Int. J. Radiat. Oncol. Biol. Phys.* **2003**, *56*, 561–572. [CrossRef] [PubMed]
25. Anscher, M.S. The irreversibility of radiation-induced fibrosis: Fact or folklore? *J. Clin. Oncol.* **2005**, *23*, 8551–8552. [CrossRef] [PubMed]
26. Wolff, K.; Johnson, R.; Saavedra, A. Skin reactions to ionizing radiation. In *Fitzpatrick's Color Atlas and Synopsis of Clinical Dermatology*; McGraw-Hill: New York, NY, USA, 2013.
27. Porock, D. Factors influencing the severity of radiation skin and oral mucosal reactions: Development of a conceptual framework. *Eur. J. Cancer Care* **2002**, *11*, 33–43.
28. Hegedus, F.; Schwartz, R.A. Cutaneous radiation damage: Updating a clinically challenging concern. *G. Ital. Dermatol. Venereol.* **2019**, *154*, 550–556. [CrossRef] [PubMed]
29. Meyer, F.; Fortin, A.; Wang, C.S.; Liu, G.; Bairati, I. Predictors of severe acute and late toxicities in patients with localized head-and-neck cancer treated with radiation therapy. *Int. J. Radiat. Oncol. Biol. Phys.* **2012**, *82*, 1454–1462. [CrossRef]

30. Kawamura, M.; Yoshimura, M.; Asada, H.; Nakamura, M.; Matsuo, Y.; Mizowaki, T. A scoring system predicting acute radiation dermatitis in patients with head and neck cancer treated with intensity-modulated radiotherapy. *Radiat. Oncol.* **2019**, *14*, 14. [CrossRef] [PubMed]
31. Toledano, A.; Garaud, P.; Serin, D.; Fourquet, A.; Bosset, J.F.; Breteau, N.; Body, G.; Azria, D.; Le Floch, O.; Calais, G. Concurrent administration of adjuvant chemotherapy and radiotherapy after breast-conserving surgery enhances late toxicities: Long-term results of the ARCO-SEIN multicenter randomized study. *Int. J. Radiat. Oncol. Biol. Phys.* **2006**, *65*, 324–332. [CrossRef]

VIA MEDICA

Review article

NOWOTWORY Journal of Oncology
2020, volume 70, number 1, 9–15
DOI: 10.5603/NJO.2020.0002

ISSN 0029–540X
www.nowotwory.edu.pl

What is new when it comes to acute and chronic radiation-induced dermatitis in head and neck cancer patients?

Aleksandra Dudek[1], Tomasz Rutkowski[1], Grażyna Kamińska-Winciorek[2], Krzysztof Składowski[1]

[1]*Inpatient Department of Radiation and Clinical Oncology, Maria Sklodowska-Curie National Research Institute of Oncology, Gliwice Branch, Gliwice, Poland*

[2]*Department of Bone Marrow Transplantation and Oncohematology, Maria Sklodowska-Curie National Research Institute of Oncology, Gliwice Branch, Gliwice, Poland*

Head and neck cancer is a serious clinical and social problem. Surgery and radiotherapy play the most important role in treatment and give the chance of cure. Optimal treatment of patients with head and neck cancer should provide for the maximum destruction of cancerous tissue, saving as much healthy tissue as possible. Despite this, due to radiotherapy still almost 90% of patients develop skin symptoms. It seems that the mechanism of radiodermatitis is quite clear, but studies assume that its pathogenesis is not fully understood and there is much to be clarified. Acute and chronic dermatitis caused by radiotherapy is usually diagnosed according to clinical criteria. It seems that it would be useful to have a photographic classification that would facilitate and unify the clinical evaluation. In this article we shall summarize the current knowledge about the mechanisms of formation, risk factors, clinical classifications and methods for the prevention and treatment of acute and chronic radiation dermatitis. We have included clinical photos that depict individual stages according to the clinical classification of RTOG.

NOWOTWORY J Oncol 2020; 70, 1: 9–15

Key words: acute and chronic radiation-induced dermatitis

Introduction

Head and neck cancer is a serious clinical and social problem. The major reason for poor treatment results is the advanced stage of disease at diagnosis. Surgery and radiotherapy are the main treatment options that give a chance of a complete cure [1]. Radiotherapy utilizes ionizing radiation that usually covers relatively large volumes of tissue surrounding the tumor [2]. The optimal treatment of patients with head and neck cancer involves a compromise between destroying as much cancerous tissue as possible, and saving as much healthy tissue as possible [3]. Radiotherapy should be carried out with the use of modern technologies, such as conformal 3D radiation, and, in particular, intensity-modulated radiation therapy (IMRT) [1]. This method allows for a significant reduction in tissue volume subject to the high radiation dose, and in the intensity of acute radiation-related reactions of these tissues. Despite this, still almost 90% of patients develop skin symptoms after radiotherapy [4]. Radiation-induced reactions can be divided into early and late as regards the time of their appearance in the relation to radiotherapy. Acute (early) ones appear during radiotherapy and usually disappear a few weeks after the completion of the treatment. Late reactions appear months after radiotherapy and may leave chronic results [5]. In turn, as far as the extent of radiation is concerned, reactions can be local or generalized [2, 3].

Pathogenesis

According to the Michalowski and Wheldon classification, proliferative tissues can be divided into "hierarchical" and "flexible",

and consequently, the course of radiation injury differs in these two groups [6]. The skin belongs to hierarchical tissues and is made of mature cells, maturing cells and stem cells. Radiotherapy causes cells, 70% of which is composed of water, to become ionized [6]. Hydrolysis of water and the formation of free radicals, be it direct or indirect, causes breaks in the DNA and cell death. The lethal effect mainly pertains to stem cells and, to some extent, to maturing cells [3]. Consequently, the balance between normal cell production at skin's basal layer and cell destruction at skin surface is disrupted [3]. The radiation-induced skin reaction reflects the degree of cell damage. Its intensity depends on the radiation dose, and increases with the number of stem cells that die. The first phase, transient erythema, may occur 24 hours after radiotherapy, with vessels becoming wider and more permeable [5]. Inflammatory cytokines, prostaglandins, and many other mediators are secreted [3, 5]. This inflammatory reaction causes the development of a secondary erythematous response. Immune cells, keratinocytes, fibroblasts and other cells are stimulated. Subsequent radiation doses create a vicious circle and correlate with the degree of radiodermatitis [7]. In the next phase, dry exfoliation usually occurs, which results from the disturbed balance between the division of new cells and the exfoliation of the old ones. In the final stage, stem cells are lacking and the skin has no material from which to rebuild individual layers. Wet exfoliation and exudates occur [7]. The inflammation that started in the epidermis after the beginning of irradiation lasts for months, and even years. Inflammatory cytokines are secreted, including interleukin IL-1α, IL-1β, tumor necrosis factor TNF-α, TGF-β, IL-6, IL-8 [7]. The secretion of TGF-β, which is a central mediator of fibrogenesis, increases following the exposure to ionizing radiation, and it is proportional to the radiation dose delivered [8, 9]. Huang and Glick summarize the knowledge about major genes and polymorphisms, and delineate the role of TGF-β as a peptide protein gene associated with an immune response that plays an important role in both early and late dermatitis [10]. Studies using the rat and mice model show that those less equipped with this protein are not as sensitive to radiotherapy as wild rats [9, 11].

Despite this knowledge, the studies at the National Jewish Health Biological Resource Center assumed that pathogenesis of radiodermatitis is not fully understood. Using mouse models in their project, the researchers at the Center discovered that the transient receptor potential melastatin 2 (TRPM2) ion channel plays a major role in developing radiation injury. They suggest that TRPM2 may be a potential target for a systemic medicine which would inhibit this channel and reduce the severity of radiodermatitis [12]. However, other researchers who have also used mouse models say that plasminogen plays a major role in the development of radiation injury. Among other things, it participates in the activation of many inflammatory factors, such as TGF-β. Fallah et al. used tranexamic acid, postulating that inhibiting plasminogen could be used as treatment or as a preventive option in the future [13]. The pathogenesis of bio-radiation dermatitis differs from that associated with radiotherapy alone. Inhibition of the EGFR pathway results in a disruption of physiological processes associated with the migration and proliferation process, and the development of inflammation in the skin. The type of response depends on the degree of interaction between the inhibitor of EGFR pathway and radiotherapy [14]. The multitude of reports on factors that may be involved in the development of acute and chronic radiation-induced dermatitis is certainly attributable to the fact that many studies are still needed to find out the actual pathogenesis of this process.

Risk factors

The risk factors associated with the development of radiodermatitis can be divided into patient- and treatment-related [3, 7], where the letter include the type and energy of irradiation, the dose per fraction, the duration of treatment, and the total radiation dose [3]. An additional factor associated with the treatment may be concurrent chemotherapy. Researchers have shown that chemotherapy improves the therapeutic effect [15–17], but also increases the intensity of radiodermatitis [18]. EGFR inhibitor – cetuximab given during radiotherapy increases the intensity more seriously compared to radiotherapy alone [14]. Concomitant diseases, a patient's age, past injuries and surgeries in the irradiated area should be considered as the main patient-related factors [3]. Patients with genetic disorders, such as ataxia-telangiectasia or the Nijmegen syndrome, show a genetically determined susceptibility to the development of radiation damage. Consequently, their normal cells are hypersensitive to the radiation-related damage [3].

The neoplastic tissue itself is a constant factor affecting the severity and development of radiodermatitis. It secretes factors that increase the number of cells that divide both cancerous and healthy tissues [3]. Undoubtedly, the study conducted by Huang and Glick shows how many risk factors are associated with human genetic material and how many factors affect the development of radiodermatitis [10]. Kawamura et al. present a new radiation dermatitis scoring system. The results of their study show that radiation dose, concurrent chemotherapy, age and body mass index (BMI) have a predictive significance. On this basis, they constructed a score system combining the above parameters [18]. Apart from this, there are no other commonly used score systems that allow predicting the risk and intensity of acute and late skin reactions in patient before radiotherapy.

Clinical classification

In clinical practice, various clinical scales are applied in the assessment of acute and chronic radiodermatitis. The Radiation Therapy Oncology Group and the European Organization for Research and Treatment of Cancer (RTOG/EORTC), Common Terminology Criteria for Adverse Events (CTCAE), and the Late

Effects Normal Tissue Task Force-Subjective, Objective, Management, Analytic (LENTSOMA) scales are used most often [19]. RTOG/EORTC scale is dedicated to assessing early and late post-radiation reactions (Tab. I) [20].

LENTSOMA scores only late reactions [4]. In turn, CTCAE does not describe the late effect, but only its acute phase [19] (Tab. II).

Generally, RTOG scale refers to various tissues and organs. At grade 0, no skin reactions are observed. Reactions of different intensities are scored between grades I to IV, with death due to dermatitis at grade V [20]. In our review, we include figures presenting the individual grades in line with the RTOG classification.

At grade I, erythema of moderate intensity is observed. Hair loss and dry exfoliation may also occur (Fig. 1) [20]. At grade II, usually, tender or bright erythema is visible with moist desquamation. This is accompanied by moderate swelling (Fig. 2) [20]. At grade III, erythema is accompanied by swelling and moist exfoliation, which includes areas outside the skinfolds (Fig. 3) [20]. Grade IV is characterized by ulceration, bleeding

Figure 1. Follicular dull erythema with epilation and red dermographism in the course of acute radiodermatitis, RTOG/EORTC grade I

Table I. Early and late post-radiation reactions

	Grade I	Grade II	Grade III	Grade IV
Acute radiodermatitis	follicular, faint or dull erythema, epilation, dry desquamation, decrease sweating	tender or bright erythema, patchy moist desquamation, moderate edema	confluent, moist desquamation other then skin folds, pitting edema	ulceration, hemorrhage, necrosis
Chronic radiodermatitis	slight atrophy, pigmentation change, some hair loss	patchy atrophy, moderate teleangiectasia, total hair loss	marked atrophy, gross teleangiectasia	ulceration

Table II. Late post-radiation reactions – proposed modifications

	Grade I	Grade II	Grade III	Grade IV
NCI-CTCAE v 4.03 radiation dermatitis	faint erythema or dry desquamation	moderate to brisk erythema; patchy moist desquamation, mostly confined to skin folds and creases; moderate edema	moist desquamation in areas other than skin folds and creases; bleeding induced by minor trauma or abrasion	life-threatening consequences; skin necrosis or ulceration of full-thickness dermis; spontaneous bleeding from involved site; skin graft indicated
Proposed modifications	faint erythema or dry desquamation	moderate to brisk erythema and/or dry desquamation; patchy moist desquamation, **or nonhemorrhagic crusts mostly confined to skin folds and creases**	moist desquamation **or hemorrhagic crusts; nonhemorrhagic crusts other** than in skin folds and mostly confined to skin folds and creases; bleeding induced by minor trauma or abrasion; **superinfection requiring oral antibiotics**	life-threatening consequences; **extensive confluent hemorrhagic crusts or ulceration (>50% of involved field); extensive spontaneous bleeding from involved site (>40% of the involved site); skin necrosis or ulceration of full-thickness dermis or any size ulcer with extensive destruction, tissue necrosis or damage to muscle, bone or supporting structures with or without full-thickness skin loss; skin graft indicated; ulceration associated with extensive superinfection with i.v. antibiotics indicated**

Figure 2. Tender and bright erythema with moderate edema-within the irradiated area in the course of acute radiodermatitis, RTOG/EORTC grade II

and necrosis [20]. In contrast to the acute cutaneous reaction after radiation therapy, chronic dermatitis occurs not earlier than 90 days from completing radiotherapy and may develop even a few years after irradiation [5]. It is clinically characterized by moderate (Fig. 4) to severe atrophy (Fig. 7) accompanied by telangiectasia (Fig. 4–7), as well as ulceration (Fig. 7) (grade IV) [20]. RTOG, CTCAE and LENTSOMA are descriptive scales, with a risk of subjective evaluation and classification of acute and chronic radiation dermatitis [21]. Zenda et al. provide an atlas of radiodermatitis with pictures showing grades from I to IV according to CTCAE. A photographic classification could be useful in supporting and unifying the clinical one [21]. Acute and chronic dermatitis caused by radiotherapy is usually diagnosed based

Figure 3. Sharp demarcated, exacerbated erythema accompanied by swelling and moist exfoliation, expanding to non-irradiated neighbouring areas in the course of acute radiodermatitis, RTOG/EORTC grade III

Figure 4. Slight atrophy, poikilodermic pigmentation (mainly depigmentation) with permanent hair loss and several thin telangiectasias in the course of chronic radiodermatitis, RTOG/EORTC grade I

Figure 5. Patchy atrophy areas with thin, moderate telangiectasias accompanied by total hair loss and skin discoloration (depigmented and brownish spots) in the course of chronic radiodermatitis, RTOG/EORTC grade II

Figure 6. Marked skin atrophy presented as multiple whitish scarred lines with multiple gross telangiectasias in the course of chronic radiodermatits, RTOG/EORTC grade III

Figure 7. Advanced atrophy with multiple gross telangiectasias and desquamation of the skin. Diffused white atrophy with multiple thick telangiectasias also observed. Thinning of the skin of epidermis also seen in the course of chronic radiodermatitis, RTOG/EORTC grade IV

on the above-mentioned clinical criteria. CTCAE 4.0 appears to be the most commonly used scale during clinical assessment, but it is not a unified, unambiguous system for the assessment of post-radiation reactions [19]. It is worth mentioning that the combined treatment involving concomitant radiotherapy and EGFR inhibitor may result in reaction called bio-radiation dermatitis [22]. This type of reaction has a different pathogenesis and clinical characteristics [14]. Bernier et al. propose guidelines on the classification and treatment of bio-radiation dermatitis. These would help clinicians to properly assess and manage it. The treatment could be optimized, and there would be a greater chance of a good clinical outcome [14, 23]. Table II shows the changes proposed by Bernier et al. in relation to CTCEA. In grades II–IV, the change in type and extent of crusting can be observed. Infections may influence the intensity of bio-radiation and therefore appropriate local or systemic treatment should be considered (Tab. II) [14]. The extent of spontaneous bleeding is concerned at grade IV (Tab. II) [14].

Prevention and treatment

The latest recommendation on prevention and treatment was published in 2013 by the Multinational Association of Supportive Care in Cancer (MASCC) Skin Toxicity Study Group [19], and showed that randomized studies have confirmed that skin hygiene with the use of water, with or without gentle soap, and the use of antiperspirants is recommended. A positive effect of using topical glucocorticosteroids has also been shown [19].

In 2015 O'Donnovan carried out an anonymous online survey in Europe and in the United States [24]. It turned out that there is a large discrepancy between the clinical management, prevention and treatment of acute radiodermatitis, and what has been confirmed in scientific studies. Many of the commercially available products have no scientific support [24].

In 2017 Lucey et al. began another such study in the United States. They conclude that there is a considerably wide variety in the prevention and treatment of acute radiodermatitis [25]. At the same time, this type of research shows that, in fact, no recommendations are available yet. However, since clinical experience shows that this process yields some effects, it requires confirmatory research. Lucey et al. show that aloe vera, gentle soap, and topical glucocorticosteroids are most commonly used for the prevention of acute radiation injury [25]. When it comes to treatment, it is correlated with the degree of the development of radiodermatitis [25]. Dry desquamation is mostly treated with emollients and aloe vera [25]. For grade II and III, silver sulfadiazine cream is most commonly used. A comparison of procedures at different centers in the country showed that the procedures result from observation in 89% of cases, and only in 51,4% from scientifically confirmed studies [25]. There is evidently a need to carry out tests confirming the effectiveness of individual intervention. In 2018 a randomized Radiotherapy Related Skin Toxicity (RAREST-01) study commenced [26]. It compares standard care and Mepitel Film (gentle, transparent, breathable dressings) in patients with locally advanced squamous-cell carcinoma of the head and neck receiving radiotherapy or radiochemotherapy [26]. One of the surveys done in China confirmed the effectiveness of Mepitel Film dressings and it decreases acute radiation injury in head and neck cancer patients [27].

At the same time, the third phase of the study protocol of J-SUPPORT 1602 (TOPICS study) began, comparing topical glucocorticosteroids with placebo as prevention of radiation

injury [28]. Zhang et al. used red light therapy and it turned out that such an intervention may accelerate wound healing, reduce pain, and improve the patient's life [29]. Ferreira et al. published a review of 13 randomized studies. Intervention with trolamine, aloe vera, allantoin, Lianbai liquid (Chinese remedy), sucralfate, Na-sucrose octasulfate, olive oil, hyaluronic acid, and dexpanthenol did not show any benefits in prevention and treatment of radiation injury [30]. At the same time, there was no difference between the control group using institution routine, aqueous cream, mild soap, water thermal gel, placebo, and no intervention [30]. Regarding bio-radiation dermatitis, Bonomo et al. confirmed the effectiveness of calcium dressing for moist exfoliation [22]. Side effects like radiodermatitis which is particularly visible may significantly impair the quality of life. Non-pharmacological recommendations and patient education should not be forgotten [31].

It is very important to minimize the risk of infection using an appropriate standard of hygiene and choose the right cosmetics and cleaning products that are clinically tested and adapted to this group of patients. In addition, patients should remember about photoprotection [31]. Experts believe that in the interests of patient's well-being, the use of deodorants and non-irritating perfumes can be part of daily routine [31]. It is very important to conduct regular dermatological follow-ups due to the fact that chronic radiation dermatitis predisposes patients to secondary malignant tumors [32, 33].

Conclusions

At this time, there is a lot of reports on factors that may be involved in the pathogenesis of acute and chronic radiodermatitis. Further studies are still needed to confirm and find out the actual nature of the pathogenesis of this process. Clinical assessment is carried out using various clinical scales. There is no one unified system which would make our assessments uniform, and thanks to which we could subsequently proceed with treatment. There is a good chance that the photographic atlas presenting the selected grade of acute and chronic radiodermatitis may unify the clinical evaluation.

Currently, apart from one study, there are no specific prognostic factors and predictors that could indicate the dynamics and severity of acute dermatitis caused by radiotherapy or prognostic factors related to the late reaction of skin. Genetic susceptibility testing and the determination of the final pathogenesis pathway in the future may bring the target for treatment and prevention. Currently, the last recommendations come from 2013; they were published by MASCC Skin Toxicity Study Group [17]. By 2019, no new recommendations have been issued, and the clinics today are based on observation in 89% of cases and only in 51.4% on clinically confirmed results [23].

Appropriate assessment of the severity of acute and chronic radiation induced skin injury makes it possible to decide how to proceed with patients, especially with such groups for which the cosmetic effect has special importance for personal, social and professional reasons.

Conflict of interest: none declared

Grażyna Kamińska-Winciorek
Maria Sklodowska-Curie National Research Institute of Oncology, Gliwice Branch
Department of Bone Marrow Transplantation and Oncohematology
ul. Wybrzeże Armii Krajowej 15
44-101 Gliwice, Poland
e-mail: grazyna.kaminskawinciorek@gmail.com

Received: 4 Nov 2019
Accepted: 13 Jan 2020

References

1. Wierzbicka M, Bień S, Osuch-Wójcikiewicz E, et al. The recommendations of diagnostic and therapeutic in the treatment of head and neck cancers. Pol. Przegląd Otorynolaryngol. ; 2011: 17–43.
2. Biedka M, Dutsch-Wicherek M. Side effects of postoperative radiotherapy in patient with laryngeal cancer receiving immunosuppressive drugs after renal transplant. Otorynolaryngologia. 2015; 14(2): 108–116.
3. Ziółkowska E, Biedka M, Windorbska W. Odczyn popromienny u chorych na raka regionu głowy i szyi: mechanizmy i konsekwencje. Otorynolaryngologia. 2011; 10(4): 147–153.
4. Michalewska J. Odczyny popromienne w radioterapii oraz popromienne zapalenie skóry. Letters in Oncology Science. 2017; 14(4): 104–109, doi: 10.21641/los.14.4.41.
5. Hegedus F, Mathew LM, Schwartz RA. Radiation dermatitis: an overview. Int J Dermatol. 2017; 56(9): 909–914, doi: 10.1111/ijd.13371, indexed in Pubmed: 27496623.
6. Wheldon TE, Michalowski AS, Kirk J. The effect of irradiation on function in self-renewing normal tissues with differing proliferative organisation. Br J Radiol. 1982; 55(658): 759–766, doi: 10.1259/0007-1285-55-658-759.
7. Robijns J, Laubach HJ. Acute and chronic radiodermatitis. Journal of the Egyptian Women's Dermatologic Society. 2018; 15(1): 2–9, doi: 10.1097/01.ewx.0000529960.52517.4c.
8. Biernacka A, Dobaczewski M, Frangogiannis NG. TGF-β signaling in fibrosis. Growth Factors. 2011; 29(5): 196–202, doi: 10.3109/08977194.2011.595714, indexed in Pubmed: 21740331.
9. de Andrade CB, Ramos IP, de Moraes AC, et al. Radiotherapy--Induced Skin Reactions Induce Fibrosis Mediated by TGF-β1 Cytokine. Dose Response. 2017; 15(2): 1559325817705019, doi: 10.1177/1559325817705019, indexed in Pubmed: 28507463.
10. Huang A, Glick SA. Genetic susceptibility to cutaneous radiation injury. Arch Dermatol Res. 2017; 309(1): 1–10, doi: 10.1007/s00403-016-1702-3, indexed in Pubmed: 27878387.
11. Flanders K, Major C, Arabshahi A, et al. Interference with Transforming Growth Factor-β/ Smad3 Signaling Results in Accelerated Healing of Wounds in Previously Irradiated Skin. The American Journal of Pathology. 2003; 163(6): 2247–2257, doi: 10.1016/s0002-9440(10)63582-1.
12. Perraud AL, Rao DM, Kosmacek EA, et al. The ion channel, TRPM2, contributes to the pathogenesis of radiodermatitis. Radiat Environ Biophys. 2019; 58(1): 89–98, doi: 10.1007/s00411-018-0769-y, indexed in Pubmed: 30483886.
13. Fallah M, Shen Y, Brodén J, et al. Plasminogen activation is required for the development of radiation-induced dermatitis. Cell Death Dis. 2018; 9(11): 1051, doi: 10.1038/s41419-018-1106-8, indexed in Pubmed: 30323258.
14. Bernier J, Russi EG, Homey B, et al. Management of radiation dermatitis in patients receiving cetuximab and radiotherapy for locally advanced squamous cell carcinoma of the head and neck: proposals for a revised grading system and consensus management guidelines. Ann Oncol. 2011; 22(10): 2191–2200, doi: 10.1093/annonc/mdr139, indexed in Pubmed: 21606209.
15. Brizel DM, Albers ME, Fisher SR, et al. Hyperfractionated irradiation with or without concurrent chemotherapy for locally advanced head and neck cancer. N Engl J Med. 1998; 338(25): 1798–1804, doi: 10.1056/NEJM199806183382503, indexed in Pubmed: 9632446.
16. Pignon JP, le Maître A, Maillard E, et al. MACH-NC Collaborative Group. Meta-analysis of chemotherapy in head and neck cancer (MACH-NC):

an update on 93 randomised trials and 17,346 patients. Radiother Oncol. 2009; 92(1): 4–14, doi: 10.1016/j.radonc.2009.04.014, indexed in Pubmed: 19446902.
17. Tobias JS, Monson K, Gupta N, et al. UK Head and Neck Cancer Trialists' Group. Chemoradiotherapy for locally advanced head and neck cancer: 10-year follow-up of the UK Head and Neck (UKHAN1) trial. Lancet Oncol. 2010; 11(1): 66–74, doi: 10.1016/S1470-2045(09)70306-7, indexed in Pubmed: 19875337.
18. Kawamura M, Yoshimura M, Asada H, et al. A scoring system predicting acute radiation dermatitis in patients with head and neck cancer treated with intensity-modulated radiotherapy. Radiat Oncol. 2019; 14(1): 14, doi: 10.1186/s13014-019-1215-2, indexed in Pubmed: 30665451.
19. Wong RKS, Bensadoun RJ, Boers-Doets CB, et al. Clinical practice guidelines for the prevention and treatment of acute and late radiation reactions from the MASCC Skin Toxicity Study Group. Support Care Cancer. 2013; 21(10): 2933–2948, doi: 10.1007/s00520-013-1896-2, indexed in Pubmed: 23942595.
20. Radiation Therapy Oncology Group (RTOG). RTOG/EORTC Late Radiation Morbidity Scoring Schema. https://www.rtog.org/ResearchAssociates/AdverseEventReporting/RTOGEORTCLateRadiationMorbidityScoringSchema.aspx..
21. Zenda S, Ota Y, Tachibana H, et al. A prospective picture collection study for a grading atlas of radiation dermatitis for clinical trials in head-and-neck cancer patients. J Radiat Res. 2016; 57(3): 301–306, doi: 10.1093/jrr/rrv092, indexed in Pubmed: 26850926.
22. Bonomo P, Desideri I, Loi M, et al. Management of severe bio-radiation dermatitis induced by radiotherapy and cetuximab in patients with head and neck cancer: emphasizing the role of calcium alginate dressings. Support Care Cancer. 2019; 27(8): 2957–2967, doi: 10.1007/s00520-018-4606-2, indexed in Pubmed: 30569265.
23. Russi EG, Bensadoun RJ, Merlano MC, et al. Bio-radiation dermatitis: the need of a new grading: in regard to Bernier et al: Ann Oncol 2011; 22(10): 2191-2200. Ann Oncol. 2013; 24(9): 2463–2465, doi: 10.1093/annonc/mdt281, indexed in Pubmed: 23897703.
24. O'Donovan A, Coleman M, Harris R, et al. Prophylaxis and management of acute radiation-induced skin toxicity: a survey of practice across Europe and the USA. Eur J Cancer Care (Engl). 2015; 24(3): 425–435, doi: 10.1111/ecc.12213, indexed in Pubmed: 24986477.
25. Lucey P, Zouzias C, Franco L, et al. Practice patterns for the prophylaxis and treatment of acute radiation dermatitis in the United States. Support Care Cancer. 2017; 25(9): 2857–2862, doi: 10.1007/s00520-017-3701-0, indexed in Pubmed: 28411323.
26. Narvaez C, Doemer C, Idel C, et al. Radiotherapy related skin toxicity (RAREST-01): Mepitel® film versus standard care in patients with locally advanced head-and-neck cancer. BMC Cancer. 2018; 18(1): 197, doi: 10.1186/s12885-018-4119-x, indexed in Pubmed: 29454311.
27. Wooding H, Yan J, Yuan L, et al. The effect of Mepitel Film on acute radiation-induced skin reactions in head and neck cancer patients: a feasibility study. Br J Radiol. 2018; 91(1081): 20170298, doi: 10.1259/bjr.20170298, indexed in Pubmed: 29072852.
28. Zenda S, Yamaguchi T, Yokota T, et al. Topical steroid versus placebo for the prevention of radiation dermatitis in head and neck cancer patients receiving chemoradiotherapy: the study protocol of J-SUPPORT 1602 (TOPICS study), a randomized double-blinded phase 3 trial. BMC Cancer. 2018; 18(1): 873, doi: 10.1186/s12885-018-4763-1, indexed in Pubmed: 30189840.
29. Zhang X, Li H, Li Q, et al. Application of red light phototherapy in the treatment of radioactive dermatitis in patients with head and neck cancer. World J Surg Oncol. 2018; 16: 222.
30. Ferreira EB, Vasques CI, Gadia R, et al. Topical interventions to prevent acute radiation dermatitis in head and neck cancer patients: a systematic review. Support Care Cancer. 2017; 25(3): 1001–1011, doi: 10.1007/s00520-016-3521-7, indexed in Pubmed: 27957620.
31. Bensadoun RJ, Humbert P, Krutman J, et al. Daily baseline skin care in the prevention, treatment, and supportive care of skin toxicity in oncology patients: recommendations from a multinational expert panel. Cancer Manag Res. 2013; 5: 401–408, doi: 10.2147/CMAR.S52256, indexed in Pubmed: 24353440.
32. Chapter 8. In: Wells M, MacBride S. ed. Radiation skin reactions. Churchill Livingstone, Elsevier, London 2003.
33. Mendelsohn FA, Divino CM, Reis ED, et al. Wound care after radiation therapy. Adv Skin Wound Care. 2002; 15(5): 216–224, doi: 10.1097/00129334-200209000-00007, indexed in Pubmed: 12368711.

VIA MEDICA

Review article

NOWOTWORY Journal of Oncology
2021, volume 71, number 2, 103–110
DOI: 10.5603/NJO.a2021.0013

ISSN 0029–540X, e-ISSN: 2300-2115
www.nowotwory.edu.pl

The role of dermoscopy in dermato-oncological diagnostics – new trends and perspectives

Grażyna Kamińska-Winciorek[1], Aleksandra Pilśniak[2]

[1]*Skin Cancer and Melanoma Team, Department of Bone Marrow Transplantation and Oncohematology, M. Sklodowska-Curie National Research Institute of Oncology, Gliwice Branch, Poland*
[2]*Inpatient Department of Radiation and Clinical Oncology, M. Sklodowska-Curie National Research Institute of Oncology, Gliwice Branch, Poland*

Medical history and clinical examination are the most basic elements of medical diagnostics. Clinical examination in the context of dermatology should be combined with the taking and archiving of clinical, dermoscopic and/or video dermoscopic photographs. Dermoscopy is a non-invasive examination and is the recommended method of examining skin lesions. It requires many years of experience and extensive training, and subsequently can be very helpful in the diagnostic process since it allows for a more thorough examination than the unarmed eye. The diagnosis of malignant skin tumours has been significantly improved by noninvasive real-time diagnostic devices. Based on the data from the literature available, we discussed the most commonly used algorithms in the diagnostic process. It should be emphasized that a dermoscopic evaluation may facilitate the diagnosis and early treatment of micromelanoma and basal cell carcinoma. Finally, the role of dermoscopy in the follow-up procedure of oncologic patients should not be forgotten.

Key words: dermoscopy, dermato-oncology, skin cancer, cutaneous melanoma, skin malignancies

Introduction

Medical history and clinical examination are the most basic elements of medical diagnostics. It should be emphasized that a clinical examination in the context of dermatology should be combined with taking and archiving of clinical, dermoscopic and/or videodermoscopic photographs [1, 2]. Dermoscopy is a non-invasive examination and it is the recommended method of examining skin lesions since it allows for a more thorough examination than the unarmed eye. This diagnostic tool has several uses. The first one is self training, when a specific diagnosis is straightforward. In this case, this method provides us with an enormous amount of data. We are able to correlate our macroscopic thinking with the dermoscopic image, which consequently broadens our knowledge. In the second situation, a diagnosis is very likely and we use a dermoscope to confirm our assumptions and this ensures we can refrain from performing a biopsy. In the next case, a dermoscopy reverses the diagnosis and corrects mistakes. In the latter case, a dermoscopy can lead to a diagnosis by visualizing the feature, resulting in a list of differential diagnoses.

Diagnosis of malignant skin tumours

The diagnosis of malignant skin tumours has been significantly improved by noninvasive real-time diagnostic devices. It is obvious that such a diagnosis must be confirmed by histopathological diagnosis [3]. Dermoscopy requires several years of experience and extensive training, and subsequently can be very helpful in the diagnostic process leading to the final confirmation in the form of a histopathological examination [4]. Consequently, it is worth mentioning and characterizing the

How to cite:
Kamińska-Winciorek G, Pilśniak A. ***The role of dermoscopy in dermato-oncological diagnostics – new trends and perspectives.*** *NOWOTWORY J Oncol* 2021; 71: 103–110.

classic patterns of the most common skin cancer, i.e. basal cell carcinoma (BCC) in dermoscopy. Undoubtedly, the presence of arborizing vessels, large blue-grey ovoid nests, ulceration, leaf-like areas and spoke wheel-like structures and numerous blue-grey globules indicate the basal cell carcinoma (fig. 1A, B) [5].

The second diagnosis we should look at is melanoma. We observe an increasing number of algorithms that help in the early diagnosis of melanoma which are listed and described below. We have dealt with the differences between patients with a solitary lesion, of which a surgical excision is the best procedure. On the other hand, there are patients with numerous lesions which cannot all be cut out; in this case, a dermoscopy with computerized photo archiving is very useful. In addition to tumour diagnosis, the morphological features of the tumour may be important in designing a treatment strategy. It is suggested that the presence of multiple minor erosions or ulceration is a crucial predictor of basal cell carcinomas' response to imiquimod and the presence of pigmentation is a negative predictor of a worse response of this cancer to photodynamic therapy [6, 7].

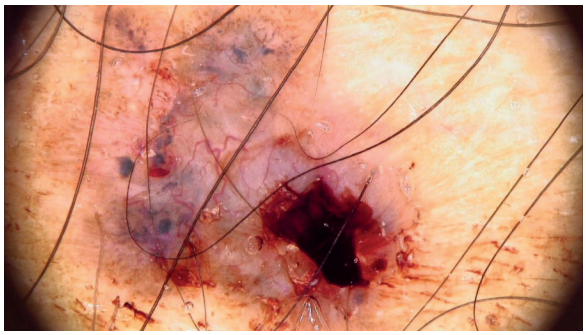

Figure 1A. Dermoscopic features in a non-polarized dermoscopy (NPD) of basal cell carcinoma include the presence of arborizing vessels (bright red, thick diameter vessels (0.2 mm or more) from which emanate branching vessels with progressively thinner diameters), large blue-grey ovoid nests (confluent, well-circumscribed, pigmented ovoid areas), multiple blue-grey dots (pinpoint blue-grey structures) and globules (well-defined round or oval structures), ulceration (shallow erosions that may be covered with congealed blood). Dermoscopic definitions based on dermoscopedia.org [49]

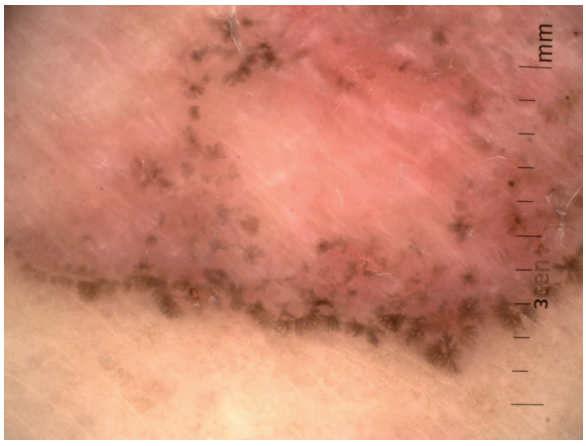

Figure 1B. Dermoscopy in a polarized dermoscopy (PD) of basal cell carcinoma indicates the presence of leaf-like structures (linear to bulbous extensions connected at an off-center base area) and spoke wheel-like structures (radial projections that surround a central darker point). Moreover, in the centre of the lesion shiny white strands (parallel and linear white areas that do not usually intersect) are noticed. Dermoscopic definitions based on dermoscopedia.org [49]

Algorithms for melanocytic lesions

A dermoscopic examination performed by experienced doctors is more accurate than the clinical examination itself. In the study of the observed features visible in a dermoscopy, many algorithms have been established that allow an approximation of an accurate diagnosis. The most commonly used algorithms are discussed below. Kamińska-Winciorek et al. in their review present in detail the older algorithms widely previously used and described in literature [8].

Three-Point Checklist

The Three-Point Checklist algorithm takes into account three criteria to which it belongs:

1. asymmetry in dermoscopic structures' distribution,
2. an atypical pigmented network and
3. blue-white structures.

This Three-Point Checklist can be used by clinicians in diagnostics not only for melanoma (fig. 2A) but also basal cell carcinoma [9]. Soyer et al. showed that the presence of either of these two criteria indicates a high probability of melanoma [9].

Seven-Point Checklist

The Seven-Point Checklist algorithm includes seven characteristics, including: atypical pigment network, gray-blue areas, atypical vascular pattern, radial streaming (streaks), irregular diffuse pigmentation (blotches), irregular dots and globules, regression pattern (a presence of white scar-like depigmentation or peppering known as multiple scattered blue-grey granules) (fig. 2B). Historically, a minimum score of three for adding individual features of the above-mentioned seven is required for the diagnosis of melanoma [10]. Previously, at least

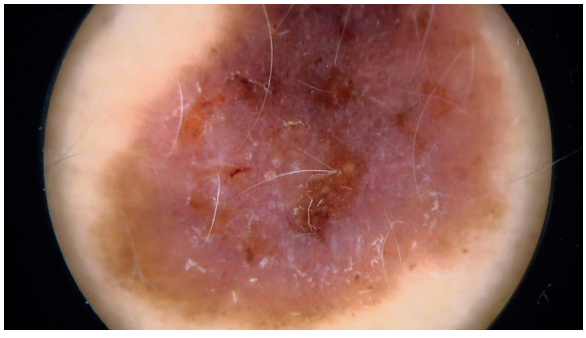

Figure 2A. Dermoscopic assessment of a superficial spreading melanoma (SSM) according to the Three-Point Checklist reveals the presence of asymmetry in dermoscopic structures' distribution (according to two axes), an atypical pigmented network and blue-white structures. Moreover, white structures which are seen in the presented case of SSM in polarized light, so-called shiny white streaks (former synonyms: chrysalis – chrysalids – crystalline) in definition as lines, white, perpendicular shiny white streaks usually correspond with invasive type of melanomas. Dermoscopic definitions based on dermoscopedia.org [49]

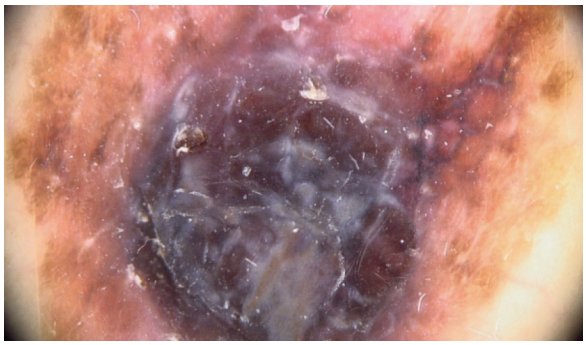

Figure 2B. Dermoscopy of a nodular melanoma in polarized light. The Seven-Point Checklist algorithm indicates the presence of 7 characteristic features, including: atypical pigment network, grey-blue areas, atypical vascular pattern, radial streaming (streaks), irregular diffuse pigmentation (blotches), irregular dots and globules, regression pattern. Moreover, multiple shiny white streaks and strands corresponding with deep dermal fibrosis are visible

two dermoscopic criteria (one major and one minor) must be present for a suspicious diagnosis (a score of three or more). In 2011, Argenziano et al. revised Seven-Point Checklist. They showed in their study that in order to increase the sensitivity of the assessment in the Seven-Point Checklist, the excision threshold of the lesion should be adjusted compared to the original [11]. In the revised Seven-Point Checklist, each criterion receives 1 point, the notch threshold is 1 point, not 3 points like in the earlier version [11].

Two Step Algorithm

In the previous traditional two-step algorithm, assessment is divided into two steps including the differentiation between melanocytic and non-melanocytic changes. When the lesion is classified as melanocytic, the observer then proceeds to the second stage consisting in qualifying the change as mild or malignant. During this second step a decision must be made whether the melanocytic lesion is benign, suspect, or malignant. For this purpose, the mentioned algorithms can be useful, including pattern analysis, ABCD rule, Menzies method and the Seven-Point Checklist which was discussed above [12, 13].

Pattern analysis is a method that involves assessing all the dermoscopic features that a lesion shows. In general terms, malignant – suspected lesions have several colors that are disordered in structure and are asymmetrical in dermoscopic distribution. The ABCD rule of dermoscopy is based on the following criteria: asymmetry (A), border (B), colour (C) and differential structures (D) [14].

The Menzies method aims to distinguish between benign lesions and melanomas. This method includes negative features (symmetrical pattern, single color) indicating benign changes and positive features indicating melanoma. The positive features include blue-white veil, multiple brown dots, pseudopods, radial streaming, scar-like depigmentation, multiple (5–6) colors, multiple blue/grey dots, broadened network [15]. Exceptions to the two-step algorithms have been observed over the years. Moreover *hybrid* dermoscopes allow the user to toggle between polarized and non-polarized light and consequently a diagnosis becomes more likely. Some dermoscopic structures are more prominent in non-polarized dermoscopy (NPD) and others in polarized (PD) [16]. In 2010, an update of this 2-step algorithm was proposed, which consists in adding 2 decision levels to help doctors correctly classify some of the so-called featureless neoplasms as melanocytic or non-melanocytic tumours. In the revised two-step algorithms, the main queries of conducted analysis is to establish a specific diagnosis (step 1) and to rule out melanoma (step 2). This algorithm impedes the use of unpolarized dermoscopy [17].

Triage Amalgamated Dermoscopic Algorithm (TADA)

It is worth noting that the algorithms mentioned so far have been used to detect specific subsets of pigmented skin neoplasms – mainly pigmented melanoma. This is a limitation of these algorithms because many melanomas, basal cell carcinomas and squamous cell carcinomas do not have this pigment. Thus, compared to the above algorithms, the TADA algorithm allows the identification of pigmented and non-pigmented skin malignancies. At the very beginning, this algorithm requires the exclusion of three common and clearly benign lesions, i.e. cherry haemangioma (fig. 3A), dermatofibroma (fig. 3B) or seborrheic keratosis (fig. 3C. In the next step, dermoscopic patterns are taken into account, i.e. the distribution of colours and structures within the lesion. If there is an architectural disorder/disorganized pattern, a biopsy should be performed. If we have organized lesions with a starburst pattern (fig. 3D) or with any of the following features: blue-black/grey colour, shiny white structures, negative network, ulcer/erosion, vessels (fig. 3E, F) a biopsy should be performed [18, 19].

Metaphoric and descriptive terminology

According to Blum et al., the more metaphorical assessment called *blink* and more descriptive one colloquially called *think* complement each other and are used all over the world [20]. However, in a clinical and scientific context, clear and universal language should be the basis. In 2016, Kittler et al. published a consensus aimed at standardizing the dermoscopic description [21].

Early detection of micro-melanoma and basal cell carcinoma

We should pay attention to the change of the type of micro-melanoma, which, due to its size, i.e. 5 mm, does not meet the criterion D of the ABCD assessment and is often overlooked. In this case, a dermoscopic evaluation may facilitate diagnosis and early treatment. So far, there are very few published studies evaluating micro-melanomas. Megaris et al. in their retrospective study suggest features that increase the probability

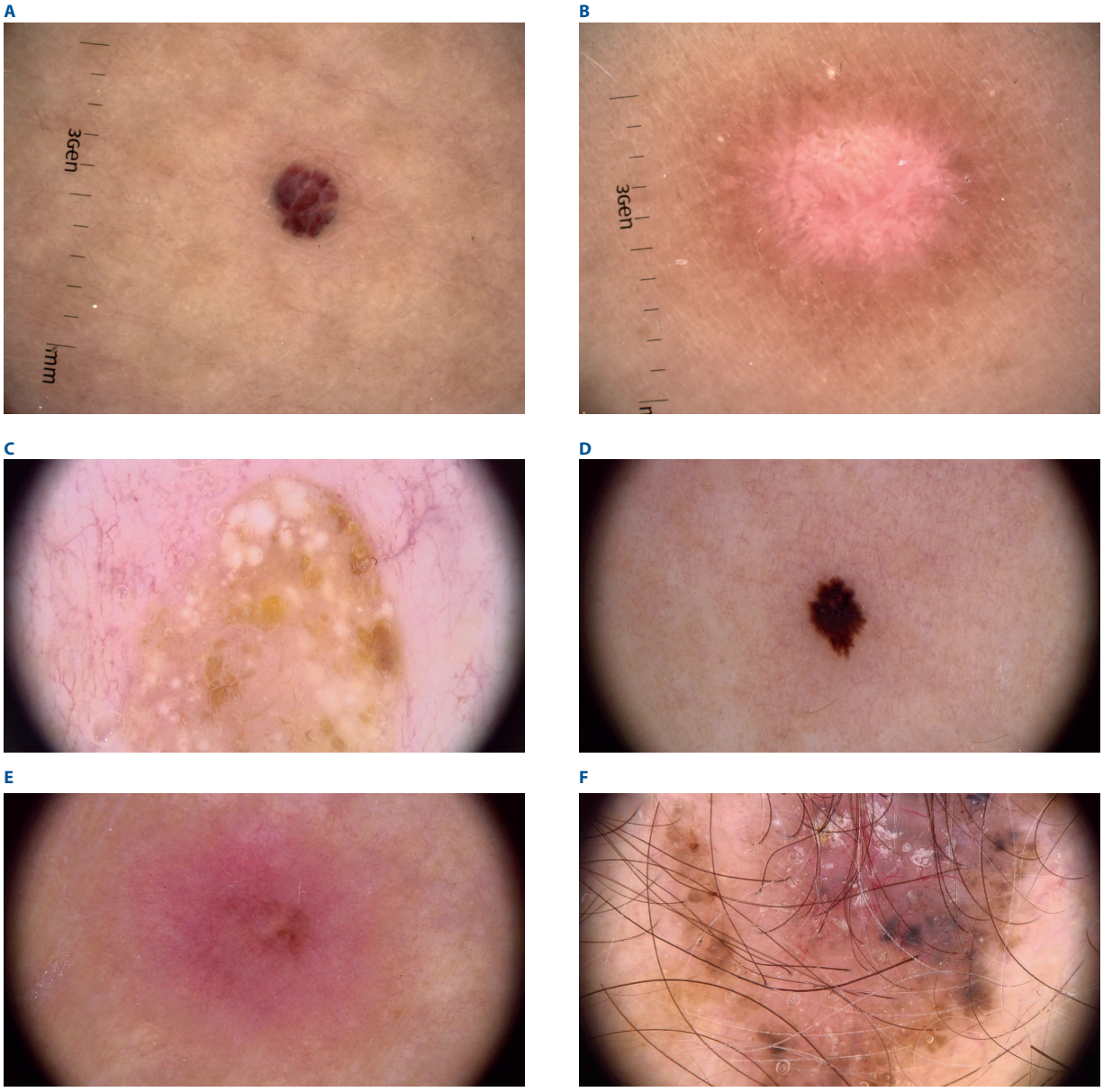

Figure 3. At the very beginning, theTriage Amalgamated Dermoscopic Algorithm (TADA) requires the exclusion of three common and clearly benign lesions; **A** - cherry haemangioma (with the presence of lacunae defined as round to oval red, reddish-brown or reddish-blue areas that commonly vary in size and colour - PD); **B** - dermatofibroma (the peripheral network with a central white scar-like area with a pink hue and shiny white lines in polarized light) or **C** - seborrheic keratosis (with multiple dots or clods white disseminated in NPD). In the TADA algorithm, if we have organized lesions with **D** - a starburst pattern (typified by streaks, pseudopods, or finger-like projections regularly distributed on the periphery; Reed nevus in NPD) or any of the following features: **E** - vessels (multiple dotted and linear irregular vessels in SSM in NPD); **F** - blue-black/grey colour (BCC in NPD), negative network, shiny white structures, ulcer/erosion, a biopsy should be performed

of malignancy in lesions up to 5 mm. Such features include irregular hyperpigmented areas, atypical dots/globules, and an atypical network, within a reticular or unstructured global pattern (fig. 4A) [22].

The routine use of dermoscopy allows the detection of melanomas of which patients are unaware [23]. Moreover, the digital follow-up enables recognition of early melanoma when specific structures or criteria for malignancy may not be present [24]. The combined use of total-body photography and sequential digital dermoscopy enables the detection of incipient melanomas that might have been overlooked if assessed solely by the naked eye [23, 24]. Moreover most melanomas are diagnosed with digital dermoscopy monitoring by side-by-side image comparison [25].

Dermoscopy can also aid early diagnosis of small basal cell carcinomas less than 5 mm in diameter, especially characterized newly arised lesions located on the skin of the head and neck [26]. They are characterized by the presence of multiple blue grey dots and large blue-grey ovoid nests [26] especially in its pigmented variants of very small BCC (3 mm-sized) (fig. 4B) [27]. Moreover the presence of arborizing vessels with the existence of shiny white blotches and strands may also help

can the BCC recognition although 1/3 of small lesions did not exhibit the typical dermoscopic criteria of BCC [28]. It is evident that in small size BCC classic dermoscopic criteria (the presence of arborizing vessels and ulceration) are often substituted by non-classical criteria [29]. Only blue-whitish veil and blue in--focus dots dermoscopic features among non-classic criteria which represent the neoplasm's early phase indicated a good agreement among low experience observers [29].

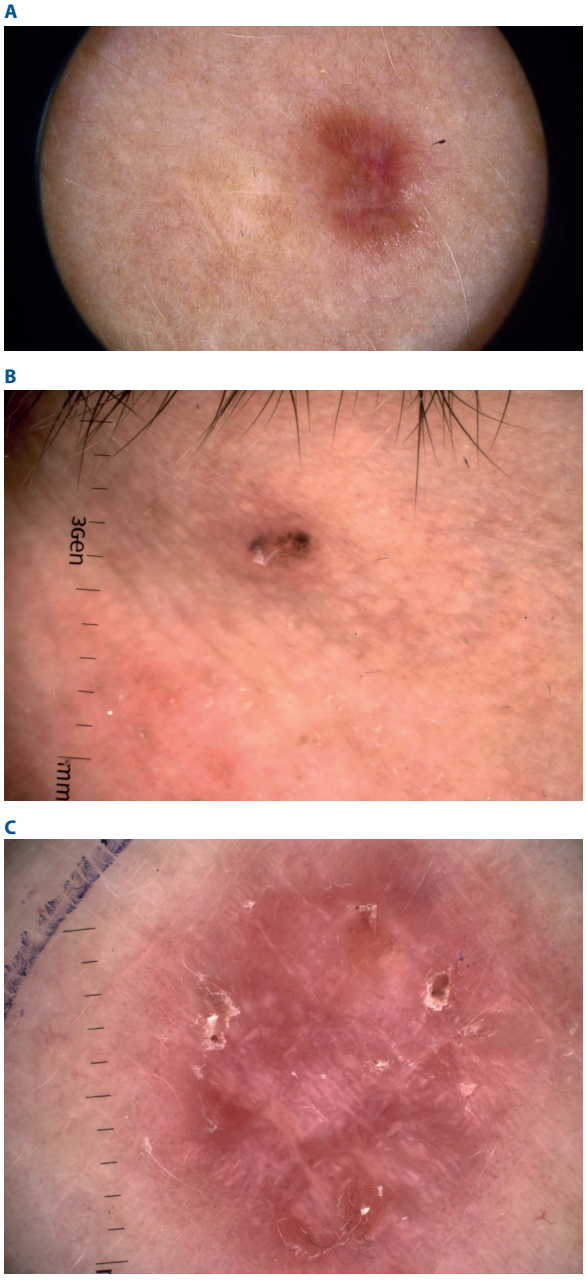

Figure 4. A - a micro-melanoma measuring 3 mm proved histopathologically as SSM located on the décolletage. Dermoscopy in polarized light exhibits the presence of short shiny white streaks and an atypical network, within an unstructured global pattern; **B** - small basal cell carcinoma sized less than 2 mm in diameter located on the skin of the face, characterized by the presence of multiple blue grey dots and globules; **C** - non-classic BCC criteria include inter alia: pink-white areas with: white strands (bright-white less well defined lines, oriented parallel or distributed haphazardly) and shiny white blotches (as white structures in the form of large areas, clods or circles), micro-erosions (covered by crusts and blood) and short fine telangiectasias seen in polarized dermoscopy. Dermoscopic definitions based on dermoscopedia.org [49]

Dermoscopic follow-up in dermato-oncology

Dermoscopic assessment of the surgical margins before excision

Preoperative digital dermoscopy is a better method for detecting tumoral margins than clinical evaluation, and is an effective, simple, non-invasive method for the pre-surgical evaluation of margins [30]. Preoperative dermoscopy is a better method to determine the margins of neoplasms than clinical evaluation alone [31]. Moreover, the preoperative dermoscopic assessment using non-classic BCC criteria including pink-white areas and short telangiectasias in the area between clinically and dermoscopically detected margins, helps define the neoplasm's margins and to achieve a really radical excision (fig. 4C) [32].

Dermoscopic follow-up after surgical procedures

Dermoscopy, as a non-invasive method, works well in secondary prevention, i.e., early detection of neoplasms with the use of dermoscopic assessment of the entire skin, covering areas that are difficult to access during the examination. We should emphasize the importance of this method in the follow-up stages of patients after cancer treatment. These are high-risk patients at risk of relapse and should be regularly monitored using the above method along with image archiving. Dermoscopic follow-up is used in the control of post-excision malignant tumour scars enabling the diagnosis and assessment of tumour (eg. lentigo maligna melanoma – LMM) persistence after surgery (fig. 5A) [33], rapid recognition of the features of tumour recurrence among others, melanoma within the scar (fig. 5B) [34] with an assessment of its healing or leaving sutures (fig. 5C). In addition, a dermoscopic observation of the whole body of patients with diagnosed malignant neoplasms enables early detection of metastases the nature of satellitosis, *in-transit* (fig. 5D) or distant localized within the skin and subcutaneous tissue [35, 36] as well as allowing for additional monitoring dermoscopic effects of the therapies used in patients with, inter alia, metastatic melanoma (blood vessel morphology and distribution, degree of vascularization, ulceration, background). Dermoscopy is also used in patients diagnosed with cutaneous malignancies for the early detection of synchronous melanoma [37, 38] and basal or squamous cell carcinoma (SCC) with dermoscopic assessment of the selected therapies of skin cancers.

Dermoscopic assessment of the selected therapies of skin cancers

Moreover, patients' response to treatment can be easily monitored with this noninvasive medical device, thus allowing further modulation of the therapy [4]. It is worth mentioning

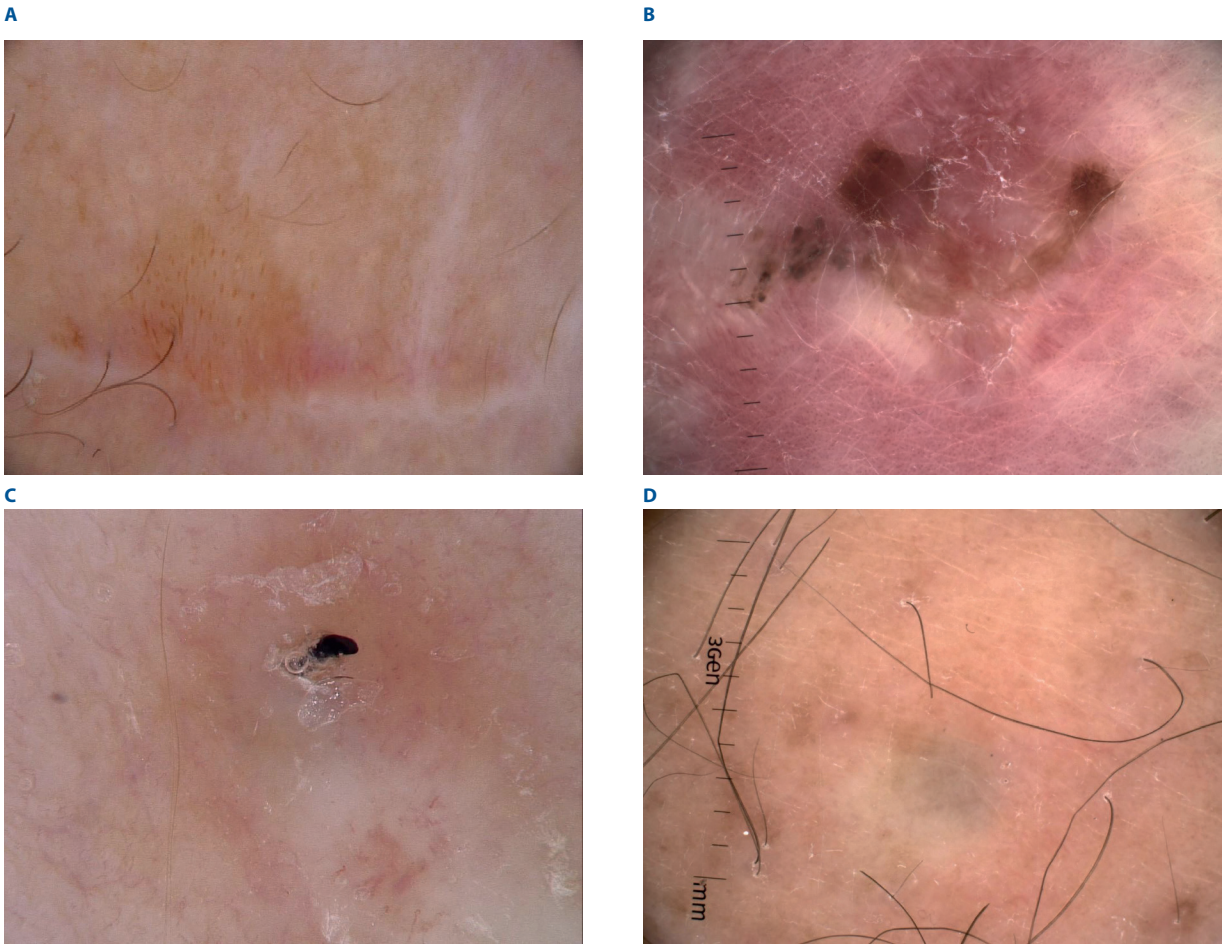

Figure 5. Dermoscopic follow-up in the control of post-excision scars of malignant tumours enabling diagnosis and the assessment of tumour persistence after surgery; **A** - lentigo maligna in NPD (with a pattern of hyperpigmented follicular openings as fine circles and semicircles), rapid recognition of the features of tumour recurrence; **B** - thick melanoma within the scar (the presence of an atypical pigmented network and irregular grey and brown clods, PD); **C** - assessment of leaving sutures (black-blue solitary clod corresponding with a non-absorbable suture within the scar, NPD); **D** - according to melanoma metastasis, dermoscopic classification [35] distinguish four dermoscopic patterns based on metastases' colour: blue, pink, brown and mixed pattern. The blue pattern of in-transit melanoma metastasis revealed the presence of structureless bluish areas in polarized dermoscopy

the treatment with the use of appropriate methods that can be considered and applied in the case of BCC and SCC, characterized by low risk of recurrence or in patients with contraindications to the use of basic methods such as surgery. Imiquimod (5%) is used in the treatment of actinic keratosis, *in situ* SCC/Bowen's disease, and non-invasive forms of superficial spreading BCC [39]. Based on the Husein-ElAhmed study, dermoscopic evaluation improves the accuracy of the assessment of clinical response to imiquimod in pigmented BCC [40].

Dermoscopic follow-up was useful in monitoring the therapeutic response to selected topical therapies including ingenol mebutate in BCC [41], Bowen's disease [42] and imiquimod in LMM [33] as well as systemic therapy with vismodegib in BCC [43]. Dermoscopy was also used in monitoring BCC's treatment effects using high dose ionizing radiation therapy [44], changes in the course of LMM radiotherapy [45], or dermoscopic margin delineation in radiotherapy planning for superficial or nodular basal cell carcinoma [46]. In addition, the dermoscope can be used to assess skin toxicity or lesions occurring in existing and newly formed melanocytic changes during the treatment of melanoma, including with the use of BRAF inhibitors [47, 48].

Conclusions

Modern perspectives regarding dermoscopy emphasize its multidisciplinary scope and nature concerning not only the preoperative diagnosis of skin cancers but also the post-operative and post-therapeutic stages – including topical and systemic implemented therapies.

The high-resolution illustrations are available in the electronic version of this article in the *Supplemetary materials* section on the website nowotwory.edu.pl.

Conflict of interest: none declared

Grażyna Kamińska-Winciorek
M. Sklodowska-Curie National Research Institute of Oncology Gliwice Branch
Department of Bone Marrow Transplantation and Oncohematology
ul. Wybrzeże Armii Krajowej 15
44-101 Gliwice, Poland
e-mail: grazyna.kaminskawinciorek@gmail.com

Received: 4 Jan 2021
Accepted: 11 Jan 2021

References

1. Kamińska-Winciorek G, Gajda M, Wydmański J, et al. What do Web users know about skin self-examination and melanoma symptoms? Asian Pac J Cancer Prev. 2015; 16(7): 3051–3056, doi: 10.7314/apjcp.2015.16.7.3051, indexed in Pubmed: 25854404.
2. Forsea AM, Tschandl P, Zalaudek I, et al. Eurodermoscopy Working Group. The impact of dermoscopy on melanoma detection in the practice of dermatologists in Europe: results of a pan-European survey. J Eur Acad Dermatol Venereol. 2017; 31(7): 1148–1156, doi: 10.1111/jdv.14129, indexed in Pubmed: 28109068.
3. Rutkowski P, Wysocki PJ, Nasierowska-Guttmejer A, et al. Cutaneous melanoma. Oncol Clin Pract. 2020; 16(4): 163–182, doi: 10.5603/OCP.2020.0021.
4. Bakos RM, Blumetti TP, Roldán-Marín R, et al. Noninvasive Imaging Tools in the Diagnosis and Treatment of Skin Cancers. Am J Clin Dermatol. 2018; 19(Suppl 1): 3–14, doi: 10.1007/s40257-018-0367-4, indexed in Pubmed: 30374899.
5. Que SK. Research Techniques Made Simple: Noninvasive Imaging Technologies for the Delineation of Basal Cell Carcinomas. J Invest Dermatol. 2016; 136(4): e33–e38, doi: 10.1016/j.jid.2016.02.012, indexed in Pubmed: 27012561.
6. Lallas A, Apalla Z, Argenziano G, et al. The dermatoscopic universe of basal cell carcinoma. Dermatol Pract Concept. 2014; 4(3): 11–24, doi: 10.5826/dpc.0403a02, indexed in Pubmed: 25126452.
7. Russo T, Piccolo V, Lallas A, et al. Dermoscopy of Malignant Skin Tumours: What's New? Dermatology. 2017; 233(1): 64–73, doi: 10.1159/000472253, indexed in Pubmed: 28486238.
8. Kamińska-Winciorek G, Spiewak R. [Basic dermoscopy of melanocytic lesions for beginners]. Postepy Hig Med Dosw (Online). 2011; 65: 501–508, doi: 10.5604/17322693.955121, indexed in Pubmed: 21918252.
9. Soyer HP, Argenziano G, Zalaudek I, et al. Three-point checklist of dermoscopy. A new screening method for early detection of melanoma. Dermatology. 2004; 208(1): 27–31, doi: 10.1159/000075042, indexed in Pubmed: 14730233.
10. Argenziano G, Fabbrocini G, Carli P, et al. Epiluminescence microscopy for the diagnosis of doubtful melanocytic skin lesions. Comparison of the ABCD rule of dermatoscopy and a new 7-point checklist based on pattern analysis. Arch Dermatol. 1998; 134(12): 1563–1570, doi: 10.1001/archderm.134.12.1563, indexed in Pubmed: 9875194.
11. Argenziano G, Catricalà C, Ardigo M, et al. Seven-point checklist of dermoscopy revisited. Br J Dermatol. 2011; 164(4): 785–790, doi: 10.1111/j.1365-2133.2010.10194.x, indexed in Pubmed: 21175563.
12. Scope A, Benvenuto-Andrade C, Agero AL, et al. Nonmelanocytic lesions defying the two-step dermoscopy algorithm. Dermatol Surg. 2006; 32(11): 1398–1406, doi: 10.1111/j.1524-4725.2006.32312.x, indexed in Pubmed: 17083595.
13. Argenziano G, Soyer HP, Chimenti S, et al. Dermoscopy of pigmented skin lesions: results of a consensus meeting via the Internet. J Am Acad Dermatol. 2003; 48(5): 679–693, doi: 10.1067/mjd.2003.281, indexed in Pubmed: 12734496.
14. Stolz W, Riemann A, Cognetta AB, et al. ABCD rule of dermatoscopy: a new practical method for early recognition of malignant melanoma. Eur J Dermatol. 1994: 4521–4527.
15. Menzies SW, Ingvar C, Crotty KA, et al. Frequency and morphologic characteristics of invasive melanomas lacking specific surface microscopic features. Arch Dermatol. 1996; 132(10): 1178–1182, indexed in Pubmed: 8859028.
16. Braun RP, Scope A, Marghoob AA. The „blink sign" in dermoscopy. Arch Dermatol. 2011; 147(4): 520, doi: 10.1001/archdermatol.2011.82, indexed in Pubmed: 21482914.
17. Marghoob AA, Braun R. Proposal for a revised 2-step algorithm for the classification of lesions of the skin using dermoscopy. Arch Dermatol. 2010; 146(4): 426–428, doi: 10.1001/archdermatol.2010.41, indexed in Pubmed: 20404234.
18. Seiverling EV, Ahrns HT, Greene A, et al. Teaching Benign Skin Lesions as a Strategy to Improve the Triage Amalgamated Dermoscopic Algorithm (TADA). J Am Board Fam Med. 2019; 32(1): 96–102, doi: 10.3122/jabfm.2019.01.180049, indexed in Pubmed: 30610147.
19. Jaimes N, Marghoob AA. Triage amalgamated dermoscopic algorithm. J Am Acad Dermatol. 2020; 82(6): 1551–1552, doi: 10.1016/j.jaad.2020.01.079, indexed in Pubmed: 32045619.
20. Blum A, Argenziano G. Metaphoric and descriptive terminology in dermoscopy: Combine „blink" with „think". Dermatol Pract Concept. 2015; 5(3): 23, doi: 10.5826/dpc.0503a05, indexed in Pubmed: 26336619.
21. Kittler H, Marghoob AA, Argenziano G, et al. Standardization of terminology in dermoscopy/dermatoscopy: Results of the third consensus conference of the International Society of Dermoscopy. J Am Acad Dermatol. 2016; 74(6): 1093–1106, doi: 10.1016/j.jaad.2015.12.038, indexed in Pubmed: 26896294.
22. Megaris A, Lallas A, Bagolini LP, et al. Dermoscopy features of melanomas with a diameter up to 5 mm (micromelanomas): A retrospective study. J Am Acad Dermatol. 2020; 83(4): 1160–1161, doi: 10.1016/j.jaad.2020.04.006, indexed in Pubmed: 32289392.
23. Salerni G, Alonso C, Fernández-Bussy R. Multiple Primary Invasive Small-Diameter Melanomas: Importance of Dermoscopy and Digital Follow-up. Dermatol Pract Concept. 2019; 9(1): 69–70, doi: 10.5826/dpc.0901a16, indexed in Pubmed: 30775153.
24. Salerni G, Alonso C, Fernández-Bussy R. A series of small-diameter melanomas on the legs: dermoscopic clues for early recognition. Dermatol Pract Concept. 2015; 5(4): 31–36, doi: 10.5826/dpc.0504a08, indexed in Pubmed: 26693087.
25. Babino G, Lallas A, Agozzino M, et al. Melanoma diagnosed on digital dermoscopy monitoring: A side-by-side image comparison is needed to improve early detection. J Am Acad Dermatol. 2020 [Epub ahead of print], doi: 10.1016/j.jaad.2020.07.013, indexed in Pubmed: 32652193.
26. Longo C, Specchio F, Ribero S, et al. Dermoscopy of small-size basal cell carcinoma: a case-control study. J Eur Acad Dermatol Venereol. 2017; 31(6): e273–e274, doi: 10.1111/jdv.13988, indexed in Pubmed: 27685248.
27. Takahashi A, Hara H, Aikawa M, et al. Dermoscopic features of small size pigmented basal cell carcinomas. J Dermatol. 2016; 43(5): 543–546, doi: 10.1111/1346-8138.13173, indexed in Pubmed: 26458728.
28. Liopyris K, Navarrete-Dechent C, Yélamos O, et al. Clinical, dermoscopic and reflectance confocal microscopy characterization of facial basal cell carcinomas presenting as small white lesions on sun-damaged skin. Br J Dermatol. 2019; 180(1): 229–230, doi: 10.1111/bjd.17241, indexed in Pubmed: 30239981.
29. di Meo N, Damiani G, Vichi S, et al. Interobserver agreement on dermoscopic features of small basal cell carcinoma (<5 mm) among low-experience dermoscopists. J Dermatol. 2016; 43(10): 1214–1216, doi: 10.1111/1346-8138.13426, indexed in Pubmed: 27129742.
30. Carducci M, Bozzetti M, de Marco G, et al. Preoperative margin detection by digital dermoscopy in the traditional surgical excision of cutaneous squamous cell carcinomas. J Dermatolog Treat. 2013; 24(3): 221–226, doi: 10.3109/09546634.2012.672711, indexed in Pubmed: 22390630.
31. Carducci M, Bozzetti M, De Marco G, et al. Usefulness of margin detection by digital dermoscopy in the traditional surgical excision of basal cell carcinomas of the head and neck including infiltrative/morpheaform type. J Dermatol. 2012; 39(4): 326–330, doi: 10.1111/j.1346-8138.2011.01449.x, indexed in Pubmed: 22150641.
32. Conforti C, Giuffrida R, Zalaudek I, et al. Dermoscopic Findings in the Presurgical Evaluation of Basal Cell Carcinoma. A Prospective Study. Dermatol Surg. 2021; 47(2): e37–e41, doi: 10.1097/DSS.0000000000002471, indexed in Pubmed: 32804889.
33. Hamilko de Barros M, Conforti C, Giuffrida R, et al. Clinical usefulness of dermoscopy in the management of lentigo maligna melanoma treated with topical imiquimod: A case report. Dermatol Ther. 2019; 32(5): e13048, doi: 10.1111/dth.13048, indexed in Pubmed: 31365164.
34. Blum A, Hofmann-Wellenhof R, Marghoob AA, et al. Recurrent melanocytic nevi and melanomas in dermoscopy: results of a multicenter study of the International Dermoscopy Society. JAMA Dermatol. 2014; 150(2): 138–145, doi: 10.1001/jamadermatol.2013.6908, indexed in Pubmed: 24226788.
35. Avilés-Izquierdo JA, Ciudad-Blanco C, Sánchez-Herrero A, et al. Dermoscopy of cutaneous melanoma metastases: A color-based pattern

classification. J Dermatol. 2019; 46(7): 564–569, doi: 10.1111/1346-8138.14926, indexed in Pubmed: 31120139.
36. Farnetani F, Manfredini M, Longhitano S, et al. Morphological classification of melanoma metastasis with reflectance confocal microscopy. J Eur Acad Dermatol Venereol. 2019; 33(4): 676–685, doi: 10.1111/jdv.15329, indexed in Pubmed: 30394598.
37. Moscarella E, Rabinovitz H, Puig S, et al. Multiple primary melanomas: do they look the same? Br J Dermatol. 2013; 168(6): 1267–1272, doi: 10.1111/bjd.12260, indexed in Pubmed: 23374221.
38. De Giorgi V, Salvini C, Sestini S, et al. Triple synchronous cutaneous melanoma: a clinical, dermoscopic, and genetic case study. Dermatol Surg. 2007; 33(4): 488–491, doi: 10.1111/j.1524-4725.2007.33098.x, indexed in Pubmed: 17430385.
39. Rutkowski P, Owczarek W, Nejc D, et al. Skin carcinomas. Oncol Clin Pract. 2018; 14(3): 129–147, doi: 10.5603/OCP.2018.0019.
40. Husein-ElAhmed H, Fernandez-Pugnaire MA. Dermatoscopy-guided therapy of pigmented basal cell carcinoma with imiquimod. An Bras Dermatol. 2016; 91(6): 764–769, doi: 10.1590/abd1806-4841.20165255, indexed in Pubmed: 28099598.
41. Diluvio L, Bavetta M, Di Prete M, et al. Dermoscopic monitoring of efficacy of ingenol mebutate in the treatment of pigmented and non-pigmented basal cell carcinomas. Dermatol Ther. 2017; 30(1), doi: 10.1111/dth.12438, indexed in Pubmed: 27860083.
42. Mainetti C, Guillod C, Leoni-Parvex S. Successful Treatment of Relapsing Bowen's Disease with Ingenol Mebutate: The Use of Dermoscopy to Monitor the Therapeutic Response. Dermatology. 2016; 232 Suppl 1: 9–13, doi: 10.1159/000447389, indexed in Pubmed: 27513936.
43. Tognetti L, Cinotti E, Fiorani D, et al. Long-term therapy of multiple basal cell carcinomas: Clinicodermoscopic score for monitoring of intermittent vismodegib treatment. Dermatol Ther. 2019; 32(6): e13097, doi: 10.1111/dth.13097, indexed in Pubmed: 31612619.
44. Navarrete-Dechent C, Cordova M, Liopyris K, et al. In vivo imaging characterization of basal cell carcinoma cutaneous response to high dose ionizing radiation therapy: A prospective study of reflectance confocal microscopy, dermoscopy, and ultrasound. J Am Acad Dermatol. 2020 [Epub ahead of print], doi: 10.1016/j.jaad.2020.07.130, indexed in Pubmed: 32827607.
45. Richtig E, Arzberger E, Hofmann-Wellenhof R, et al. Assessment of changes in lentigo maligna during radiotherapy by in-vivo reflectance confocal microscopy: a pilot study. Br J Dermatol. 2015; 172(1): 81–87, doi: 10.1111/bjd.13141, indexed in Pubmed: 24889911.
46. Ballester Sánchez R, Pons Llanas O, Pérez Calatayud J, et al. Dermoscopy margin delineation in radiotherapy planning for superficial or nodular basal cell carcinoma. Br J Dermatol. 2015; 172(4): 1162–1163, doi: 10.1111/bjd.13402, indexed in Pubmed: 25204461.
47. Rajczykowski M, Kaminska-Winciorek G, Nowara E, et al. Dermoscopic assessment of skin toxicities in patients with melanoma during treatment with vemurafenib. Postepy Dermatol Alergol. 2018; 35(1): 39–46, doi: 10.5114/ada.2018.73163, indexed in Pubmed: 29599670.
48. Cohen PR, Bedikian AY, Kim KB. Appearance of New Vemurafenib-associated Melanocytic Nevi on Normal-appearing Skin: Case Series and a Review of Changing or New Pigmented Lesions in Patients with Metastatic Malignant Melanoma After Initiating Treatment with Vemurafenib. J Clin Aesthet Dermatol. 2013; 6(5): 27–37, indexed in Pubmed: 23710269.
49. https://dermoscopedia.org/.

Aleksandra Pilśniak
Oddział Chorób Wewnętrznych,
Autoimmunologicznych i Metabolicznych,
Śląski Uniwersytet Medyczny w Katowicach

Oświadczam, że w pracy: Dudek A, Rutkowski T, Kamińska-Winciorek G, Krzysztof Składowski K. What is new when it comes to acute and chronic radiation-induced dermatitis in head and neck cancer patients?

opublikowanej w czasopiśmie Nowotwory. Journal of Oncology, 2020, 70, 1, 9-15.

mój udział w jej powstawaniu polegał na zebraniu i analizie piśmiennictwa, napisaniu pierwotnej i ostatecznej wersji pracy, edycji manuskryptu oraz wizualizacji.

A Pilśniak

dr hab. n. med. Tomasz Rutkowski
I Klinika Radioterapii i Chemioterapii
Narodowy Instytut Onkologii
im. Marii Skłodowskiej-Curie,
Państwowy Instytut Badawczy
Oddział w Gliwicach.

Oświadczam, że w pracy: Dudek A, Rutkowski T, Kamińska-Winciorek G, Krzysztof Składowski K. What is new when it comes to acute and chronic radiation-induced dermatitis in head and neck cancer patients?

opublikowanej w czasopiśmie Nowotwory. Journal of Oncology, 2020, 70, 1, 9-15.

mój udział w jej powstawaniu polegał na opracowaniu koncepcji pracy oraz recenzji i redakcji manuskryptu.

Prof. dr hab. n. med. Grażyna Kamińska-Winciorek
Klinika Transplantacji Szpiku i Onkohematologii,
Kierownik Zespołu ds. Raka i Czerniaka Skóry,
Narodowy Instytut Onkologii
im. Marii Skłodowskiej-Curie,
Państwowy Instytut Badawczy
Oddział w Gliwicach.

Oświadczam, że w pracy: Dudek A, Rutkowski T, Kamińska-Winciorek G, Krzysztof Składowski K. What is new when it comes to acute and chronic radiation-induced dermatitis in head and neck cancer patients?

opublikowanej w czasopiśmie Nowotwory. Journal of Oncology, 2020, 70, 1, 9-15.

mój udział w jej powstawaniu polegał na opracowaniu koncepcji pracy, opracowaniu metodologii, wizualizacji, recenzji i redakcji manuskryptu oraz nadzorze nad pracą.

3475587
prof. dr hab. n. med.
Grażyna Kamińska-Winciorek
SPECJALISTA DERMATOLOG - WENEROLOG

Prof. dr hab. n. med. Krzysztof Składowski
I Klinika Radioterapii i Chemioterapii
Narodowy Instytut Onkologii
im. Marii Skłodowskiej-Curie,
Państwowy Instytut Badawczy
Oddział w Gliwicach.

Oświadczam, że w pracy: Dudek A, Rutkowski T, Kamińska-Winciorek G, Krzysztof Składowski K. What is new when it comes to acute and chronic radiation-induced dermatitis in head and neck cancer patients?

opublikowanej w czasopiśmie Nowotwory. Journal of Oncology, 2020, 70, 1, 9-15.

mój udział w jej powstawaniu polegał na recenzji i redakcji manuskryptu.

Prof. dr hab. n. med. Grażyna Kamińska-Winciorek
Klinika Transplantacji Szpiku i Onkohematologii,
Kierownik Zespołu ds. Raka i Czerniaka Skóry,
Narodowy Instytut Onkologii
im. Marii Skłodowskiej-Curie,
Państwowy Instytut Badawczy
Oddział w Gliwicach.

Oświadczam, że w pracy: Kamińska-Winciorek G, Pilśniak A. The role of dermoscopy in dermato-oncological diagnostics – new trends and perspectives.

opublikowanej w czasopiśmie Nowotwory. Journal of Oncology, 2021, 71, 103-110.

mój udział w jej powstawaniu polegał na opracowaniu koncepcji pracy, opracowaniu metodologii i planu pracy, walidacji, wizualizacji, recenzji i redakcji manuskryptu oraz nadzorze nad pracą.

3475587
prof. dr hab. n. med.
Grażyna Kamińska-Winciorek
SPECJALISTA DERMATOLOG - WENEROLOG

Aleksandra Pilśniak
Oddział Chorób Wewnętrznych,
Autoimmunologicznych i Metabolicznych,
Śląski Uniwersytet Medyczny w Katowicach

Oświadczam, że w pracy: Kamińska-Winciorek G, Pilśniak A. The role of dermoscopy in dermato-oncological diagnostics – new trends and perspectives.

opublikowanej w czasopiśmie Nowotwory. Journal of Oncology, 2021, 71, 103-110.

mój udział w jej powstawaniu polegał na zebraniu i analizie piśmiennictwa, napisaniu pierwotnej i ostatecznej wersji pracy oraz edycji manuskryptu.

A. Pilśniak

KOMISJA BIOETYCZNA
Centrum Onkologii Instytut im. Marii Skłodowskiej-Curie
Oddział w Gliwicach
ul. Wybrzeże Armii Krajowej 15, 44-101 Gliwice
tel. 48-32-278 98-24 tel./fax. 48-32-231-35-12

UCHWAŁA KOMISJI BIOETYCZNEJ
NUMER KB/430- 44/19

Na podstawie § 2.ust.2 rozporządzenia Ministra Zdrowia i Opieki Społecznej z dnia 11 maja 199 r. w sprawie szczegółowych zasad powoływania i finansowania oraz trybu działania komisji bioetycznych (Dz. U. z 1999 r Nr 47), art. 29, ust 2, ustawy z dnia 5 grudnia 1996 r. o zawodach lekarza i lekarza dentysty(Dz.U.2017 poz. 125 z późn. zm, poz.480), Rozporządzenia Ministra Zdrowia z dnia 12 października 2018 r (poz. 1994), Zarządzenia Dyrektora Centrum Onkologii- Instytutu nr 44/2017 z dnia 7 czerwca 2017 roku i Regulaminu działania komisji

Dr hab. Grażyna Kamińska-Winciorek
Klinika Transplantacji Szpiku i Onkohematologii
Prof. dr hab. Krzysztof Składowski
I Klinika Radioterapii i Chemioterapii
Dr hab. Tomasz Rutkowski
I Klinika Radioterapii i Chemioterapii
Pani Aleksandra Dudek

Komisja Bioetyczna przy Centrum Onkologii Instytut im. Marii Skłodowskiej-Curie Oddział w Gliwicach na posiedzeniu w dniu 02.04.2019 r. zapoznała się z wnioskiem dot. eksperymentu medycznego pt. „ Analiza obrazów kliniczno- dermoskopowych zmian skórnych w przebiegu ostrego i przewlekłego zapalenia skóry wywołanego radioterapią u pacjentów z rozpoznanym złośliwym nowotworem głowy i szyi leczonych promieniowaniem jonizującym ”

Do Komisji wpłynęły:

- Wniosek do Komisji Bioetycznej przy Centrum Onkologii- Instytucie, Oddział w Gliwicach o wyrażenie opinii o projekcie eksperymentu medycznego (zał.1 do Regulaminu Pracy Komisji Bioetycznej)
- Opis projektu eksperymentu medycznego
- Dane o spodziewanych korzyściach leczniczych i poznawczych oraz ewentualnych innych korzyściach dla osób poddanych eksperymentowi medycznemu
- Formularz Świadomej Zgody Pacjenta na udział w badaniu
- Formularz Informacyjny dla Pacjenta biorącego udział w badaniu
- Wzór „Oświadczenia” – zobowiązanie do uzyskania Świadomej Zgody Udziału w projekcie od wszystkich badanych osób lub ich przedstawicieli ustawowych
- Oświadczenie dotyczące zgody na przetwarzanie danych osobowych osoby uczestniczącej w eksperymencie medycznym w Centrum Onkologii Instytucie im. Marii Skłodowskiej – Curie Oddziale w Gliwicach
- Recenzja dr n. med. Grzegorz Woźniak

Po dyskusji i głosowaniu Komisja postanowiła zaakceptować wyżej wymienione dokumenty i wyraziła zgodę na przeprowadzenie projektu eksperymentu medycznego.

Pan dr hab. n. med. Tomasz Rutkowski nie brał udziału w głosowaniu.

Gliwice, dn.02.04.19 r

Z poważaniem

PRZEWODNICZĄCY
Komisji Bioetycznej
prof. dr hab. n. med. Rafał Suwiński

Skład osobowy Komisji Bioetycznej przy Centrum Onkologii Instytucie im Marii Skłodowskiej Curie oddz. w Gliwicach w dniu ……**02.04.2019 r.**……

Komisja działa zgodnie z zasadami GCP.

Lp.	Imię i Nazwisko	Pracownik Instytutu	Podpis
1.	prof. dr hab. n. med. Rafał Suwiński Radioterapeuta	Tak	
2.	prof. dr hab.n. med. Dariusz Lange Patolog	Tak	
3.	dr hab. n. med. Daria Handkiewicz-Junak Radioterapeuta	Tak	
4.	dr hab. n. med. Tomasz Rutkowski Radioterapeuta	Tak	
5.	dr hab. n. med. Sławomir Blamek Radioterapeuta	Tak	
6.	dr n. med. Aleksander Zajusz Radioterapeuta	Tak	
7.	dr n. med. Janusz Wierzgoń Chirurg	Tak	
8.	dr n. med. Krzysztof Olejnik Anestezjolog	Tak	
9.	lek. med. Hanna Grzbiela Radioterapeuta	Tak	
10.	ks. dr hab. Stanisław Bafia Duchowny	Nie	
11.	dr n. prawn. Michał Synoradzki Prawnik	Nie	
12.	mgr farm. Małgorzata Wolańska Farmaceuta	Nie	
13.	piel. Urszula Broja Pielęgniarka	Nie	